

Rooftop Unit Embedded Diagnostics: Automated Fault Detection and Diagnostics (AFDD) Development, Field Testing and Validation

September 2015

Prepared for the U.S. Department of Energy

By:

S Katipamula

W Kim

R Lutes

RM Underhill

Pacific Northwest National Laboratory

Disclaimer

This document was prepared as an account of work sponsored by the United States Government. While this document is believed to contain correct information, neither the United States Government nor any agency thereof, nor Pacific Northwest National Laboratory, nor any of their employees, makes any warranty, express or implied, or assumes any legal responsibility for the accuracy, completeness, or usefulness of any information, apparatus, product, or process disclosed, or represents that its use would not infringe privately owned rights. Reference herein to any specific commercial product, process, or service by its trade name, trademark, manufacturer, or otherwise, does not constitute or imply its endorsement, recommendation, or favoring by the United States Government or any agency thereof, or Pacific Northwest National Laboratory. The views and opinions of authors expressed herein do not necessarily state or reflect those of the United States Government or any agency thereof or Pacific Northwest National Laboratory.

The work described in this report was funded by the U.S. Department of Energy under Contract No. DE-AC05-76RL01830.

Acknowledgements

The authors would like to acknowledge the Buildings Technologies Office of the U.S. Department of Energy (DOE) Office of Energy Efficiency and Renewable Energy for supporting the research and development effort. The authors would also like to thank Charles Llenza, Technical Development Manager at DOE, Linda Sandahl (Program Manager at PNNL) for thoughtful comments and insights and Sue Arey for editorial support. We also want to thank Ken Hellewell, Jerry Scott and Justin Sipe from Transformative Wave Technologies (TW) of Kent, WA for the help they provided in programming the rooftop unit controllers, deploying the embedded controls on selected RTUs in the field and working with PNNL to test and validate the embedded diagnostics. We also want to thank TW for valuable feedback on the potential for deploying embedded diagnostics.

For more information contact:

Tech Demo Reports
Mail Stop EE-5B
US Department of Energy
1000 Independence Ave, SW
Washington, DC 20585-0121
techdemo@ee.doe.gov

I. Executive Summary

Packaged rooftop units (RTUs) are used in 46% (2.1 million) of all commercial buildings, serving over 60% (39 billion square feet) of the commercial building floor space in the U.S. (EIA 2003). The primary energy consumption associated with RTUs is over 2.6 quads annually. Therefore, even a small improvement in efficiency or part-load operation of these units can lead to significant reductions of energy use and carbon emissions.

In addition to finding ways to improve the part-load performance, there is also a need to improve the persistence of RTU operations. For example, an air-side economizer can offset a significant fraction of the cooling needs in mild and dry climates. However, a number of studies have shown that a significant fraction of the economizer controls on RTUs do not work as intended. Therefore, the State of California has mandated automated fault detection and diagnostics (AFDD) for new RTUs sold in California after July 2014. In addition to the operational problems with air-side economizers, a number of studies also have reported problems with the refrigerant-side operations as well.

To find solutions to improve the operating efficiency of the installed RTU stock, the U.S. Department of Energy's (DOE's) Building Technologies Office (BTO) initiated a multi-year research, development and deployment (RD&D) effort in FY11. Initially through detailed simulations, it was shown that significant energy (between 24% and 35%) and cost savings (~38%) from fan, cooling and heating energy consumption is possible when RTUs were retrofitted with advanced control packages. Because the simulation analysis showed a significant savings potential from advanced RTU controls retrofits, DOE and the Bonneville Power Administration (BPA) funded an extensive evaluation of a retrofit advanced RTU controller in the field. In FY12, a total of 66 RTUs on 8 different buildings were retrofitted with a commercially available advanced controller for improving RTU operational efficiency. Of the 66 RTUs, 17 were packaged heat pumps and the rest were packaged air conditioners with gas heat. The eight buildings cover four building types, including mercantile (both retail and shopping malls), office, food sales, and healthcare. The field demonstration showed that the advanced controller reduced the normalized annual RTU energy consumption by an average of 57% for all RTUs.

Although the advanced controller provides a significant improvement in part-load efficiency, it does not ensure persistence of operations. To ensure persistence, there is a need for automated fault detection and diagnostics (AFDD). RTU diagnostics (both air-side and refrigerant-side) have been mostly deployed offline by collecting data from the RTUs that are integrated to a building automation system or using a retrofit package. Diagnostics using offline methods have limited use because most RTUs typically do not install all the sensors necessary for diagnostics, especially to do a refrigerant-side diagnostics. Use of a retrofit monitoring and diagnostics package can alleviate the problem of sensors. However, it can be expensive to deploy such an AFDD approach. To address the cost, DOE has funded development of a low-cost monitoring and diagnostics approach. The low-cost approach reduces the need for sensing by using two (unit power and outdoor-air temperature) or three sensors. The low-cost approach can detect the degradation in RTU operations overtime, but has limitations in diagnosing the actual cause of the fault. Field tests of this approach are still on going.

It is possible to deploy advanced RTU controls and AFDD by integrating both features on a single controller. By integrating these two features, both the part-load efficiency improvements and persistence of operations can be addressed more cost effectively because an integrated solution can be easily programmed into the controller with very little incremental cost.

Therefore, in FY14, BTO funded PNNL to develop and integrate AFDD methods for both air-side and refrigerant-side fault detection and diagnostics with one of the leading advanced RTU controllers sold in the market today. The work also includes testing and validating the integrated solution in the field. If the results from the field demonstrations show reliable fault diagnostics, it will encourage utilities to provide incentives to pursue the integrated technology because it makes the retrofit controller more cost effective and could make market adoption of the retrofit controller even more attractive to building owners.

Seven AFDD algorithms were developed, deployed and tested on the RTU controller for detecting and diagnosing faults with RTU economizer and ventilation operations using sensors that are commonly installed for advanced control purposes. The algorithms utilize rules derived from engineering principles of proper and improper RTU operations:

- Compare discharge-air temperatures (DAT) with mixed-air temperatures (MAT) for consistency (AFDD0)
- Check if the outdoor-air damper (OAD) is modulating (AFDD1)
- Detect RTU sensor faults (outdoor-air, mixed-air and return-air temperature sensors) (AFDD2)
- Detect if the RTU is not economizing when it should (AFDD3)
- Detect if the RTU is economizing when it should not (AFDD4)
- Detect if the RTU is using excess outdoor air (AFDD5)
- Detect if the RTU is bringing in insufficient ventilation air (AFDD6).

The intent of these algorithms is to provide actionable information to building owners and operations staff while minimizing false alarms. Therefore, the algorithms have been designed to minimize false alarms. These seven algorithms were embedded in the RTU controller. This implementation has been validated by comparing the outputs from the embedded diagnostics with output generated by offline analysis.

The savings that results from correcting the operational problems detected by these algorithms can vary significantly by the size of the unit, utility cost and the severity of the problem. The user has the ability to set the threshold for reporting the errors. Any problem that does not result in energy cost exceeding the threshold are not reported to the user. There are very few documented studies that report the cost impact from the improper economizer operations. Katipamula et al. (2003) reported a wide range of annual cost savings from improper economizer operations (\$100 – \$12,000) depending on the problem and severity of the problem. The problems ranged from improper supply air controls, scheduling, not fully economizing, excess ventilation air, stuck damper, etc. In addition to these problems other problems were reported as well for which the cost impacts are difficult to estimate (e.g temperature sensor problems, mis-calibrated sensor, etc.). Other problems, such as lack of adequate ventilation will not result in excess energy use.

In addition to the air-side diagnostics, refrigerant-side diagnostics were also deployed on the RTU controller. The refrigerant-side diagnostics included: 1) low and high refrigerant charge, 2) condenser fouling and 3) liquid line restriction. Similar to the air-side diagnostics, the refrigerant-side diagnostics were also validated by comparing the outputs from the embedded diagnostics with the output generated by offline analysis.

The refrigerant-side diagnostics embedded in the RTU controller run passively when the operating conditions are favorable (when the compressor is running and after the conditions reach steady-state). Based on the results reported by Kim (2014), a 25% undercharge of refrigerant can lead to an average reduction of 20% in

cooling capacity and 15% in energy efficiency. Furthermore, an undercharge of about 25% would cause an average reduction of SEER (seasonal EER) of about 16% and a cost penalty of \$60/yr/ton assuming an electricity rate of 0.12\$/kWh. For evaporator fouling, a reduction of air flow rate of 50% will result in an average capacity reduction of 14% and 12% in the energy efficiency. The average SEER reduction is about 10% and annual cost penalty of \$24/yr/ton. For condenser fouling, a 50% reduction of air flow will result in an average capacity reduction of 9% and 22% reduction in the energy efficiency. It can lead to SEER reduction 20% and cost penalty of \$80/yr/ton.

These diagnostics will report a code, which includes normal operation, warning and a fault. In addition to the code, the diagnostics also report the impact (capacity and efficiency degradation) of the fault. Combination of the fault and impact will result in a recommendation to the user/building operator on the action to take, which can include a recommendation for immediately repair if the fault is severe.

The air-side diagnostics like refrigerant-side diagnostics run in a passive mode and report a code for each of the seven diagnostics. However, these diagnostics can also be initiated in a proactive way to isolate the fault quickly.

The project has shown that air-side and refrigerant-side AFDD can be easily integrated with advanced RTU controls. With the exception of the mixed-air temperature sensor, all other sensors required to conduct the air-side AFDD are readily available on the RTU controller because they are needed for the advanced control operations. Therefore, the incremental cost of adding air-side diagnostics is minimal. Although the project has shown that integration of the refrigerant-side diagnostics on to the RTU controller is possible, there are a number of additional sensors that are needed to deploy the refrigerant-side diagnostics. Both the air-side and the refrigerant-side algorithms assume that the accuracy of the temperature sensor measurement is at least +/- 1°F.

For refrigerant side diagnostics, in addition to the cost for the additional sensors, locating the sensors in the correct location to measure the parameters also turned out to be a challenge. Because temperature sensors were being used as proxies for pressure measurements, mounting these sensors in the right location was critical; otherwise, the uncertainty in the measurement was high. Accommodating additional sensors also means either increasing the input/output capability of the RTU controller or adding another controller to handle the additional sensors, which increases the cost of deployment significantly.

Therefore, for deploying refrigerant-side diagnostics along with advanced RTU controls three hurdles have to be overcome: 1) cost of additional sensors, 2) cost of upgrading the RTU controller to handle additional sensors and 3) solving the installation difficulties of the sensors in the right location.

Table of Contents

I.	Executive Summary.....	3
II.	Introduction	12
III.	Background	13
	A. Current State of Art of Deploying Advanced RTU Controls	14
	B. Current State of Art of Deploying RTU Diagnostics.....	14
	C. Opportunity.....	15
IV.	Development of Air-side RTU Diagnostics	16
	A. AFDD0: Compare Discharge-air Temperature with Mixed-air Temperature for Consistency.....	18
	Input Parameters Required for AFDD0 Fault.....	19
	AFDD0 Fault Detection and Diagnostics Process.....	19
	B. AFDD1: Check if the Outdoor-air Damper is Modulating	23
	Input Parameters Required for AFDD1 Fault.....	24
	AFDD1 Fault Detection and Diagnostics Process.....	24
	C. AFDD2: Detect Temperature Sensor Faults (Outside-, Mixed- and Return-air Temperature)	28
	Input Parameters Required for AFDD2 Fault.....	28
	AFDD2 Fault Detection and Diagnostics Process.....	29
	D. AFDD3: Detect if the RTU is not Economizing when it Should.....	32
	Input Parameters Required for AFDD3 Fault.....	32
	AFDD3 Fault Detection and Diagnostics Process.....	33
	E. AFDD4: Detect if the RTU is Economizing When it Should Not.....	38
	Input Parameters Required for AFDD4 Fault.....	39
	AFDD4 Fault Detection and Diagnostics Process.....	40
	F. AFDD5: Detect if the RTU is Using Excess Outdoor Air	42
	Input Parameters Required for AFDD5 Fault.....	43
	AFDD5 Fault Detection and Diagnostics Process.....	44
	G. AFDD6: Detect if the RTU is Using Insufficient Outdoor Air.....	49
	Input Parameters Required for AFDD6 Fault.....	49
	AFDD6 Fault Detection and Diagnostics Process.....	50
V.	Development of Refrigerant-side RTU Diagnostics	56
	A. Refrigerant Charge (undercharge/overcharge) Fault Detection and Diagnostics	56
	Input Parameters Required for Refrigerant Charge Fault	57

Constant Parameters Required for Refrigerant Charge Fault	59
Other Constant Parameters Required for Refrigerant Charge Fault	59
Refrigerant Fault Detection and Diagnostics Process	60
B. Methodology to Estimate the Fault Impact	66
Input Parameters Required for Estimating the Fault Impact	66
Estimating the Fault Impact.....	68
C. Condenser Fouling Fault Detection.....	72
Input Parameters Required for Condenser fouling Fault	72
Condenser Fouling Fault Detection and Diagnostics Process.....	72
D. Liquid Line Restriction Fault Detection and Diagnostics.....	77
Liquid Line Fault Detection and Diagnostic Process	77
VI. Testing and Validation Methodology for both Air- and Refrigerant-side Embedded Diagnostics..	80
A. Demonstration Site Description	80
B. Metering and Monitoring Plan.....	82
VII. Validation of Air-side Embedded Diagnostics.....	84
VIII. Validation of Refrigerant-Side Embedded Diagnostics.....	92
A. Validation of Refrigerant-side Diagnostics using Artificial “Faults” in the Field	92
B. Refrigerant Undercharge and Overcharge Tests	93
Improper Condenser Air Flow (condenser blockage) Tests	96
Simultaneous Refrigerant Undercharge and Condenser Fouling Fault Tests.....	99
C. Summary of Validation of the Embedded Refrigerant-side Diagnostics with Artificial Faults.....	101
Validation of the Embedded Refrigerant-side Diagnostics with Offline Analysis	101
Parameters needed for the Refrigerant-Side Fault Detection and Diagnostics	101
Validation of Refrigerant-Side Embedded Diagnostics with Offline Analysis.....	102
IX. Summary and Discussion	108
A. Discussion and Lessons Learned	108
X. References	110
Appendix - Refrigerant Property Table	112

List of Figures

Figure 1: Illustration of the Automated Fault Detection and Diagnostic Process	16
Figure 2: Schematic Showing the Location of Various Temperature Sensors.....	18
Figure 3: Mixed-air and Discharge-air Temperature Consistency Diagnostic Process	22
Figure 4: Check if the Outdoor-air Damper is Modulating	27
Figure 5: Air-side Temperature Sensor (Outside-, Mixed- and Return-air) Diagnostic	31
Figure 6: Detect if the RTU is not Economizing When it Should	38
Figure 7: Detect if the RTU is Economizing When it Should Not	42
Figure 8: Excess Outdoor-air Intake Diagnostic.....	48
Figure 9: Insufficient Outdoor-air Intake Diagnostic	55
Figure 10: Temperature and Power Sensor Locations in a RTU	57
Figure 11: Saturation Temperature Sensor Locations of Condenser and Evaporator	58
Figure 12: Fixed-length Sliding Window of Suction Superheat	62
Figure 13: Implementation Details of Detect Improper Refrigerant Charge	65
Figure 14: Fault Impact Estimation Process	71
Figure 15: Condenser Fouling Fault Detection and Diagnostic Process	76
Figure 16: Liquid Line Restriction Fault Detection and Diagnostic Process	79
Figure 17: External View for Office Building, Kent, WA	81
Figure 18: Locations of RTUs on the Office Building	81
Figure 19: External View for Grocery Store in Phoenix, AZ	82
Figure 20: Locations of RTUs on the Grocery Store.....	82
Figure 21: Schematic of the RTU Monitoring	83
Figure 22: Validation of Embedded AFDD0 Air-side Diagnostics	85
Figure 23: Validation of Embedded AFDD1 Air-side Diagnostics	86
Figure 24: Validation of Embedded Air-side Diagnostics AFDD2	87
Figure 25: Validation of Embedded Air-side Diagnostics for AFDD3.....	88
Figure 26: Execution of Economizer Control Logic (AFDD3 and AFDD4) for RTU 449.....	89
Figure 27: Validation of Embedded Air-side Diagnostics AFDD5	90
Figure 28: Validation of Embedded Air-side Diagnostic AFDD6	91
Figure 29 Refrigerant Charging Method: Adding Refrigerant (left) and Removing Refrigerant (right)	93
Figure 30 Comparison of Predicted Refrigerant Charge Amount with Actual Charge Level.....	94
Figure 31 Validation of Embedded Refrigerant Undercharge Diagnostics.....	95
Figure 32: Screen Shots of Undercharge Refrigerant-side AFDD Results Generated by the RTU Controller: 60% Charge (left) and 100% Charge (right).....	96
Figure 33 Simulation of Condenser Blockage: 50% (Left) and 75% (Right)	97
Figure 34 Estimated Condenser Air Flow Rate as a Function of Condenser Blockage	97
Figure 35 Percent Reduction in COP as a Function of Percent Condenser Air Flow Reduction.....	98
Figure 36 Screen Shots of Condenser Fouling Refrigerant-Side AFDD Results Generated by the RTU Controller: 75% Condenser Fouling (left) and 0% Condenser Fouling (right).....	99
Figure 37 Refrigerant-Charge Fault and Condenser-Fouling Fault: 70% Charge and 50% Blockage (left) and 70% Charge and 75% Blockage (right).....	100

Figure 38 Screen Shots of Combined Charge and Condenser Fouling Refrigerant-Side AFDD Results Generated by the RTU Controller: 70% Refrigerant Charge Level + 50% Condenser Fouling (left) and 70% Refrigerant Charge + 75% Condenser Fouling (right)	100
Figure 39: Outputs Showing the Estimated Fault Level from the Embedded Diagnostics for Refrigerant Charge, Liquid line Restriction, and Condenser Fouling for one Unit in WA.....	104
Figure 40: Comparison of Degradation Parameters Estimated by the Embedded Diagnostics and Offline Analysis	104
Figure 41 Outputs Showing the Performance Impact Estimated by the Embedded Diagnostics for Refrigerant Charge, Liquid line Restriction, and Condenser Fouling for one Unit in WA.....	105
Figure 42: Comparison of Capacity and COP Degradation Estimated by the Embedded Diagnostics and Offline Analysis.....	105
Figure 43 Outputs Showing the Estimated Fault Level from the Embedded Diagnostics for Refrigerant Charge, Liquid line Restriction, and Condenser Fouling for one Unit in AZ	106
Figure 44: Comparison of Degradation Parameters Generated by the Embedded Diagnostics and Offline Analysis	106
Figure 45 Outputs Showing the Performance Impact Estimated by the Embedded Diagnostics for Refrigerant Charge, Liquid line Restriction, and Condenser Fouling for one Unit in AZ	107
Figure 46: Comparison of Capacity and COP degradation Estimated by the Embedded Diagnostics and Offline Analysis.....	107

List of Tables

Table 1: Input Parameter Required for AFDD0 Fault	19
Table 2: Configuration Parameters Required of AFDD0 Fault Implementation.....	19
Table 3: Input Parameters Required for AFDD1 Fault.....	24
Table 4: Configuration Parameters Required of AFDD1 Fault Implementation.....	24
Table 5: Input Parameter Required for AFDD2 Fault	29
Table 6: Configuration Parameters Required of AFDD2 Fault Implementation.....	29
Table 7: Input Parameter Required for AFDD3 Fault	32
Table 8: Configuration Parameters Required of AFDD3 Fault Implementation.....	33
Table 9: Input Parameter Required for AFDD4 Fault	39
Table 10: Configuration Parameters Required of AFDD4 Fault Implementation.....	40
Table 11: Input Parameter Required for AFDD5 Fault	43
Table 12: Configuration Parameters Required of AFDD5 Fault Implementation.....	43
Table 13: Input Parameter Required for AFDD6 Fault	50
Table 14: Configuration Parameters Required of AFDD6 Fault Implementation.....	50
Table 15: Input Parameter Required to Detect and Diagnosis the Refrigerant Charge Fault	57
Table 16: Required Constants (at rated condition) for Refrigerant Charge Fault Detection	59
Table 17: Default Constants for Refrigerant Charge Model 1	59
Table 18: Default Parameters for Refrigerant Charge Algorithm Model 2	59
Table 19: Input for Model 1 and Model 2	60
Table 20: State Condition after Steady-state Detection Process	61
Table 21: Warning Condition for Default Parameters.....	63
Table 22: Fault Condition for Refrigerant Charge Fault	63
Table 23: Fault Condition for Refrigerant Charge Fault	64
Table 24: Inputs Required for Estimating Fault Impact.....	66
Table 25: List of Inputs and Calculated Inputs Necessary for Estimating Enthalpies for Fault Impact	67
Table 26: State Condition after Steady-state Detection Process	69
Table 27: Rules to Flag Capacity Degradation	70
Table 28: Rules to Flag Energy Efficiency Degradation	70
Table 29: Input Parameter Required for Condenser Fouling Fault	72
Table 30: State Condition after Steady-state Detection Process is Complete	73
Table 31: Fault Condition for Capacity Impact	75
Table 32: Input Parameters Required to Detect and Diagnosis Liquid Line Restriction	77
Table 33: State Condition after Steady-state Detection Process	78
Table 34: Rules to Flag Liquid Line Restriction Fault Condition	78
Table 35: Details of the RTUs on the Office Building in Kent, WA (FXO: Fixed Orifice and TXV: Thermal Expansion Valve).....	81
Table 36: Details of the RTUs on the Grocery Store Building in Phoenix, AZ (FXO: Fixed Orifice and TXV: Thermal Expansion Valve).....	82
Table 37: Details of the RTUs at a Retail Site in Seattle, WA.....	82
Table 38: Summary of RTU Cooling Operations	84

Table 39 Details of the RTUs used for AFDD Validation	92
Table 40 Validation Tests for Refrigerant-Side Diagnostics	93
Table 41 Comparison of Default Parameter and “Tuned” Parameter (first row below the labels represents the default parameter for all units)	101
Table 42 Fault Detection Thresholds used by the AFDD Algorithms	102

II. Introduction

Packaged rooftop units (RTUs) are used in 46% (2.1 million) of all commercial buildings, serving over 60% (39 billion square feet) of the commercial building floor space in the U.S. (EIA 2003). The primary energy consumption associated with RTUs is over about 2.6 quads annually. Therefore, even a small improvement in efficiency or part-load operation of these units can lead to significant reductions of energy use and carbon emissions.

Efforts to increase the energy efficiency in commercial buildings have focused mainly on improving the efficiency of heating, ventilation and air conditioning (HVAC) equipment at rated (or design) conditions. Focusing on improving the rated efficiency will yield some savings, but to make significant reductions in energy consumption, solutions that improve the part-load efficiency of RTUs are needed. Approaches that address the improvement in the part-load performance will lead to a significant increase in the operating efficiency of equipment and buildings.

In addition to finding ways to improve the part-load performance, there is also a need to improve the persistence of RTU operations. For example, an air-side economizer can offset a significant fraction of the cooling needs in mild and dry climates. However, a number of studies have shown that a significant fraction of the economizer controls on RTUs do not work as intended (New Buildings Institute 2003). Therefore, California State has mandated automated fault detection and diagnostics (AFDD) for new RTUs sold in California after July 2014. In addition to the operational problems with air-side economizers, a number of studies also have reported problem with the refrigerant-side operations as well (Kim and Braun 2012; New Buildings Institute 2003).

The part-load efficiency of an RTU can be significantly improved (over 50%) by use of advanced RTU controls (Wang et al. 2011, 2012, 2013; Katipamula et al. 2014). Similarly, the persistence of correct RTU operations can be improved by deploying AFDD tools on RTUs.

This report documents the development, testing and field validation of the integrated AFDD and advanced RTU controls using a single controller. Section III provides the background for the project. Sections IV and V describe the development of air-side and refrigerant-side diagnostics processes, respectively, that can be implemented on an advanced RTU controller. Section VI describes the testing and validation methodology, including measurement, verification and evaluation plan. Sections VII and VIII documents the results from validating air-side and refrigerant-side AFDD methods, respectively. Section IX provides a summary and discussion, including the lessons learned from this effort. A list of reference used in the reported are provided in Section X.

The following convention is used in this report to identify the various variables used for diagnostics:

- **Bold style:** Constant value
- *Italic style:* Calculated value
- Normal Style: Real-time measurement.

III. Background

To find solutions to improve the operating efficiency of the installed RTUs stock, the U.S. Department of Energy's (DOE's) Building Technologies Office (BTO) initiated a multi-year research, development and deployment (RD&D) effort in FY11. The objective of the multi-year RD&D effort was to determine the magnitude of energy savings achievable by retrofitting existing RTUs with advanced control strategies not ordinarily used on RTUs. In FY11, Pacific Northwest National Laboratory (PNNL) was funded to estimate the potential energy and the associated cost savings from widespread use of advanced control strategies with RTUs. For that study, the savings were estimated based on detailed EnergyPlus (DOE 2014) simulation. The FY11 study was limited to air conditioners with gas furnaces (Wang et al. 2011). The results from detailed simulation analysis showed significant energy (between 24% and 35%) and cost savings (38%) from fan, cooling and heating energy consumption when RTUs were retrofitted with advanced control packages. In FY12, the simulation analysis was extended to packaged heat pumps (Wang et al. 2012). The simulation analysis showed that combining multi-speed fan control and demand controlled ventilation (DCV) lead to between 35% and 47% savings across all 11 locations for the retail building and between 20% and 57% savings for the office building.

Because the simulation analysis showed a significant savings potential from advanced RTU controls retrofits, DOE and Bonneville Power Administration (BPA) decided to fund an extensive evaluation of a retrofit advanced RTU controller in the field. In FY12, a total of 66 RTUs on 8 different buildings were retrofitted with a commercially available advanced controller for improving RTU operational efficiency. Of the 66 RTUs, 17 were packaged heat pumps and the rest were packaged air conditioners with gas heat. The eight buildings cover four building types, including mercantile (both retail and shopping malls), office, food sales, and healthcare. These buildings are located in four different climate zones, including warm and coastal climate, mixed and humid climate, mixed and marine climate, and cool and moist climate. One-minute interval data was collected from these 66 units over a 12-month period. During the 12-month monitoring period, the controls on the RTUs were alternated between standard (pre-retrofit mode) and advanced control modes on a daily basis. The measured actual savings, the normalized annual energy savings, and the savings uncertainties were calculated using the methods described in the American Society of Heating, Refrigeration and Air Conditioning Engineers (ASHRAE) Guideline 14. Major findings from this work are highlighted below:

- The advanced controller reduced the normalized annual RTU energy consumption by an average of 57% for all RTUs. The fractions savings uncertainty was 12% for normalized savings, significantly lower than the average savings.
- Normalized annual electricity savings were in the range between 0.47 kWh/h (kWh per hour of fan/unit operation) and 7.21 kWh/h, with an average of 2.39 kWh/h.
- Fan energy savings made a dominant contribution to the total RTU electricity savings, while the heating and cooling energy savings varied with units and were relatively smaller in comparison to fan energy savings. In general, fan energy savings had much less uncertainty than heating and cooling energy savings.
- As expected, savings increased with the RTU size. The electricity savings increased from about 1.0 kWh/h for the group with RTU cooling capacity less than 10 tons, to 1.9 kWh/h for the group with RTU

capacity between 10 and 15 tons, and then to 3.9 kWh/h for the group with RTU capacity greater than 15 tons.

- On average, packaged air conditioners (AC units) with gas heat achieved more electricity savings than heat pumps (HP units). The AC units saved 2.60 kWh/h, while the HP group saved 1.75 kWh/h. The reason for this is that the average size of HPs was smaller than the average size of the ACs.
- Normalizing the annual savings with unit runtime and fan horse power appeared to be a better indicator of the potential savings from this retrofit. The variation of annual normalized RTU electricity savings were between 500 and 800 Wh/h/hp, with average savings of approximately 703 Wh/h/hp across all eight sites.

Based on the normalized annual electricity savings and the installed cost of the advanced controller, the simple payback period was calculated for three arbitrary electricity rates including 0.05 \$/kWh, 0.10 \$/kWh, and 0.15 \$/kWh. Note that the gas energy savings were not considered in estimating the payback periods because gas consumption was not directly measured. Major findings from the economic analysis include the following:

- For all RTUs, the average payback period was 6, 3, and 2 years, respectively for the three utility rates. These payback periods account for the controller retail cost and labor to install the controller. The simple payback period for individual units varied from 9 months to 10 years for the electricity rate of 0.15 \$/kWh. The units with the shortest payback period were either large units (e.g., greater than 15 tons) or had the longest runtime (e.g., 24/7 operations).

A. Current State of Art of Deploying Advanced RTU Controls

There are number of vendors that are offering advanced RTU controls; some have more mature products than others (Criscione 2011). Some also provide remote monitoring and limited diagnostics. Some new RTUs, for example, the RTU Challenge units, also come with some advanced control features that improve the part-load efficiency of the RTU significantly.

Over the past decade DOE and California Energy Commission (CEC) has funded PNNL to develop and test economizer and ventilation AFDD (AEC 2003). During the same period, a number of other researchers were also funded by DOE and CEC to develop the refrigerant-side diagnostics for RTUs (Smith and Braun, 2003).

B. Current State of Art of Deploying RTU Diagnostics

RTU diagnostics (both air-side and refrigerant-side) have been mostly deployed offline by collecting the data from the RTUs that are integrated to a building automation system or using a retrofit package (Quimby et al., 2014). Diagnostics using offline methods have limited use because most RTUs typically do not install all the sensors necessary for diagnostics, especially to do a refrigerant-side diagnostics. Use of a retrofit monitoring and diagnostics package can alleviate the problem of sensors. However, it can be expensive to deploy such an AFDD approach. To address the cost, DOE has funded development of a low-cost monitoring and diagnostics approach. The low-cost approach reduces the need for sensing by using two (unit power and outdoor-air temperature) or three sensors (the third sensor is the supply-air temperature)¹. The low-cost approach can

¹ <http://buildingsystems.pnnl.gov/building/smds.stm>

detect the degradation in RTU operations overtime, but has limitations in diagnosing the actual cause of the fault. Field tests of this approach are still on going.

C. Opportunity

It is possible to deploy advanced RTU controls and AFDD by integrating both features on a single controller. By integrating these two features, both the part-load efficiency improvements and persistence of operations can be addressed more cost effectively because an integrated solution can be easily programmed into the controller with very little incremental cost.

Therefore, in FY14, BTO funded PNNL to develop and integrate AFDD methods for both air-side and refrigerant-side fault detection and diagnostics with one of the leading advanced RTU controllers sold in the market today. The work also includes testing and validating the integrated solution in the field. If the results from the field demonstrations show reliable fault diagnostics, it will encourage utilities to provide incentives to pursue the integrated technology because it makes the retrofit controller more cost effective and could make market adoption of the retrofit controller even more attractive to building owners. The field demonstrations are important to establish both to the user and the utility confidence in the persistent energy and cost saving benefits of the integrated RTU retrofit controller.

IV. Development of Air-side RTU Diagnostics

The automated fault detection and diagnostic process is a two-step process where 1) a fault with equipment operation is detected and 2) the cause of the fault is isolated (Figure 1). The process generally relies on analytical or physical redundancies to isolate faults during the diagnostic step. Most rooftop units (RTUs) on commercial buildings lack physical redundancy because heating, ventilation, and air conditioning (HVAC) systems in commercial buildings are considered non-critical. An AFDD process can use proactive diagnostic processes to create analytical redundancy to help isolate the cause of a fault.

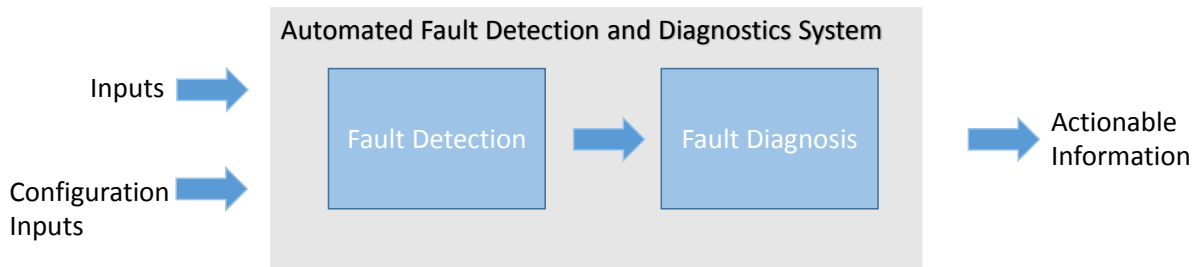


Figure 1: Illustration of the Automated Fault Detection and Diagnostic Process

Proactive AFDD is a process that involves automatically initiating changes to cause or to simulate operating conditions that may not occur for some time, thus producing results that might not be available for months otherwise. Such tests could be automated to cover a more complete range of conditions or to deepen diagnosis beyond what might be possible without this capability. The proactive diagnostic process can help diagnose and isolate faulty operations to a much greater extent than passive diagnostics, but it is intrusive. Proactive diagnostic procedures are capable of providing continuous persistence of performance if they are frequently triggered (e.g., once a day, once a week, once a month or perhaps seasonal). These procedures might be scheduled to occur during building startup hours or at the end of the day to reduce their intrusiveness or could be scheduled on demand. Because the proactive diagnostics are scheduled during unoccupied period, there could be slight increase in energy consumption but not impact on the comfort.

Seven AFDD algorithms were developed and deployed on the RTU controller for detecting and diagnosing faults with RTU economizer and ventilation operations using sensors that are commonly installed for advanced control purposes (with exception to mixed-air sensor). The algorithms utilize rules derived from engineering principles of proper and improper RTU operations. The seven algorithms include:

- Compare discharge-air temperatures (DAT) with mixed-air temperatures (MAT) for consistency (AFDD0)
- Check if the outdoor-air damper (OAD) is modulating (AFDD1)
- Detect RTU sensor faults (outdoor-air, mixed-air and return-air temperature sensors) (AFDD2)
- Detect if the RTU is not economizing when it should (AFDD3)
- Detect if the RTU is economizing when it should not (AFDD4)
- Detect if the RTU is using excess outdoor air (AFDD5)

- Detect if the RTU is bringing in insufficient ventilation air (AFDD6).

The diagnostics are available as a proactive test, that can be run on demand, and as a passive test that continuously monitors the RTUs sensor readings and command outputs. The passive test does not alter the RTU's control sequence in any way. During the passive diagnostics, all seven diagnostics run concurrently and diagnostic results are generated as operational conditions permit.

The intent of these algorithms is to provide actionable information to building owners and operations staff while minimizing false alarms. Therefore, the algorithms have been designed to minimize false alarms. On the other hand, if HVAC systems and their controls start to fail, having an indicator (a.k.a. "check engine light") of a real problem is always helpful – especially if it allows operations and maintenance staff to be proactive, rather than reactive. The remainder of this section will provide a more detailed summary of the seven algorithms.

The temperature sensors (outdoor-air, mixed-air, return-air and discharge-air) required to implement the AFDD algorithms are shown in Figure 2. Although power consumption of the unit and CO₂ sensors are also shown in the figure, they are optional and not needed. In addition to the four temperature sensors, a number of status signals (including fan, compressor, heating, cooling and economizer) and the outdoor-air damper command are also needed. The outdoor-air temperature (OAT) sensor can be installed on an individual RTU, or a shared value across the network.

The advanced RTU controller enables economizing whenever there is a call for cooling and the OAT is less than 70°F. When the OAT is greater than 70°F and there is a call for cooling, the controller uses differential dry-bulb economizer logic. This control logic has been accounted for in the AFDD process.

The following conditions must be met before the fault diagnostic process can be initiated:

1. Supply fan status = "ON."
2. The OAT is between 50°F and 120°F.

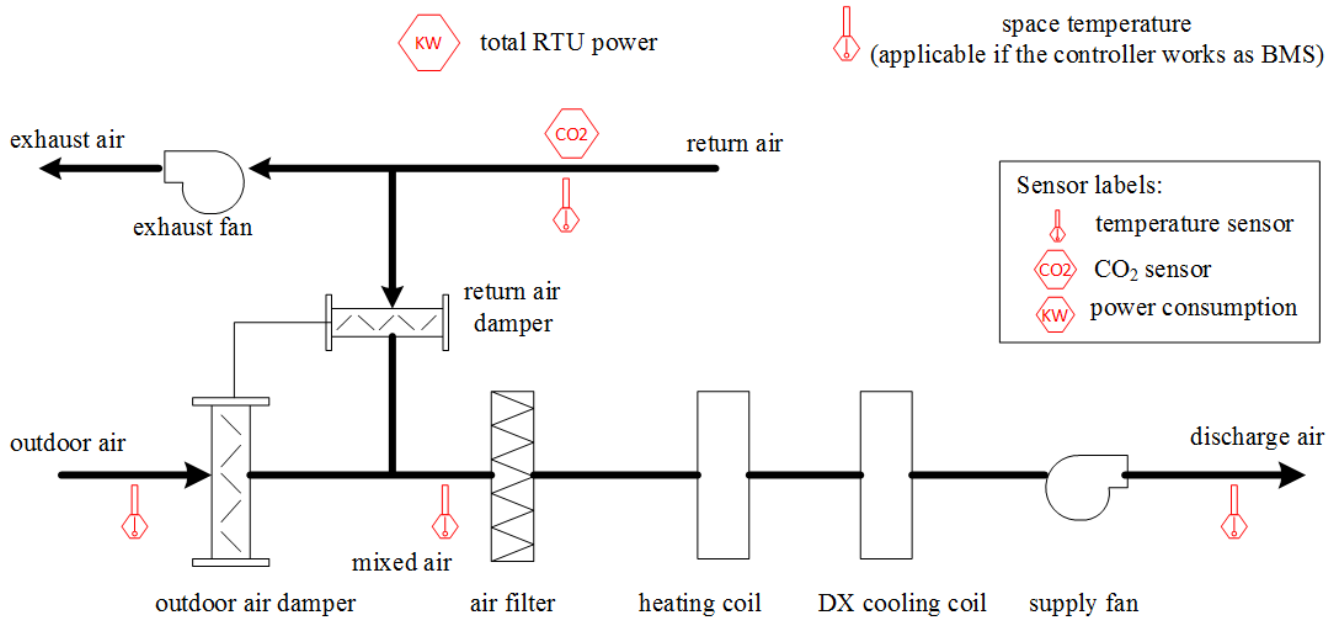


Figure 2: Schematic Showing the Location of Various Temperature Sensors

A. AFFD0: Compare Discharge-air Temperature with Mixed-air Temperature for Consistency

The first diagnostic check is designed to compare the discharge-air and mixed-air temperature sensor readings with each other. Economizer systems often use MAT measurements for feedback control of the outdoor- and return-air dampers. In addition, diagnostic methods require accurate measurements of the MAT. However, RTUs typically have small chambers for mixing outdoor and return air, and can have non-uniform temperature and velocity distributions at the inlet to the direct expansion (DX) coil. As a result, there can be significant bias errors associated with employing single-point temperature sensors. Furthermore, the mixing process can change significantly as the position of the dampers change with economizer operations. The purpose of this proactive diagnostic test is not to identify which sensor(s) is "faulty," but to establish that there is a lack of confidence in one or both sensors and their accuracy.

The compressor (and heating) will be turned off to ensure the consistency of DAT and MAT readings. The MAT may increase between 2°F and 4°F after passing the supply fan chamber because of the heat from the supply fan motor. The Threshold_AFFD0 can be adjusted to compensate for this during the diagnostic. This test will not be activated if the supply fan is off. If the RTU has variable-speed supply fans, this test will not be activated unless the fan speed is at 100% (fan speed can be proactively commanded to 100%) to ensure that there is sufficient air flow.

When heating and cooling systems are turned off, (disabled) during this diagnostic check, the temperature sensors in the air streams upstream of the fan (mixed-air plenum) and downstream of the fan (discharge-air plenum) are compared to each other. The result of this comparison should have temperature readings within 2°F to 4°F (user-adjustable, depends on the size of fan motor) of each other during steady-state conditions (user-adjustable time delay required after the heating and cooling systems are turned off). There usually is additional

heat in the discharge–air stream from the fan and motor that would create the slight difference (higher discharge-air temperature) when this check is made.

This test validates that these two temperature sensor readings are within a user-adjustable pre-set value (within 2°F to 4°F). This provides an initial confidence factor in the two sensors and their integrity. If the diagnostic check determines that the absolute value of the difference between the two temperature sensors is higher than the acceptable threshold, a fault will be generated. The fault does not identify which sensor is "faulty," only that there is a lack of confidence in one or both sensors and their accuracy. Typical causes include sensor fault, sensor location, sensor wiring, sensor software configuration, cooling (or heating) coil control valve leak (where chilled water coils exist in the RTU), etc.

This AFDD test can be run either in a proactive mode or a passive mode. If it is run in a proactive mode, the schedule established on the controller determines when this fault analysis will run for an individual RTU. It is generally preferable not to schedule this test prior to normal occupancy or during morning warm up or cool down periods (because heating or cooling would be active). The best time of day to run this fault analysis is 15 to 30 minutes prior to a scheduled unoccupied period (if the intent is to not cause additional run time on the RTU). If mixed-air temperature sensor value is not available because it is not typically measured, this test cannot be performed.

Input Parameters Required for AFDD0 Fault

The RTU controller needs two temperatures, two status and two command signals (Table 1). The configuration parameters needed for this diagnostics are listed in Table 2. The accuracy of the temperature sensors is assumed to be at least +/- 1°F.

Table 1: Input Parameter Required for AFDD0 Fault

Description	Physical sensor location	Range
Mixed-air temperature	Mixed-air plenum	50 ~ 80°F
Discharge-air temperature	Discharge-air plenum	50 ~ 140°F
Compressor status	-	On/Off
Fan status	-	On/Off
Heating/cooling command	-	1/2
Supply fan speed command	-	0 - 100%

Table 2: Configuration Parameters Required of AFDD0 Fault Implementation

Name	Description	Value
Threshold_AFDD0	Temperature threshold	5°F
Time_steadystate	Wait for steady-state condition	6 minutes
N_samples	Number of samples to average	5
Sampling_rate	Data sampling rate	1 minute
Err_code	Error code	See Figure 3

AFDD0 Fault Detection and Diagnostics Process

The primary goal of the AFDD0 process is to establish mixed-air and discharge-air temperature consistency. The implementation details for AFDD0 are shown in Figure 3.

The fault detection and diagnostics process is broken down into several steps, so it is easy to embed in a controller. The configuration parameters required for executing this diagnostic are listed in Table 2.

Step 1. Disable the heating and cooling (compressor(s)) for the RTU and command the supply fan speed to 100%.

Step 2. Send a command to open the outdoor-air damper (OAD) 100% and force it to remain in that position irrespective of the thermostat control signal. After the damper is fully open and steady-state conditions are reached (minimum 6 minutes delay time, which can be adjusted by the user), monitor and record the discharge-air temperature (DAT) and the MAT. Compute the absolute difference between the MAT and DAT (*DIFF1*) averaged over five samples (adjustable by the user).

Step 3. If the difference between DAT and MAT is greater than the AFDD0 **AFDD0_threshold**, then the diagnostic has detected a problem. Proceed to step 6, otherwise no faults were detected, proceed to the next step.

- If $DIFF1 > \text{Threshold}_{AFDD0}$ then a problem exists.
- **Err_code = 5**

Step 4. Command the OAD to a fully closed position. After the OAD closes completely and steady-state conditions are reached (minimum 6 minutes delay time, which can be adjusted by the user), monitor and record the DAT and the MAT. Compute the absolute difference between the MAT and DAT (*DIFF2*) averaged over five samples (adjustable by the user).

Step 5. If the difference between the DAT and MAT is greater than **AFDD0_threshold**, then the diagnostic has detected a problem, otherwise no faults were detected.

- If $DIFF2 > \text{Threshold}_{AFDD0}$ then a problem exists.
- **Err_code = 5**

Step 6. If no problem was detected:

- **Err_code = 0**

Step 7. Report the diagnostic results (**Err_code**).

Some common causes of the DAT and MAT sensor inconsistencies are:

- Sensor failure or communication failure
- MAT sensor is out of calibration or improperly located
- The return air and outdoor air are not well mixed in the mixing chamber

- The MAT sensor uses a point measurement instead of a temperature averaging sensor
- Temperature stratification: Outside air may stay at the bottom of the duct without good mixing.

The corrective actions could include:

- Use an averaging temperature sensor instead of the point measurement for mixed-air temperature.
- Possible ways to improve the mixing:
 - Rotate the damper sections so that the damper blades direct the air streams into each other as they close. This creates turbulence and helps to promote the mixing process.
- Add baffles to divert the air stream several times before it reaches the coils. This also creates turbulence, which promotes mixing. If the baffles are arranged so that the velocity through them is low (between 800 to 1,000 fpm), then significant benefits can be realized without significant additional pressure drop.

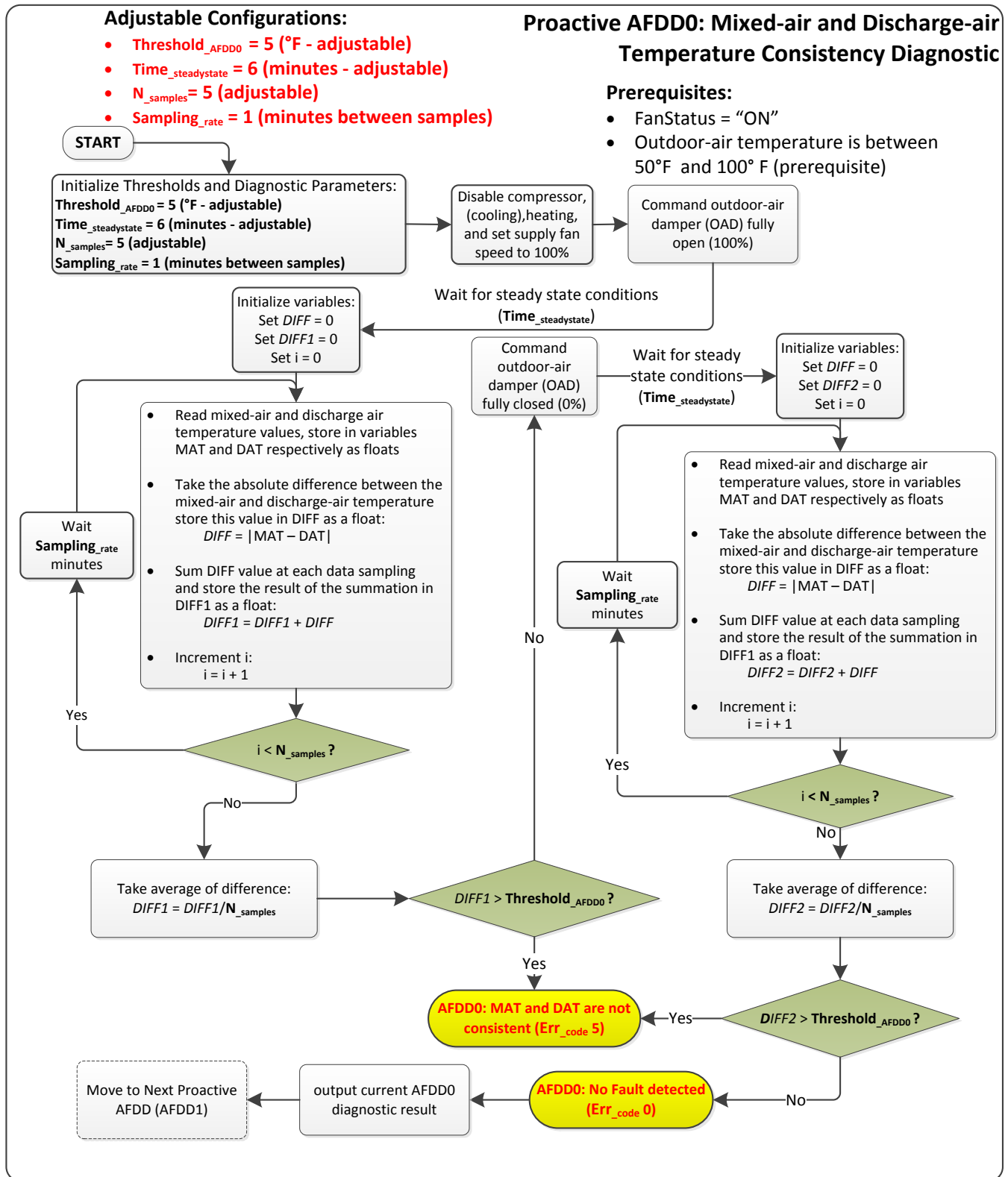


Figure 3: Mixed-air and Discharge-air Temperature Consistency Diagnostic Process

B. AFFD1: Check if the Outdoor-air Damper is Modulating

The second diagnostic checks if the outdoor-air damper (OAD) is modulating properly. When the OAD is not modulating, there is the potential for energy waste or insufficient ventilation to the spaces served by the RTU. For example, if the damper is stuck in a fully closed position, the RTU will fail to provide the necessary ventilation and the opportunity for free cooling when outdoor conditions are favorable for economizing will be missed, causing energy waste.

A broken or stuck actuator or linkage that affects damper modulation can cause an economizer to fail. The damper fault can increase energy consumption of the RTU in two ways; 1) too much OA is admitted on a cold day, this unnecessarily increases the heating load; and 2) too much OA intake on a hot or humid day unnecessarily increases the energy expended to cool or dehumidify the excess OA. On extremely hot or cold days, additional load may prevent the RTU from maintaining desired space temperature, causing occupant discomfort. Furthermore, an OAD that fails and is stuck closed may reduce the OA ventilation to levels less than those required by ANSI/ASHRAE Standard 62, *Ventilation for Acceptable Indoor Air Quality*, potentially causing indoor air quality (IAQ) problems.

The fault analysis will use the economizer damper command to create two steady-state conditions in the mixed-air plenum. This diagnostic test will also require that the heating and cooling functions be temporarily disabled (similar to “AFFD0” diagnostic check) for both steady-state condition checks. If the RTU has variable-speed supply fan, this test will not be activated unless the fan speed is at 100% to ensure that there is sufficient flow (fan speed can proactively be commanded to 100%). The first steady-state condition is obtained by commanding the OAD to a fully open position (100% outside air). The time to reach steady-state will be a user-adjustable parameter (recommended to be at least 5 minutes for steady-state conditions to be established). If the damper is fully open, the difference between the OAT and the MAT (DAT if a mixed-air temperature sensor is not installed) should be minimal (between 2°F and 4°F).

The second steady-state condition is obtained by commanding the OAD to a fully closed position (0% outside air). If the OAD is fully closed, the difference between the RAT and the MAT sensors (DAT if MAT sensor is not installed) should be minimal (between 2°F and 4°F).

The absolute difference between the sensor measurements is averaged over a user-adjustable number of samples to obtain an average absolute difference for each of the steady-state conditions. If the diagnostic check determines that the average absolute temperature difference is greater than the acceptable threshold, a fault is generated indicating the damper is not modulating properly.

If the RTU is missing the MAT sensor, the DAT sensor is used instead for both steady-state conditions with appropriate change in the threshold value (DAT will be warmer because of the heat gain from supply fan motor).

If the fault analysis returns a fault for an economizer damper that does not open 100% or close to 0%, the diagnostic will recommend that the building owner or designated operations and maintenance (O&M) staff physically inspect the damper movements.

Input Parameters Required for AFDD1 Fault

The RTU controller needs three temperatures, two status and three command signals (Table 3). The configuration parameters required for this diagnostics are list in Table 4.

Table 3: Input Parameters Required for AFDD1 Fault

Description	Physical sensor location	Range
Mixed-air temperature	Mixed-air plenum	50 ~ 80°F
Outdoor-air temperature	Outdoor-air intake hood	50 ~ 100°F
Return-air temperature	Return-air plenum	50 ~ 100°F
Compressor status	-	On/Off
Fan status	-	On/Off
Heating/cooling command	-	1/2
Supply fan speed command	-	0 – 100%
Damper command	-	0 – 100%

Table 4: Configuration Parameters Required of AFDD1 Fault Implementation

Name	Description	Value
Threshold _Temp, AFDD1	Prerequisite temperature threshold	10°F
Theshold _damper, AFDD1	OAD modulation threshold	3°F
Time _steadystate	Wait time for steady-state conditions	6 minutes
N _samples	Number of samples to average	5
Sampling _rate	Data sampling rate	1 minute
Err _code	Error code	See Figure 4

AFDD1 Fault Detection and Diagnostics Process

The primary goal of the AFDD1 process is to verify whether the OAD is functional (can modulate from 0% to 100% open) properly. The implementation details of AFDD1 are shown in Figure 4. The following conditions must be met before the fault diagnostic process can be initiated:

- The OAT is not too close to the RAT. For example, the proactive fault diagnostics process will not be initiated if the absolute value of the difference between the OAT and RAT is not greater than **Threshold**_temperature, AFDD1 (10°F by default and user adjustable) as shown below:
 - $|RAT - OAT| > \text{Threshold_Temp, AFDD1}$
- Performing a limit check on the temperature sensors can detect a hardware failure and should be performed prior to the OAD modulation diagnostic. Ensure that each temperature sensor (OAT, RAT, and MAT sensors) are not outside their expected range of operation. If any of the temperature sensors are outside their expected range, a diagnostic message will be presented to the user. O&M staff should inspect the indicated temperature sensor and fix or replace the sensor.

The fault detection and diagnostics process is broken down into several steps, so it is easy to embed in a controller. The configuration parameters required for executing this diagnostic are listed in Table 4.

Step 1. Disable the heating and cooling (compressor) for the RTU and command the supply fan speed to 100%.

Step 2. Command the OAD to a fully open position and force it to remain in that position irrespective of the control signal. After the damper is fully open and steady-state conditions are reached (minimum 6 minutes delay time, which can be adjusted by the user), monitor and record the OAT and the MAT (DAT if MAT is not available). Compute absolute difference between MAT and OAT (*DIFF1*) averaged over five samples (the number of samples over which this difference is averaged over can be adjusted by the user).

Step 3. Command the OAD to a fully closed position. After the OAD closes and steady-state conditions are reached (minimum 6 minute delay time, which can be adjusted by the user), monitor and record the RAT and the MAT (DAT if MAT is not available). Compute the absolute difference between the MAT and RAT (*DIFF2*) averaged over five samples (the number of samples over which this difference is averaged over can be adjusted by the user).

Step 4. Compare *DIFF1* and *DIFF2* to **Threshold_{damper, AFDD1}**.

- If $DIFF1 < \text{Threshold}_{\text{damper, AFDD1}}$ and $DIFF2 < \text{Threshold}_{\text{damper, AFDD1}}$ then:
 - No problem is detected, the OAD is modulating properly.
 - **Err_{code} = 10**
- If ($DIFF1 > \text{Threshold}_{\text{damper, AFDD1}}$ and $DIFF2 < \text{Threshold}_{\text{damper, AFDD1}}$) OR ($DIFF1 < \text{Threshold}_{\text{damper, AFDD1}}$ and $DIFF2 > \text{Threshold}_{\text{damper, AFDD1}}$) then:
 - Check if there was a fault detected for AFDD0. If a fault has been detected for AFDD0, then this diagnostic cannot isolate the fault.
 - **Err_{code} = 11**
 - If AFDD0 did not detect a fault, then AFDD1 indicates that there is a leaking damper (outdoor-air or return-air damper).
 - **Err_{code} = 13**
- The red dashed box in the Figure 4 shows an additional diagnostic step that may be implemented in the future. If there is a potential OAD or OAT sensor problem, then the OAT reading associated with the RTU will be compared to another OAT sensor, such as an OAT from a local weather station. This check will help to decouple temperature sensor and economizer damper problems and add an extra measure of confidence in the diagnostic results.

Step 5. Report the diagnostic results (**Err_{code}**).

The possible causes for failure of the OAD can be both mechanical or control problems:

- Broken linkage between damper actuator and damper.
- Damper or damper actuator mechanical (and/or electrical) failure (including damper seals, damper power or blockage/binding).
- Electrical connection (control wiring) fault between the local controller and the damper actuator (no signal or wrong signal).
- Actuator not rotating correct direction when signal is applied or not sequenced correctly with other actuator(s) when multiple actuators exist (first actuator has rotated 50% of travel before other actuator(s) start moving).

Possible corrective actions include:

- Fix the damper and actuator connection.
- Make sure the control wiring and data points are mapped correctly.
- Make sure the actuator sequencing and calibration set up are correct.

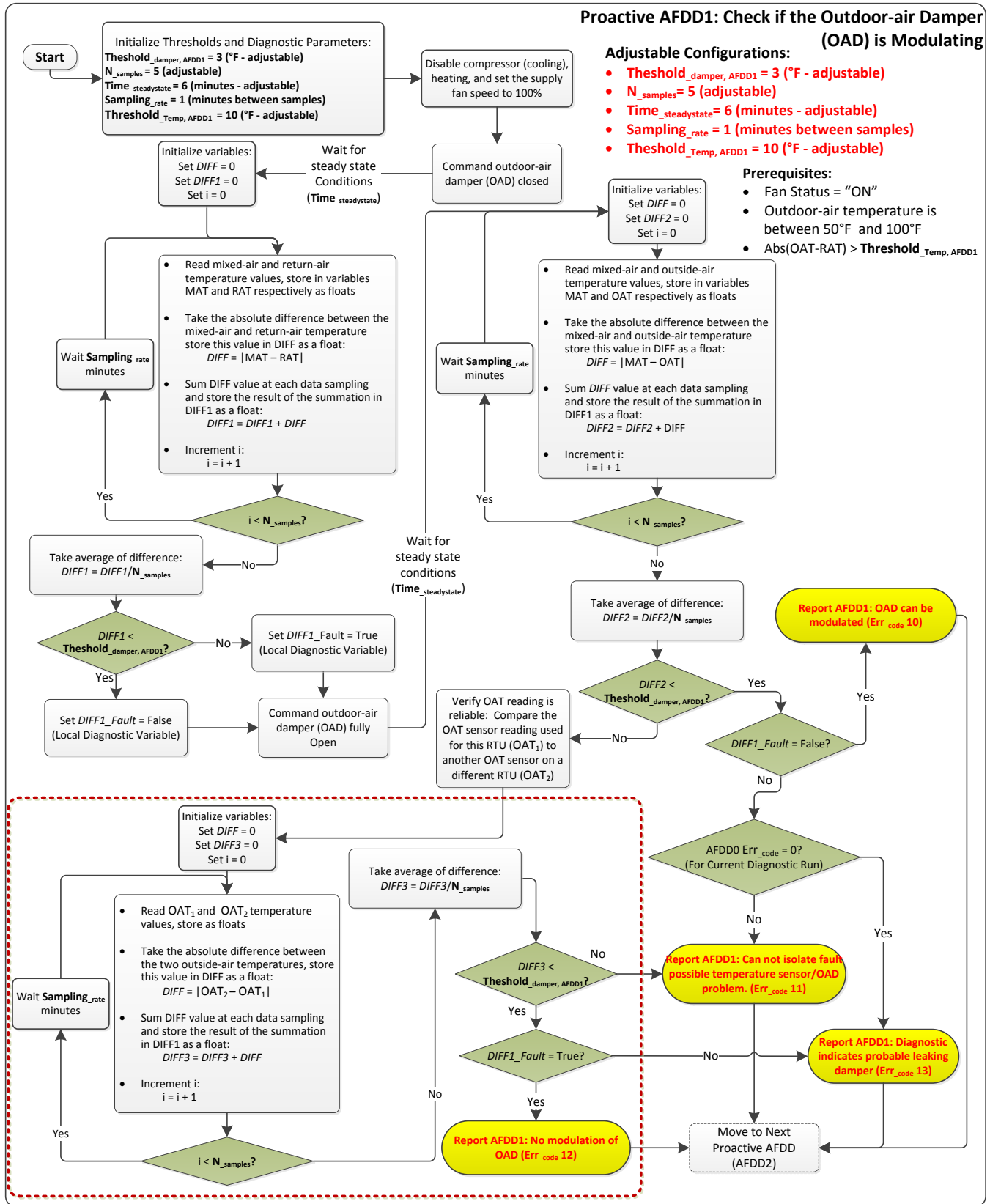


Figure 4: Check if the Outdoor-air Damper is Modulating

C. AFDD2: Detect Temperature Sensor Faults (Outside-, Mixed- and Return-air Temperature)

The third diagnostic determines if the temperature sensors used on the RTU are reliable and within accepted accuracy. This diagnostic requires that the user/owner or designated staff to visually verify that the economizer dampers are working (when “AFDD1” indicates a fault) as previously described for one or both of the steady-state conditions (0% outside-air and 100% outside-air commands).

Damaged, disconnected wiring, or mis-calibration of temperature sensors can cause an RTU to operate inefficiently, such as failing to activate the economizer cycle when OA can provide free cooling, or remaining in a high-capacity mechanical cooling mode in an attempt to maintain the DAT when a more energy-efficient economizer stage could provide adequate cooling.

In general, sensor faults fall into two broad categories: 1) complete failure (hardware faults) and 2) partial failure (software faults). Sensors with hard faults are relatively easy to detect and diagnose, while soft faults can be difficult to detect and diagnose. The most common soft faults are sensor bias and gradual drift. Unlike hard faults, soft faults can go undetected and adversely affect the health of occupants (lack of sufficient fresh air) or increase energy consumption.

When the OAD is commanded to a fully closed position (0% outside air), the temperature sensors in the return- and the mixed-air (discharge-air temperature sensor if mixed-air temperature sensor is not installed) plenums are compared to each other. The result of this comparison should be within 2°F to 4°F after steady-state conditions are reached. The time to reach steady-state could be a user-adjustable parameter (recommended to be at least 6 minutes for greater accuracy and confidence in the results).

The second steady-state condition is obtained by commanding the economizer damper to a fully open position (100% outside air). When the temperature in the mixed-air plenum is compared to the outside-air temperature, the result of this comparison should be within 2°F to 4°F after steady-state conditions are reached.

This test will not run when outside-air temperatures are extreme (too hot or too cold [OAT < 50°F or OAT > 100°F]) or when the OAT are within 4°F to 5°F of the RAT value.

Input Parameters Required for AFDD2 Fault

The RTU controller needs three temperatures, two status and three command signals (Table 5). The configuration parameters required for this diagnostics are listed in Table 6.

Table 5: Input Parameter Required for AFDD2 Fault

Description	Physical sensor location	Range
Mixed-air temperature	Mixed-air plenum	50 ~ 80°F
Outdoor-air temperature	Outdoor-air intake hood	50 ~ 100°F
Return-air temperature	Return-air plenum	50 ~ 100°F
Compressor status	-	On/Off
Fan status	-	On/Off
Heating/cooling command	-	0/1/2
Supply fan speed command	-	0 – 100%
Damper command	-	0 – 100%

Table 6: Configuration Parameters Required of AFDD2 Fault Implementation

Name	Description	Value
Threshold_Temp, AFDD2	Threshold to detect sensor problem	4°F
Threshold_AFDD2-OAT	Threshold to isolate OAT sensor fault	3°F
Threshold_AFDD2-RAT	Threshold to isolate RAT sensor fault	4°F
Time_steadystate	Wait time for steady-state conditions	6 minutes
N_samples	Number of samples to average	5
Sampling_rate	Data sampling rate	1 minute
Err_code	Error code	See Figure 5

AFDD2 Fault Detection and Diagnostics Process

The primary goal of the AFDD2 process is to validate the accuracy of the temperature sensors. The FDD process is broken down into several steps, so it is easy to embed in the RTU controller. The implementation details for AFDD2 are show in Figure 5.

Step 1. Determine if a temperature sensor fault exists.

- If (RAT - MAT > **Threshold_Temperature, AFDD2** and OAT – MAT > **Threshold_Temperature**) OR (MAT - RAT > **Threshold_Temperature, AFDD2** and MAT – OAT > **Threshold_Temperature, AFDD2**) then:
 - A temperature sensor problem is detected; continue with the diagnostic to isolate the faulty temperature sensor (proceed to step 2).
- If there is not a temperature sensor problem:
 - **Err_code** = 20
 - proceed to step 8.

Step 2. Disable heating and cooling (compressor) and command the supply fan speed to 100%.

Step 3. Command the OAD to a fully open position and force it to remain in that position irrespective of the control signal. After the damper is fully open and steady-state conditions are reached (minimum 6 minutes delay time, which can be adjusted by the user), monitor and record the OAT and the MAT (DAT if MAT is not available). Compute the absolute difference between the MAT and OAT (DIFF1) averaged over five samples (adjustable by the user).

Step 4. If $DIFF1 < \text{Threshold}_{\text{temperature, AFDD2-RAT}}$, then the RAT sensor is faulty.

- **Err_code** = 25
- Proceed to step 8.

Step 5. If the RAT sensor is not faulty, command the OAD to a fully closed position. After the OAD fully closes and steady-state conditions are reached (minimum 6 minutes delay time, which can be adjusted by the user) monitor and record the RAT and the MAT (DAT if MAT is not available). Compute the absolute difference between the MAT and RAT (*DIFF2*) averaged over five samples (adjustable by the user).

Step 6. If $DIFF2 < \text{Threshold}_{\text{temperature, AFDD2-OAT}}$, then the OAT sensor is faulty.

- **Err_code** = 24
- Proceed to step 8.

Step 7. If the both the OAT sensor and the RAT sensor are not found to be faulty then there is a MAT sensor fault.

- **Err_code** = 26

Step 8. Report the diagnostic results (**Err_code**).

The possible causes of the temperature sensors failure/fault include:

- The temperature sensor is physically broken or damaged.
- Connection fault between the local controller and the temperature sensors (no signal or wrong signal).
- Sensor is not connected to local controller.
- The temperature sensor is out of calibration.

Possible corrective actions include:

- Replace the sensor if the sensor is broken or damaged.
- Fix the sensor and RTU controller connection.
- Make sure the control wiring and sensor points are mapped and terminated correctly.
- Make sure the dampers are modulating to a fully open and a fully closed position.
- Make sure sensors are properly calibrated.

Proactive AFDD2: Air-side Temperature Sensor (Outside-air, Mixed-air, and Return-air) Diagnostic

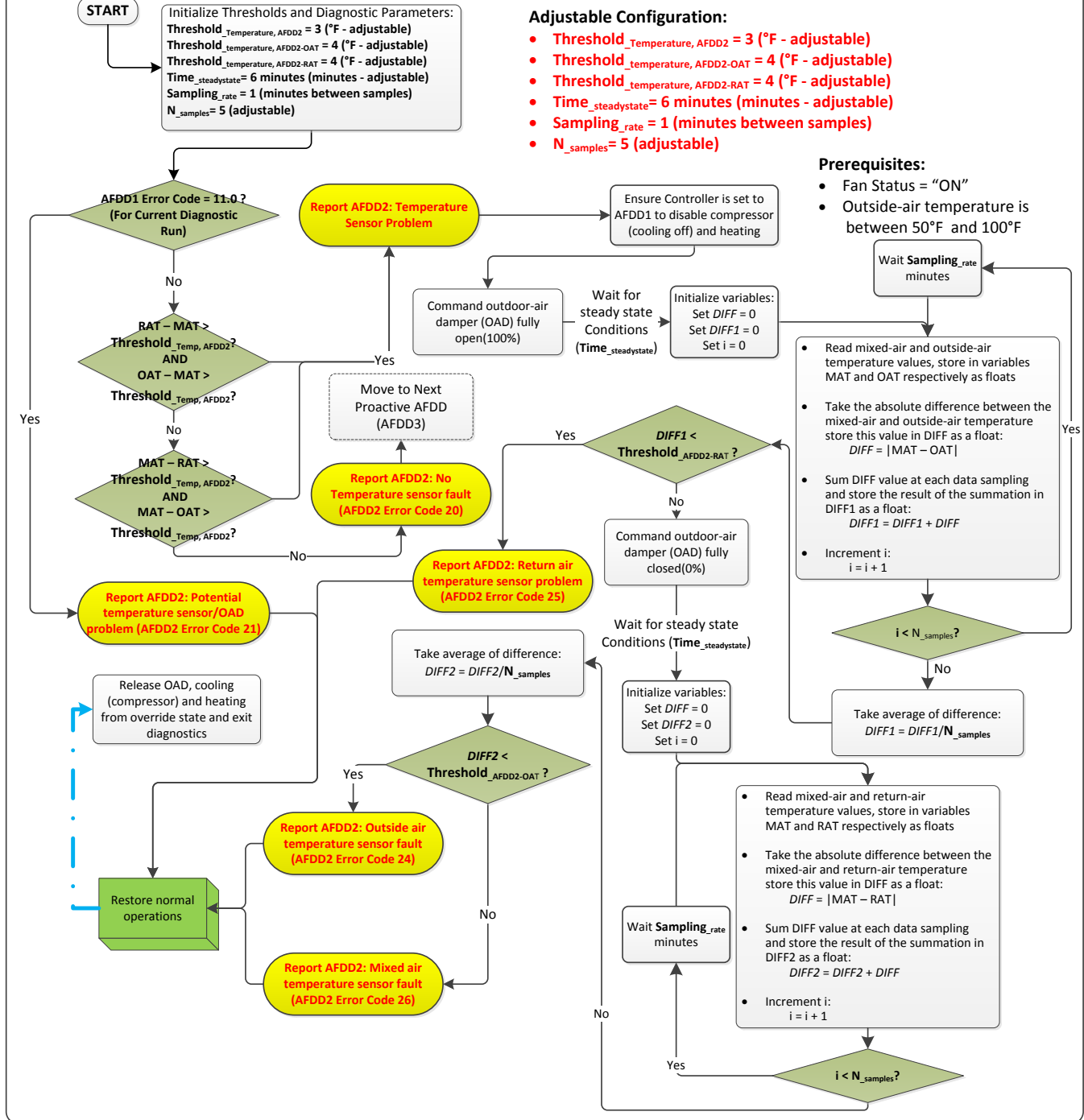


Figure 5: Air-side Temperature Sensor (Outside-, Mixed- and Return-air) Diagnostic

D. AFDD3: Detect if the RTU is not Economizing when it Should

The purpose of this proactive diagnostic measure is to verify that the economizing controls are working properly when outdoor conditions are favorable for economizing. When the economizer damper does not operate as intended, the unit fails to provide free cooling, thus causing an energy penalty during periods when free cooling is available.

The failure of the RTU to economize when it should can be caused by improper control parameter settings, improper building pressurization or failure of the actual economizer actuator and/or economizer damper components (blades, seals, linkages, etc.). When economizers fail to operate properly, their poor performance may go unnoticed for a long time. Few symptoms of failure are perceptible to building occupants because if the economizer is not working, the compressors usually picks up the slack. Only in extreme cases does a malfunctioning economizer result in unacceptable space temperatures or poor indoor air quality. The proactive AFDD process can help to minimize such problems.

The outdoor-air temperature can be overridden to test the economizer when the outdoor-air temperature is not favorable for economizing.

The embedded diagnostics run in a passive mode continuously and perform active diagnostics on demand. The *OATBias* is not set in the passive mode. In the passive mode, this diagnostic only runs when there is a call for cooling from the space served by the RTU and conditions are favorable for economizing. Each diagnostic runs independently of the other diagnostics. Ideally, if a temperature sensor problem is detected, the remainder of the diagnostics should return an inconclusive result (the economizer and ventilation diagnostics rely on accurate temperature sensors to return a valid diagnostic result). If a fault is detected that indicates a temperature sensor problem (AFDD2), this fault should be corrected first before acting on other diagnostic results.

Input Parameters Required for AFDD3 Fault

The RTU controller needs three temperatures, two status and three command signals (Table 7). The configuration parameters required for this diagnostics are listed in Table 8.

Table 7: Input Parameter Required for AFDD3 Fault

Description	Physical sensor location	Range
Mixed-air temperature	Mixed-air plenum	50 ~ 80°F
Outdoor-air temperature	Outdoor-air intake hood	50 ~ 100°F
Return-air temperature	Return-air plenum	50 ~ 100°F
Compressor status	-	On/Off
Fan status	-	On/Off
Heating/cooling command	-	0/1/2
Supply fan speed command	-	0 – 100%
Damper command	-	0 – 100%

Table 8: Configuration Parameters Required of AFDD3 Fault Implementation

Name	Description	Value
Threshold _Temp, AFDD3	Minimum difference between OAT and RAT	4°F
Threshold _damper, AFDD3	Threshold to detect proper damper position	25%
Threshold _OAF, AFDD3	Threshold to detect proper OAF value	25%
Δ	Dead band associated with economizer control	1°F
Time _steadystate	Wait time for steady-state conditions	6 minutes
N _samples	Number of samples to average	5
Sampling _rate	Data sampling rate	1 minute
OAD _minimum	Minimum OAD command	15%
OA _minimum	Minimum desired OAF	5%
Err _code	Error code	See Figure 6

To check the amount of outdoor air being brought into the RTU the outdoor-air fraction (*OAF*) is calculated:

$$\frac{\text{RAT} - \text{MAT}}{\text{RAT} - \text{OAT}}$$

The *OAF* should be close to 1.0 (100%) when the outdoor-air damper is fully open for economizing.

AFDD3 Fault Detection and Diagnostics Process

The primary goal of the AFDD3 is to validate the economizing controls when outdoor conditions are favorable for economizing. The following conditions must be met before the fault diagnostic process can be initiated. The implementation details for AFDD3 are show in Figure 6.

- The OAT is not too close to the RAT. For example, the proactive fault diagnostics process will not be initiated if the absolute value of the difference between the OAT and RAT is not greater than **Threshold**_Temp, AFDD3 (4°F by default and user adjustable) as shown below:
 - $|\text{RAT} - \text{OAT}| > \text{Threshold}_{\text{Temp, AFDD3}}$ (If this condition is not met then **Err**_code = 38)

This diagnostic will check the economizer operations during the following modes of operation:

1. There is a call for cooling from the space served by RTU and outdoor conditions are favorable for economizing.
2. There is a call for cooling from the space served by the RTU and outdoor conditions are not favorable for economizing.
3. There is no call for cooling from the space served by the RTU.

These modes of operation are handled distinctively in AFDD3 as follows:

- When there is a call for cooling from the space served by RTU and outdoor conditions are favorable for economizing ($\text{OAT} < \text{RAT} - \Delta$ or $\text{OAT} < 70^\circ\text{F} - \Delta$).

Step 1. Check the OAD command.

- If $OAT \geq DAT_{\text{set point}}$.
 - If $(100 - OAD) < \text{Threshold}_{\text{damper, AFDD3}}$, then the OAD is open and the RTU is economizing.
 - Proceed to step 2.
 - Otherwise, a problem has been detected. The RTU is not economizing when it should or is under utilizing the economizer.
 - **Err_code = 31**
 - Proceed to step 3.
- Else if the $OAT < DAT_{\text{set point}}$.
 - If $OAD > OAD_{\text{minimum}}$, then the OAD is open and the RTU is economizing.
 - Proceed to step 4.
 - Otherwise, a problem has been detected. The RTU is not economizing when it should or is under utilizing the economizer.
 - **Err_code = 31**
 - Proceed to step 3.

Step 2. If the RTU is economizing properly (no fault was detected in Step 1), the *OAF* is calculated using the *OAT*, *MAT*, and *RAT*.

- If the *OAF* is within the expected range (*OAF* such that $OAF < 1.25$ and $OAF > 0$).
 - If $OAT \geq DAT_{\text{set point}}$.
 - If $(1.0 - OAF) > \text{Threshold}_{\text{OAF, AFDD3}}$, then the RTU is not bringing in sufficient outdoor air and is not fully realizing the energy savings potential of economizing.
 - **Err_code = 32**
 - Proceed to step 3.
 - Otherwise, no problem was detected for this diagnostic.
 - **Err_code = 30**
 - Proceed to step 3.
 - If $OAT < DAT_{\text{set point}}$.

- If $OAF > OA_{\text{minimum}}$.
 - **Err_code = 30**
 - Proceed to step 3.
 - If $OAF \leq OA_{\text{minimum}}$.
 - **Err_code = 32**
 - Proceed to step 3.
 - Else the OAF is outside the expected range (OAF such that $OAF \leq 0$ or $OAF \geq 1.25$).
 - **Err_code = 38**
 - Proceed to step 3.

Step 3. Report the diagnostic results (**Err_code**).

- When there is a call for cooling from the space served by the RTU and the conditions are not favorable for economizing ($OAT > RAT + \Delta$ or $OAT > 70^{\circ}\text{F} + \Delta$):

Step 1. Send an override command to RTU controller and set the outdoor-air temperature bias (OAT_{Bias}) to simulate conditions favorable for economizing (the RTU should open the damper fully).

Step 2. Allow a sufficient delay so that conditions in the RTU will reach steady-state (6 minutes adjustable).

Step 3. Check the OAD command.

- If $OAT \geq DAT_{\text{set point}}$.
 - If $(100 - OAD) < \text{Threshold}_{\text{damper, AFDD3}}$, then the OAD is open and the RTU is economizing.
 - Proceed to step 4.
 - Otherwise, a problem has been detected. The RTU is not economizing when it should or is under utilizing the economizer.
 - **Err_code = 31**
 - Proceed to step 5.
- Else if the $OAT < DAT_{\text{set point}}$.
 - If $OAD > OAD_{\text{minimum}}$, then the OAD is open and the RTU is economizing.
 - Proceed to step 4.

- Otherwise, a problem has been detected. The RTU is not economizing when it should or is under utilizing the economizer.
 - **Err_code = 31**
 - Proceed to step 5.

Step 4. If the RTU is economizing properly (no fault was detected in Step 1), the *OAF* is calculated using the OAT (true unbiased OAT), MAT and RAT.

- If the *OAF* is within the expected range (*OAF* such that $OAF < 1.25$ and $OAF > 0$).
 - If $OAT \geq DAT_{\text{set point}}$.
 - If $(1.0 - OAF) > \text{Threshold}_{OAF, AFDD3}$, then the RTU is not bringing in sufficient outdoor air and is not fully realizing the energy savings potential of economizing.
 - **Err_code = 32**
 - Proceed to step 5.
 - Otherwise, no problem was detected for this diagnostic.
 - **Err_code = 30**
 - Proceed to step 5.
 - If $OAT < DAT_{\text{set point}}$.
 - If $OAF > OA_{\text{minimum}}$.
 - **Err_code = 30**
 - Proceed to step 5.
 - If $OAF \leq OA_{\text{minimum}}$.
 - **Err_code = 32**
 - Proceed to step 5.
- Else the *OAF* is outside the expected range (*OAF* such that $OAF \leq 0$ or $OAF \geq 1.25$).
 - **Err_code = 38**
 - Proceed to step 5.

Step 5. Release the *OATBias* (set the *OATBias* to zero).

Step 6. Report the diagnostic results (**Err_code**).

- If there is no call for cooling from the space served by the RTU, retry the diagnostic later when there is a call for cooling.

The causes improve economizer controls (not economizing when it should) can be mechanical failure or a control failure:

- An air-temperature sensor fault or failure. Refer to AFDD2 for more details.

Possible corrective actions include:

- Replace or calibrate the temperature sensors.
- Verify CO₂ sensors (if used with DCV sequences) are calibrated
- Check the implemented control logic.

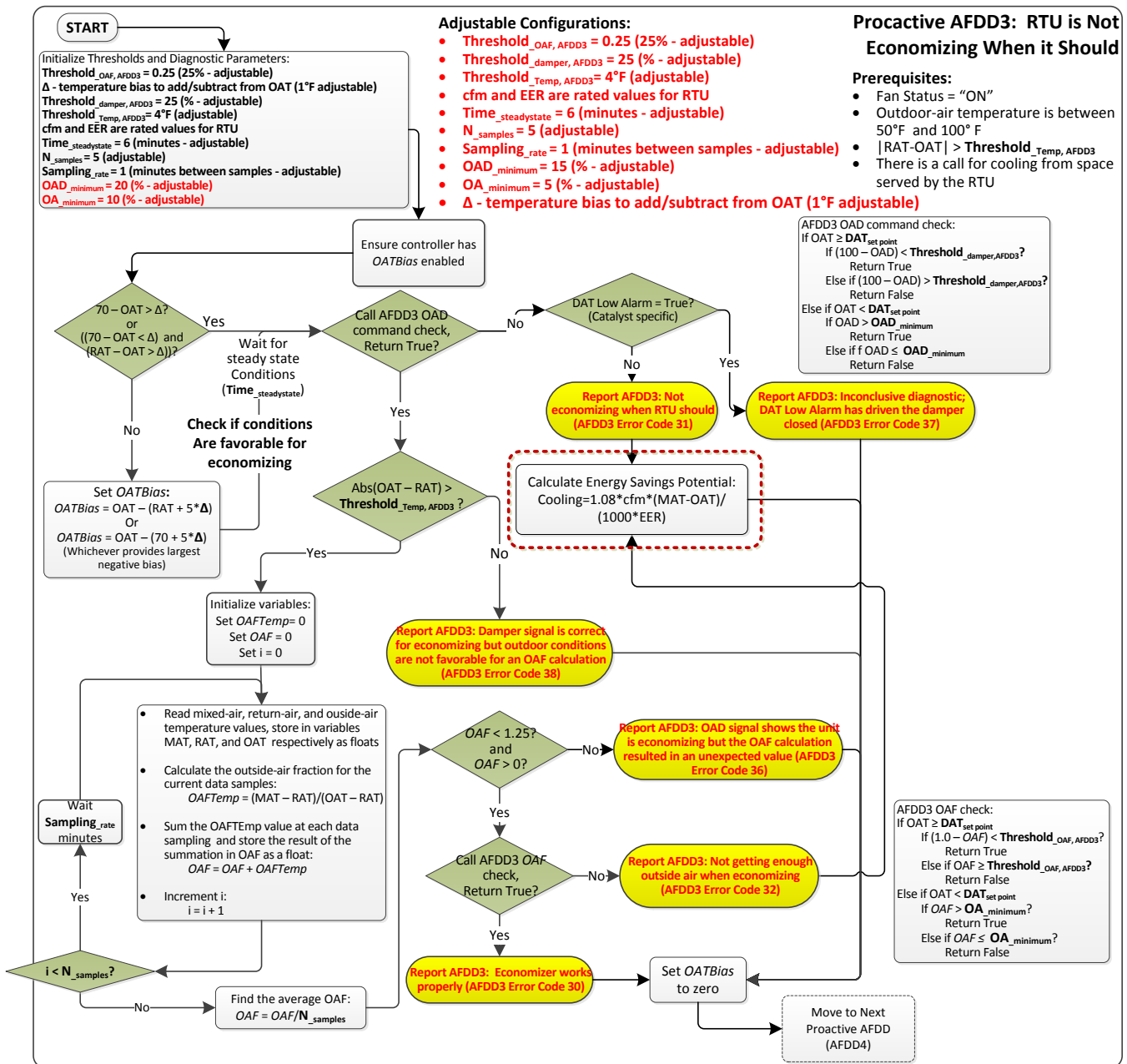


Figure 6: Detect if the RTU is not Economizing When it Should

E. AFDD4: Detect if the RTU is Economizing When it Should Not

The fifth diagnostic also validates economizer controls, but when the conditions are not favorable for economizing. This diagnostic assumes that the sensors are reliable and that the damper is able to modulate (AFDD1 and AFDD2 are fault-free). Even though economizing can reduce cooling energy consumption, economizing when it not favorable for economizing has the potential to increase heating and/or cooling energy consumption. The diagnostic will use the outdoor-air damper command from the controller to determine if it is appropriate during various heating and cooling events, as well as when there is no call for heating or cooling.

This diagnostic will look at the RTU heating and cooling commands and the outdoor-air damper’s response to varying conditions. During unoccupied periods when the controller is trying to maintain minimum or maximum space temperatures, the damper should be closed, unless the outside-air temperature is less than the return-air temperature and there is a predisposition for cooling. The same is also true during morning warm up periods and may also be true during morning cool down periods. This fault diagnostic will alert the building owner or operator of possible failure of the economizer control function.

Because there are so many possible configurations for when the damper should not be open or not be open beyond the minimum position, this diagnostic may need to run most of the time (at least during occupied periods). If natural conditions are not favorable for economizing, the outdoor-air temperatures can be temporarily changed to verify the test.

The embedded diagnostics can remain in a passive mode continuously or perform active diagnostics on demand. The *OATBias* is not set in the passive mode. In the passive mode, this diagnostic only runs when conditions are not favorable for economizing. Each diagnostic runs independently of the other diagnostics. Ideally, if a temperature sensor problem is detected, the remainder of the diagnostics should return an inconclusive result (the economizer and ventilation diagnostic rely on accurate temperature sensors to return valid diagnostic results). If a fault is detected that indicates a temperature sensor problem (AFDD2), the sensor fault should be corrected before running any other diagnostics.

Input Parameters Required for AFDD4 Fault

The RTU controller needs three temperatures, two status and three command signals (Table 9). The configuration parameters required for the diagnostics are listed in Table 10.

Table 9: Input Parameter Required for AFDD4 Fault

Description	Physical sensor location	Range
Mixed-air temperature	Mixed-air plenum	50 ~ 80°F
Outdoor-air temperature	Outdoor-air intake hood	50 ~ 100°F
Return-air temperature	Return-air plenum	50 ~ 100°F
Compressor status	-	On/Off
Fan status	-	On/Off
Heating/cooling command	-	0/1/2
Supply fan speed command	-	0 – 100%
Damper command	-	0 – 100%

Table 10: Configuration Parameters Required of AFDD4 Fault Implementation

Name	Description	Value
OAD _minimum	Minimum OAD command	20%
Threshold _damper, AFDD4	Threshold for detecting proper OAD signal	10%
Δ	Dead band associated with economizer control	1°F
Time _steadystate	Wait time for steady-state conditions	6 minutes
N _samples	Number of samples to average	5
Sampling _rate	Data sampling rate	1 minute
Err _code	Error code	See Figure 7

To check the amount of outdoor air being brought into the RTU, the *OAF* is calculated as described previously.

AFDD4 Fault Detection and Diagnostics Process

The primary goal of the AFDD4 is to validate economizer controls when the outdoor conditions are not favorable for economizing. The implementation details for AFDD4 are shown in Figure 7. During occupied periods, there are at least three conditions that should be evaluated to validate the economizer controls:

1. When there is no call for cooling or heating, the damper command should be at the minimum position.
2. When there is a call for heating, the damper command should be at the minimum position.
3. When there is a call for cooling, and the outside-air temperature is greater than the return-air temperature, the damper command should be at the minimum damper position.

These modes of operation are handled distinctively in AFDD4 as follows:

- If there is a call for cooling from the space served by the RTU and outdoor conditions are not favorable for economizing, ($OAT > RAT + \Delta$ and $OAT > 70^{\circ}F + \Delta$).

Step 1. Check the OAD command.

- If $(OAD - OAD_{\text{minimum}}) > \text{Threshold}_{\text{damper, AFDD4}}$, a fault has been detected. The OAD is significantly above the minimum value for ventilation and is potentially wasting energy.
 - **Err_code** = 41
- Otherwise, no problem is detected for this diagnostic.
 - **Err_code** = 40

Step 2. Report the diagnostic results (**Err_code**).

- If there is a call for cooling from the space served by the RTU and outdoor conditions are favorable for economizing, ($OAT < RAT - \Delta$ and $OAT < 70^{\circ}F - \Delta$).

Step 1. Send an override command to RTU controller and set the *OATBias* to simulate conditions not favorable for economizing (the RTU should close the OAD to the minimum position).

Step 2. Allow a sufficient delay so that conditions in the RTU will reach steady-state (6 minutes adjustable).

Step 3. Check the OAD command.

- If $(OAD - OAD_{\text{minimum}}) > \text{Threshold}_{\text{damper, AFDD4}}$, a fault has been detected. The OAD is significantly above the minimum value for ventilation and is potentially wasting energy.
 - **Err_code = 41**
- Otherwise, no problem is detected for this diagnostic.
 - **Err_code = 40**

Step 3. Report the diagnostic results (**Err_code**).

- If there is a no call for cooling from the space served by the RTU.

Step 1. Check the OAD command.

- If $(OAD - OAD_{\text{minimum}}) > \text{Threshold}_{\text{damper, AFDD4}}$, then a fault is detected. The OAD is significantly above the minimum value for ventilation and is potentially wasting energy.
 - **Err_code = 41**
- Otherwise, no problem is detected for this diagnostic.
 - **Err_code = 40**

Step 2. Report the diagnostic results (**Err_code**).

The causes of this fault (economizing when the RTU should not) can be mechanical failure or a control failure:

- An air-temperature sensor fault or failure. Refer to AFDD2 for more details.
- If the controls include demand control ventilation (DCV) sequences that rely on one or more CO₂ sensor(s), and if the sensors have failed or are out of calibration (reading at the high end of the sensor), this can result in the controls commanding the outside dampers to be open more than required.

Possible corrective actions include:

- Replace or calibrate the temperature sensors.
- Verify CO₂ sensors (if used with DCV sequences) are calibrated.
- Check the implemented control logic.

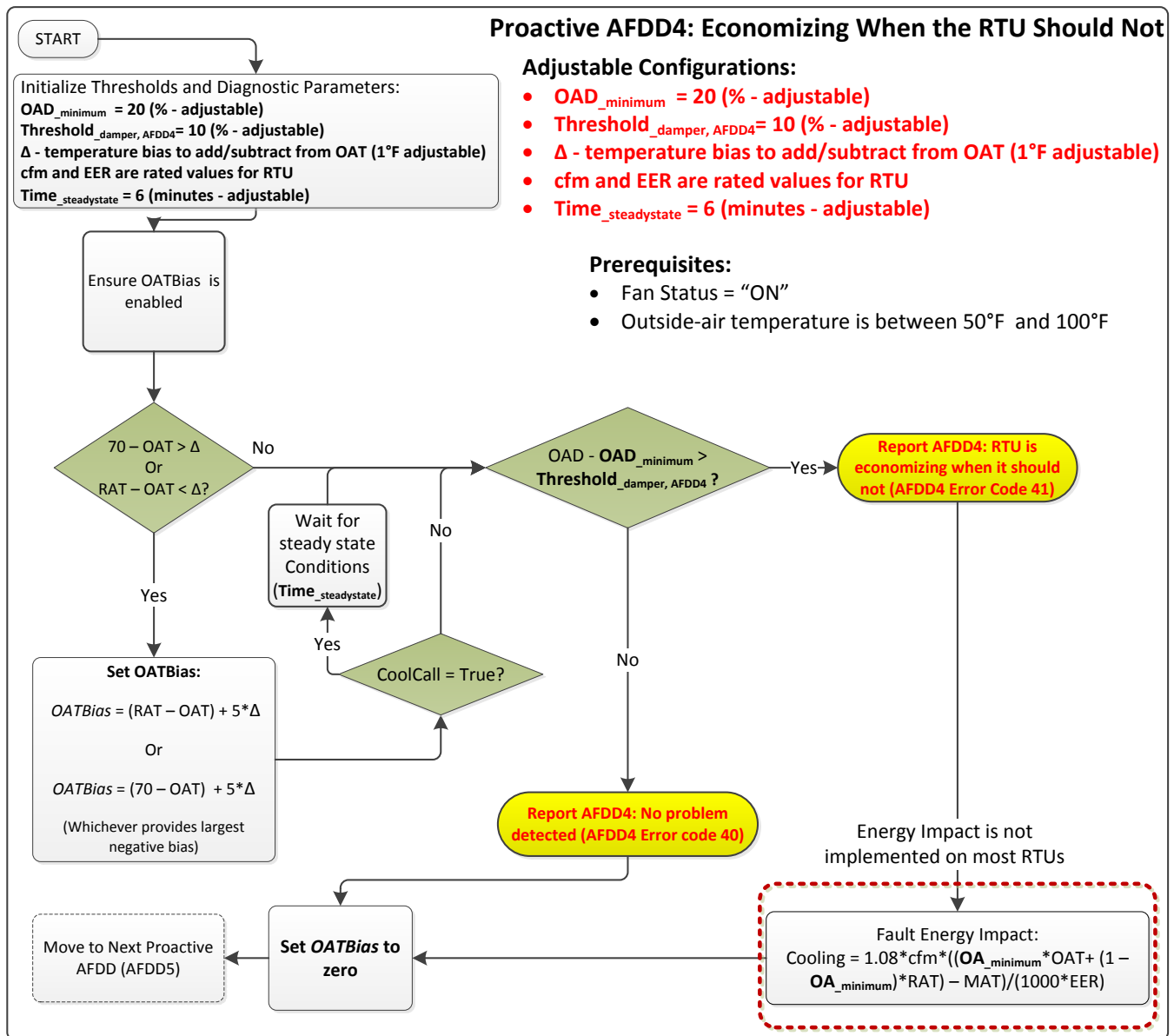


Figure 7: Detect if the RTU is Economizing When it Should Not

F. AFDD5: Detect if the RTU is Using Excess Outdoor Air

The sixth diagnostic determines if the RTU is introducing excess outdoor air beyond the minimum ventilation requirement. This diagnostic assumes that the sensors are reliable and that the damper is able to modulate (AFDD1 and AFDD2 are fault-free). Excess outdoor air, when not needed, has the potential to increase heating and/or cooling energy consumption.

This diagnostic relies on calculated outdoor air fraction (*OAF*) value, which was described previously. The accuracy of the *OAF* is less reliable when the *OAT* and the *RAT* are close to each other (within 4 to 5°F). Therefore, the diagnostic will only run when this is not the case.

The calculated *OAF* is compared to an *OAF* threshold (adjustable) to determine if excess outdoor air is being introduced into the space. If the calculated outdoor air percent ($OAF \times 100$) is **more than 25% to 50%** (user adjustable) greater than the *OAF* threshold, a fault is issued.

The embedded diagnostics can run in a passive mode continuously or perform active diagnostics on demand. The *OATBias* is not set in the passive mode. In the passive mode, this diagnostic only runs when there is a call for heating/cooling from the space served by the RTU and when the outdoor air conditions are not favorable for economizing; or when the RTU is in the ventilation mode. Ideally, if a temperature sensor problem is detected, the remainder of the diagnostics should return an inconclusive result (the other economizer and ventilation diagnostic rely on accurate temperature sensors to return valid diagnostic results). If a fault is detected that indicates a temperature sensor problem (AFDD2), the sensor fault should be corrected before attempting to run other diagnostics.

Input Parameters Required for AFDD5 Fault

The RTU controller needs three temperatures, two status and three command signals (Table 11). The configuration parameters required for this diagnostics are listed in Table 12.

Table 11: Input Parameter Required for AFDD5 Fault

Description	Physical sensor location	Range
Mixed-air temperature	Mixed-air plenum	50 ~ 80°F
Outdoor-air temperature	Outdoor-air intake hood	50 ~ 100°F
Return-air temperature	Return-air plenum	50 ~ 100°F
Compressor status	-	On/Off
Fan status	-	On/Off
Heating/cooling command	-	1/2
Supply fan speed command	-	0 – 100%
Damper command	-	0 – 100%

Table 12: Configuration Parameters Required of AFDD5 Fault Implementation

Name	Description	Value
Threshold_Temp, AFDD5	Minimum difference between <i>OAT</i> and <i>RAT</i>	4°F
OAD_minimum	Minimum <i>OAD</i> command	15%
Threshold_damper, AFDD5	Threshold to detect proper damper position	10%
OA_minimum	Minimum desired <i>OAF</i>	5%
Threshold_OAF, AFDD5	Threshold to detect proper <i>OAF</i> value	10%
Δ	Dead band associated with economizer control	1°F
Time_steadystate	Wait time for steady-state conditions	6 minutes

N_samples	Number of samples to average	5
Sampling_rate	Data sampling rate	1 minute
Err_code	Error code	See Figure 8

AFDD5 Fault Detection and Diagnostics Process

The primary goal of AFDD5 is to validate that the RTU is not bringing in excess outdoor air beyond the minimum required. The implementation details for AFDD5 are shown in Figure 8. The following conditions must be met before the fault diagnostic process can be initiated.

- The OAT is not too close to the RAT. For example, the fault diagnostics process will not be initiated if the absolute value of the difference between the OAT and RAT is not greater than **Threshold_{Temp, AFDD5}** (4 °F by default and user adjustable) as shown below:
 - $|RAT - OAT| > \text{Threshold}_{Temp, AFDD5}$ (If this condition is not met then **Err_code** = 58)

This diagnostic will check the minimum damper position setting during the following modes of operation:

1. There is a call for cooling from the space served by RTU and outdoor conditions are not favorable for economizing.
2. There is a call for cooling from the space served by the RTU and the conditions are favorable for economizing.
3. There is not a call for cooling (ventilation or heating) from the space served by the RTU.

These modes of operation are handled distinctively in AFDD5 as follows:

- If there is a call for cooling from the space served by the RTU and outdoor conditions are not favorable for economizing ($OAT > RAT + \Delta$ or $OAT > 70^{\circ}F + \Delta$):

Step 1. Check the OAD command.

- If $(OAD - OAD_{minimum}) > \text{Threshold}_{damper, AFDD5}$, a fault was detected. The OAD is significantly above the minimum set point for ventilation.
 - **Err_code** = 53
 - Proceed to the step 4.
- Otherwise, report that the OAD is commanded to the correct position, proceed to the next step.

Step 2. Calculate the *OAF* using the OAT, RAT, and MAT.

- If the *OAF* is within the expected range (*OAF* such that $OAF < 1.25$ and $OAF > 0$).
 - Proceed to step 3.

- Else if the *OAF* is outside the expected range (*OAF* such that $OAF \leq 0$ or $OAF \geq 1.25$).
 - **Err_code = 56**
 - Proceed to step 4.

Step 3. Compare the *OAF* with the pre-defined minimum outdoor-air intake ratio (**OA_{minimum}**).

- If $(OAF - OA_{minimum}) > \text{Threshold}_{OAF, AFDD5}$, a fault was detected. The OAD is commanded to the correct position for ventilation but the RTU is bringing in excess outdoor air.
 - **Err_code = 51**
- Otherwise, no problem is detected for this diagnostic.
 - **Err_code = 50**

Step 4. Report the diagnostic results (**Err_code**).

- If there is a call for cooling from the space served by the RTU and outdoor conditions are favorable for economizing ($OAT < RAT - \Delta$ or $OAT < 70^\circ\text{F} - \Delta$):

Step 1. Send an override command to RTU controller and set the *OATBias* to simulate conditions not favorable for economizing (the RTU should position the damper at the minimum position).

Step 2. Allow a sufficient delay so that conditions in the RTU will reach steady-state (6 minutes adjustable).

Step 3. Check the OAD command.

- If $(OAD - OAD_{minimum}) > \text{Threshold}_{damper, AFDD5}$, a fault was detected. The OAD is significantly above the minimum set point for ventilation.
 - **Err_code = 53**
 - Proceed to the step 6.
- Otherwise, report that the OAD is commanded to the correct position, proceed to the next step.

Step 4. Calculate the *OAF* using the OAT (true unbiased OAT), RAT, and MAT.

- If the *OAF* is within the expected range (*OAF* such that $OAF < 1.25$ and $OAF > 0$).
 - Proceed to step 5.
- Else if the *OAF* is outside the expected range (*OAF* such that $OAF \leq 0$ or $OAF \geq 1.25$).

- **Err_code** = 56
- Proceed to step 6.

Step 5. Compare the *OAF* with the pre-defined minimum outdoor-air intake ratio (**OA_{minimum}**).

- If $(OAF - OA_{minimum}) > Threshold_{OAF, AFDD5}$, a fault was detected. The OAD is commanded to the correct position for ventilation but the RTU is bringing in excess outdoor air.
 - **Err_code** = 51
- Otherwise, no problem is detected for this diagnostic.
 - **Err_code** = 50

Step 6. Set the *OATBias* to zero.

Step 7. Report the diagnostic results (**Err_code**).

- If there is no call for cooling from the space served by the RTU:

Step 1. Check the OAD command.

- If $(OAD - OAD_{minimum}) > Threshold_{damper, AFDD5}$, a fault was detected. The OAD is significantly above the minimum set point for ventilation.
 - **Err_code** = 53
 - Proceed to the step 4.
- Otherwise, the OAD is commanded to the correct position, proceed to the next step.

Step 2. Calculate the *OAF* using the OAT, RAT, and MAT.

- If the *OAF* is within the expected range (*OAF* such that $OAF < 1.25$ and $OAF > 0$).
 - Proceed to step 3.
- Else if the *OAF* is outside the expected range (*OAF* such that $OAF \leq 0$ or $OAF \geq 1.25$).
 - **Err_code** = 56
 - Proceed to step 4.

Step 3. Compare the *OAF* with the pre-defined minimum outdoor-air intake ratio (**OA_{minimum}**).

- If $(OAF - OA_{minimum}) > Threshold_{OAF, AFDD5}$, a fault was detected. The OAD is commanded to the correct position for ventilation but the RTU is bringing in excess outdoor air.

- **Err_code = 51**
 - Otherwise, no problem is detected for this diagnostic.
- **Err_code = 50**

Step 4. Report the diagnostic results (**Err_code**).

The causes of excessive outdoor-air intake can be mechanical failure or a control failure:

- The minimum OAD set point is too high. If the minimum damper position is set too high, mechanical cooling costs will increase during warm weather because of higher ventilation rates, and comfort may be compromised if this extra load exceeds available cooling capacity. Heating costs will increase during cool weather because of higher ventilation rates, and comfort may be compromised if this extra load exceeds available heating capacity.
- The OAD set to the minimum position.
- CO₂ DCV sensors are out of calibration or DCV control sequence parameters are not configured properly.

Possible corrective actions include:

- Check the outdoor-air intake requirements based on the existing occupancy. Input a reasonable minimum OAD.
- Fix the OAD if it cannot be closed to the minimum position.

G. AFDD6: Detect if the RTU is Using Insufficient Outdoor Air

The seventh and final diagnostic validates the ventilation requirements. This diagnostic assumes that the sensors are reliable and that the damper is able to modulate (AFDD1 and AFDD2 are fault-free).

Insufficient outdoor air has the potential to contribute to possible “sick building” syndrome effects, including increased levels of CO₂ gases and could also lead to potentially negative building pressurization problems, which can contribute to infiltration of unwanted dust, moisture, pollens, cold air or hot air (from other parts of the building). All of these unwanted infiltration issues can impact occupant health and in some cases the safety of the building (cold air infiltrating can freeze nearby pipes, if not adequately insulated). Moisture can contribute to the growth of molds, which is also unwanted. The intent is to ensure that ventilation air from outside is brought into the building through the RTUs outdoor-air dampers, which are designed with filtration systems, conditioning systems and moisture capture systems. If the dampers are verified to be working properly, this fault analysis will determine if there is an insufficient amount of outdoor air being introduced to the RTU’s supply-air stream.

This diagnostic will calculate the outdoor-air fraction (*OAF*), similarly to AFDD5. The accuracy of this equation is less reliable when the outside-air temperature and the return-air temperatures are within 4 to 5°F. Therefore, the diagnostic will only run when this is not the case. The calculated *OAF* is compared to a minimum *OAF* threshold to determine if insufficient ventilation air is being introduced into the space. If the difference between the calculated outdoor air percent and the minimum *OAF* is **more than 10%** (user-adjustable), a fault is issued.

The embedded diagnostics can run in a passive mode continuously or perform active diagnostics on demand. The *OATBias* is not set in the passive mode. In the passive mode, this diagnostic only runs when there is a call for heating/cooling from the space served by the RTU and conditions are not favorable for economizing or there is no call for heating/cooling from the space. Each diagnostic runs independently of the other diagnostics. Ideally, if a temperature sensor problem exists, this diagnostics will return an inconclusive result (the other economizer and ventilation diagnostic rely on accurate temperature sensors in order to return valid diagnostic results). If a fault is detected that indicates a temperature sensor problem (AFDD2) this should be corrected before other diagnostic are run.

Input Parameters Required for AFDD6 Fault

The RTU controller needs three temperatures, two status and two command signals (Table 11Table 13). The configuration parameters required for this diagnostics are listed in Table 14.

Table 13: Input Parameter Required for AFDD6 Fault

Description	Physical sensor location	Range
Mixed-air temperature	Mixed-air plenum	50 ~ 80°F
Outdoor-air temperature	Outdoor-air intake hood	50 ~ 100°F
Return-air temperature	Return-air plenum	50 ~ 100°F
Compressor status	-	On/Off
Fan status	-	On/Off
Heating/cooling command	-	0/1/2
Supply fan speed command	-	0 - 100%

Table 14: Configuration Parameters Required of AFDD6 Fault Implementation

Name	Description	Value
Threshold_Temp, AFDD6	Minimum difference between OAT and RAT	4°F
OAD_minimum	Minimum OAD command	15%
Threshold_damper, AFDD6	Threshold to detect proper damper position	15%
OA_minimum	Minimum desired OAF	5%
Threshold_OAF, AFDD6	Threshold to detect proper OAF value	10%
Δ	Dead band associated with economizer control	1°F
Time_steadystate	Wait time for steady-state conditions	6 minutes
N_samples	Number of samples to average	5
Sampling_rate	Data sampling rate	1 minute
Err_code	Error code	See Figure 9

AFDD6 Fault Detection and Diagnostics Process

The primary goal of AFDD6 is to validate the ventilation requirements. The implementation details for AFDD6 are shown in Figure 9. The following conditions must be met before the fault diagnostic process can be initiated.

- The OAT is not too close to the RAT. For example, the proactive fault diagnostics process will not be initiated if the absolute value of the difference between the OAT and RAT is not greater than **Threshold_Temp, AFDD6** (4°F by default and user adjustable) as shown below:
 - $|RAT - OAT| > \text{Threshold}_{Temp, AFDD6}$

This diagnostic will check the economizer operations during the following modes of operation:

1. There is a call for heating/cooling from the space served by RTU and outdoor conditions are not favorable for economizing.
2. There is a call for cooling from the space served by the RTU and the conditions are favorable for economizing.
3. There is not a call for heating/cooling (ventilation mode) from the space served by the RTU.

These modes of operation are handled distinctively in AFDD6 as follows:

- If there is a call for heating/cooling from the space served by the RTU and outdoor conditions are not favorable for economizing, ($OAT > RAT + \Delta$ or $OAT > 70^{\circ}F + \Delta$):

Step 1. Check the OAD command.

- If $(OAD_{\text{minimum}} - OAD) > \text{Threshold}_{\text{damper, AFDD6}}$, then a fault was detected. The OAD is significantly below the minimum set point for ventilation.
 - **Err_code = 64**
 - Proceed to the step 4.
- Otherwise, the OAD is commanded to the correct position, proceed to the next step.

Step 2. Calculate the *OAF* using the OAT, RAT, and MAT.

- If the *OAF* is within the expected range (*OAF* such that $OAF < 1.25$ and $OAF > 0$).
 - Proceed to step 3.
- Else if the *OAF* is outside the expected range (*OAF* such that $OAF \leq 0$ or $OAF \geq 1.25$).
 - **Err_code = 66**
 - Proceed to step 4.

Step 3. Compare the *OAF* with the pre-defined minimum outdoor-air intake ratio (OA_{minimum}).

- If $(OA_{\text{minimum}} - OAF) > \text{Threshold}_{\text{OAF, AFDD6}}$, then a fault was detected. The OAD is commanded to the correct position for ventilation but the RTU is bringing in insufficient outdoor air.
 - **Err_code = 61**
- Otherwise, no problem is detected for this diagnostic.
 - **Err_code = 60**

Step 4. Report the diagnostic results (**Err_code**).

- If there is a call for cooling from the space served by the RTU and outdoor conditions are favorable for economizing ($OAT < RAT - \Delta$ or $OAT < 70^{\circ}F - \Delta$):

Step 1. Send an override command to RTU controller and set the *OATBias* to simulate conditions not favorable for economizing (the RTU should open the damper fully).

Step 2. Allow a sufficient delay so that conditions in the RTU will reach steady-state (6 minutes adjustable).

Step 3. Check the OAD command.

- If $(\text{OAD}_{\text{minimum}} - \text{OAD}) > \text{Threshold}_{\text{damper, AFDD6}}$, then a problem was detected. The OAD is significantly below the minimum set point for ventilation.
 - **Err_code** = 64
 - Proceed to the step 6.
- Otherwise, the OAD is commanded to the correct position, proceed to the next step.

Step 4. Calculate the *OAF* using the OAT (true unbiased OAT), RAT, and MAT.

- If the *OAF* is within the expected range (*OAF* such that $\text{OAF} < 1.25$ and $\text{OAF} > 0$).
 - Proceed to step 5.
- Else if the *OAF* is outside the expected range (*OAF* such that $\text{OAF} \leq 0$ or $\text{OAF} \geq 1.25$).
 - **Err_code** = 66
 - Proceed to step 6.

Step 5. Compare the *OAF* with the pre-defined minimum outdoor-air intake ratio ($\text{OA}_{\text{minimum}}$).

- If $(\text{OA}_{\text{minimum}} - \text{OAF}) > \text{Threshold}_{\text{OAF, AFDD6}}$, then a problem was detected. The OAD is commanded to the correct position for ventilation but the RTU is bringing in insufficient outdoor air.
 - **Err_code** = 61
- Otherwise, no problem is detected for this diagnostic.
 - **Err_code** = 60

Step 6. Set the *OATBias* to zero.

Step 7. Report the diagnostic results (**Err_code**).

- If there is no call for heating/cooling from the space served by the RTU:

Step 1. Check the OAD command.

- If $(\text{OAD}_{\text{minimum}} - \text{OAD}) > \text{Threshold}_{\text{damper, AFDD6}}$, then a problem was detected. The OAD is significantly below the minimum set point for ventilation.

- **Err_code = 64**
- Proceed to the step 4.
- Otherwise, the OAD is commanded to the correct position, proceed to the next step.

Step 2. Calculate the *OAF* using the OAT, RAT, and MAT.

- If the *OAF* is within the expected range (*OAF* such that $OAF < 1.25$ and $OAF > 0$).
 - Proceed to step 3.
- Else if the *OAF* is outside the expected range (*OAF* such that $OAF \leq 0$ or $OAF \geq 1.25$).
 - **Err_code = 66**
 - Proceed to step 4.

Step 3. Compare the *OAF* with the pre-defined minimum outdoor-air intake ratio (**OA_{minimum}**).

- If $(\mathbf{OA}_{\text{minimum}} - OAF) > \mathbf{Threshold}_{OAF, AFDD6}$, a problem was detected. The damper is commanded to the correct position for ventilation but the RTU is bringing in insufficient outdoor air.
 - **Err_code = 61**
- Otherwise, no problem is detected for this diagnostic.
 - **Err_code = 60**

Step 4. Report the diagnostic results (**Err_code**).

The causes of insufficient outdoor-air intake can be mechanical failure or a control failure:

- The minimum outdoor-air damper set point is close to 0% open.
- The outdoor-air damper cannot be opened because of the mechanical/electrical failure.
- The static pressure in mixed-air chamber is positive.
- The intake screens and/or filters are plugged
- The return fan or powered exhaust fan cannot be overcoming the supply fan, causing more return air to spill over into the mixed-air chamber.

Possible corrective action include:

- Check the outdoor-air intake requirements based on the existing occupancy. Input a reasonable minimum outdoor-air damper position.
- Fix the outdoor-air damper, if it cannot be opened.

- Fix/replace screens or filters.
- Fix control of powered exhaust fan or return fan, if they are contributing to the problem.

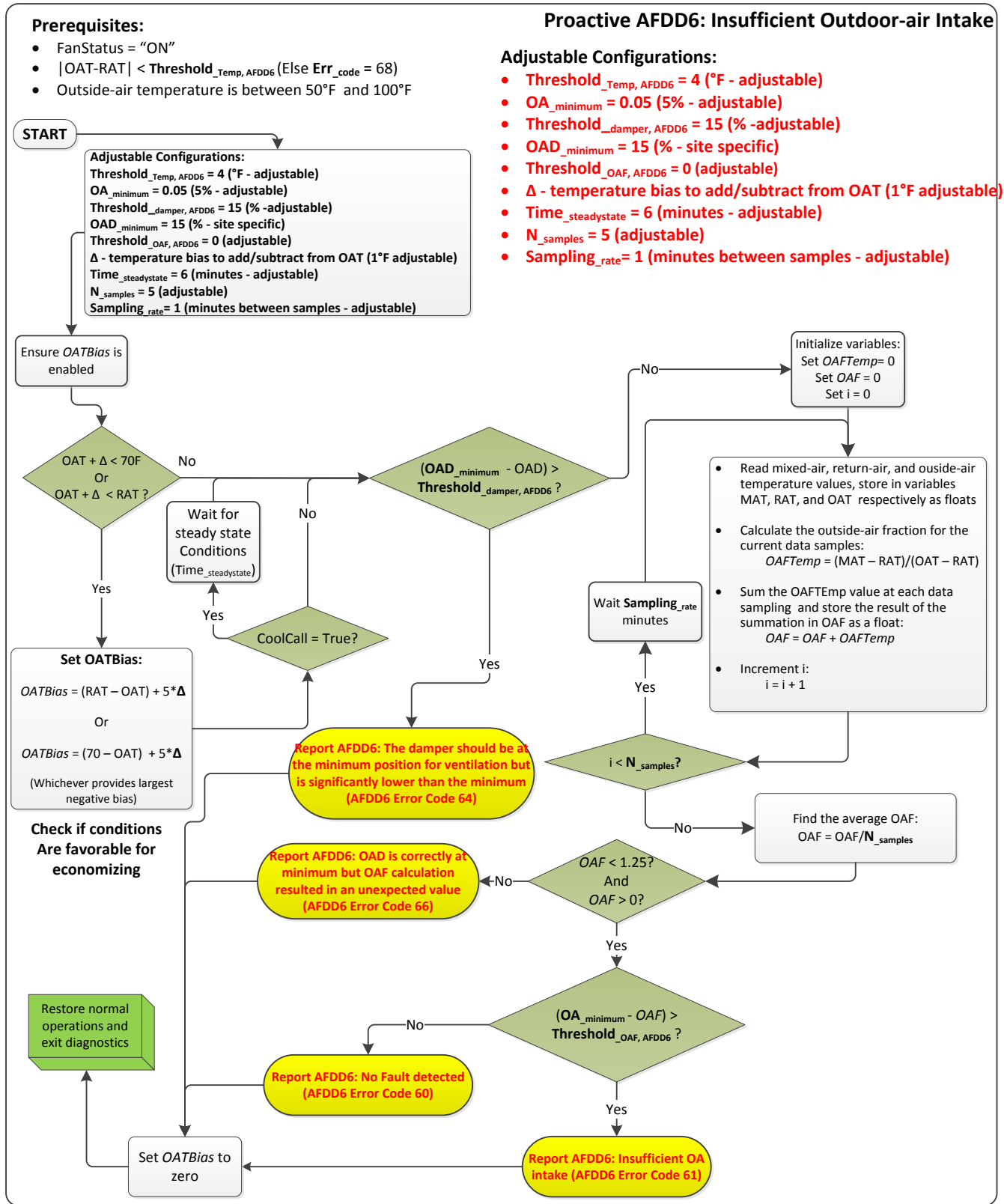


Figure 9: Insufficient Outdoor-air Intake Diagnostic

V. Development of Refrigerant-side RTU Diagnostics

This section presents the implementation details of a refrigerant-side AFDD that can be embedded on a RTU controller. The following AFDD methods are described: (1) low or high refrigerant charge, (2) condenser (outdoor coil) fouling, (3) liquid line restriction, and (4) other system fault (e.g., compressor or expansion device damage).

The AFDD methods do both detection and diagnostics in a single step, and thus no separate diagnostic classification is necessary. For fault isolation, fault detection based on decoupling models is applied to individual components (e.g., refrigerant charge, condenser, and liquid line) and isolated to choose the specific fault from the possible component faults. With the decoupling approach, it is not necessary to have a separate diagnostic classifier. Fault diagnoses results directly from fault identification when the output value from the AFDD methods deviate significantly from expected value or normal value. The output values that are generated include the cooling capacity and the energy efficiency (e.g., coefficient of performance - COP).

A. Refrigerant Charge (undercharge/overcharge) Fault Detection and Diagnostics

The purpose of this diagnostic measure is to identify and isolate refrigerant charge faults (over and under). This fault can result from improper charge by the service technician or refrigerant leak that occurs when a seal or joint within the refrigeration system is compromised and allows refrigerant to leak into the surrounding environment. Improper refrigerant charge can lead to compressor damage and a significant increase in energy consumption or reduction in system efficiency.

Kim and Braun (2012a) found that a refrigerant charge reduction of 25% led to an average energy efficiency reduction of about 15% and capacity degradation of about 20% and can lead to reduced equipment lifespan. Furthermore, refrigerant charge leakage can contribute to greenhouse effect and global warming in the long term. The other long-term impacts include additional carbon dioxide emissions from fossil-fuel power plants because of lower energy efficiency.

Despite the fact that there are slight differences between manufacturers, the typical approach currently used to verify refrigerant charge in the field involves the use of either superheat at the compressor inlet or subcooling at the condenser outlet. These approaches can only determine whether the charge is high or low, not the level of charge. To find a charge level, a technician needs to evacuate the system and weigh the removed charge. The correct amount of charge is then added to the system by weighing the charge that is added to the system. This is time-consuming and costly. In addition, the current charge verification protocols utilize compressor suction and discharge pressure to determine refrigerant saturation temperatures that are used in calculating superheat and subcooling. However, the measurement of pressures requires the installation of gauges or transducers that can lead to refrigerant leakage.

Two different models (model 1 and model 2) are used to detect the refrigerant charge level. The charge level estimated from these models is then used to detect and then diagnose the improper charge level. Model 1 is less reliable at low ambient conditions; therefore, two independent models are used to estimate the charge level. The charge levels estimated from each of the two models is compared with each other if they do not match a warning is issued. In addition, the refrigerant charge level estimated from model 2 is used to compare with a threshold to identify either undercharge or an overcharge condition. The input, the constants and the

default values used in those two models are described in the following subsection, followed by the steps required to detect and diagnose improper refrigerant charge.

Input Parameters Required for Refrigerant Charge Fault

The RTU controller needs five temperature measurements to implement the refrigerant charge fault detection (Table 15). If there are multiple refrigerant circuits, these measurements have to be repeated for each circuit as shown in Figure 10.

Table 15: Input Parameter Required to Detect and Diagnosis the Refrigerant Charge Fault

Input	Description	Physical sensor location	Range [°F]
T _{c_s}	Condenser saturation temperature	Condenser tube band	95 ~ 135
T _{e_s}	Evaporator saturation temperature	Evaporator inlet line	5 ~ 65
T _{liq}	Liquid line temperature	Condenser exit line	85 ~ 125
T _{suc}	Compressor suction temperature	Compressor suction line	0 ~ 60
T _{dis}	Compressor discharge temperature	Compressor discharge line	95 ~ 135

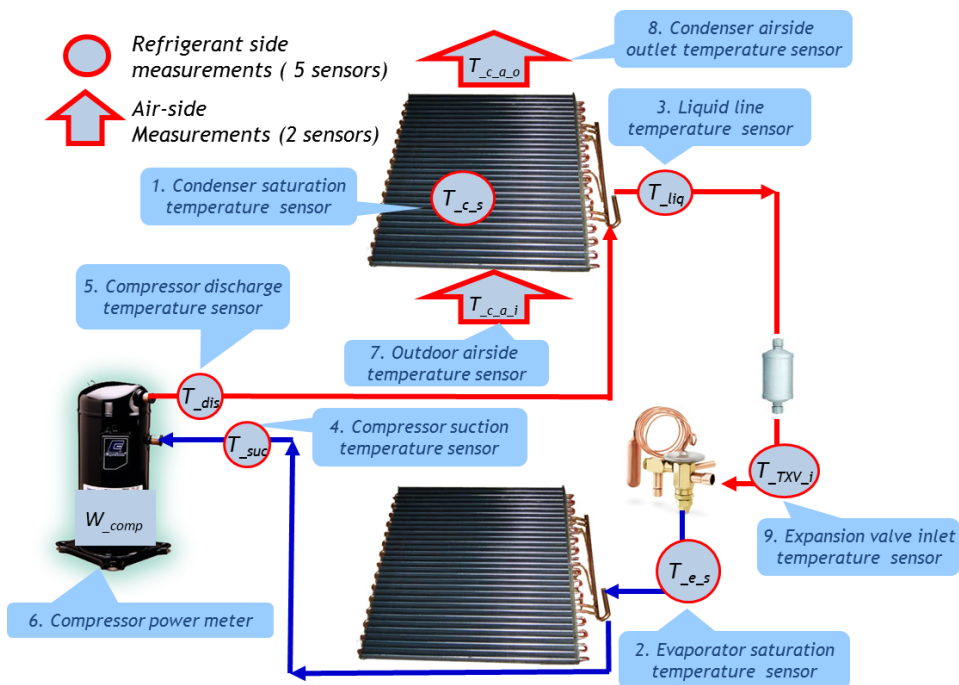


Figure 10: Temperature and Power Sensor Locations in a RTU

The location of the temperature sensors is critical for the refrigerant charge algorithms. The ideal location of the sensors is described in this section. Five temperature sensors (1. condenser saturation (T_{c_s}), 2. evaporator saturation (T_{e_s}), 3. liquid line (T_{liq}), 4. compressor suction (T_{suc}), and 5. compressor discharge (T_{dis})) are mounted on the outer surface of the refrigerant tubing and insulated by sticky foam shown in Figure 10.

The evaporator saturation temperature ($T_{e,s}$) can be measured using a surface-mounted temperature sensor located on the inlet tube to the evaporator. However, the condenser saturation temperature ($T_{c,s}$) requires that the sensor be located on a return somewhere in the middle of the coil where a two-phase condition exists under a wide variety of operating conditions. The temperature sensors should be installed at the tube bends of the condenser and evaporator inlet line and insulated to measure the saturation temperatures as shown in Figure 11.

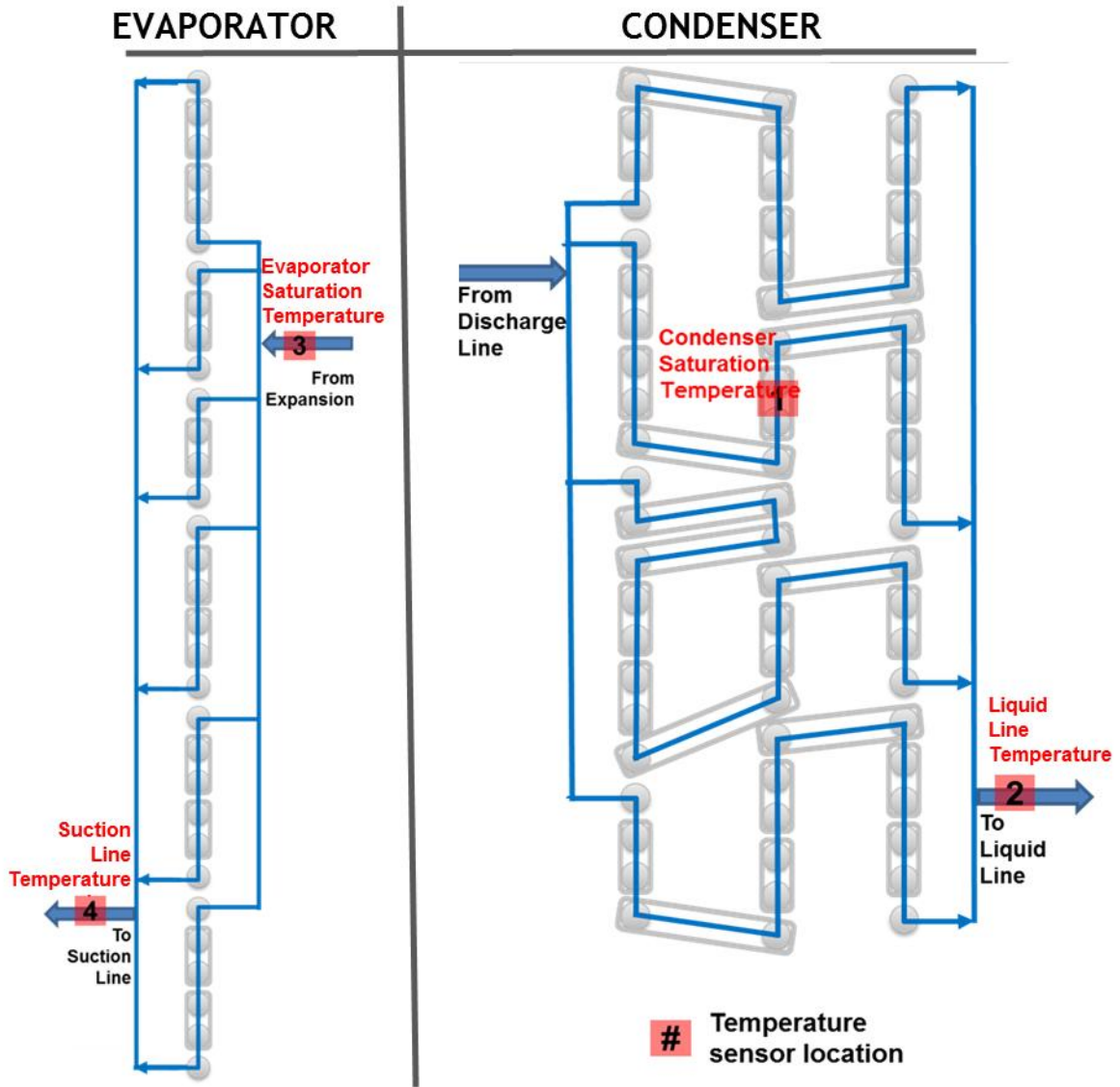


Figure 11: Saturation Temperature Sensor Locations of Condenser and Evaporator

Constant Parameters Required for Refrigerant Charge Fault

Table 16 shows three rated constant values: 1) rated subcooling ($T_{sc,r}$), 2) rated suction superheat ($T_{sh,r}$) and 3) rated discharge superheat ($T_{dsh,r}$) for the refrigerant charge model 1 and model 2. These constant are determined in the absence of faults under rated indoor and ambient conditions.

The rated conditions are not that critical as long as the values of $T_{sc,r}$, $T_{sh,r}$, and $T_{dsh,r}$ are available for the same condition and at a known refrigerant charge level. These three rated constant values can be obtained from the initial temperature measurements or from the technical data (product specification) provided by manufacturers. Table 16 shows the initial rated constant values based on data available from existing test (Kim and Braun 2012b).

Table 16: Required Constants (at rated condition) for Refrigerant Charge Fault Detection

Value	Description	Range [°F]	Initial values [°F]
$T_{sc,r}$	Subcooling	0 ~ 30	10
$T_{sh,r}$	Suction superheat	0 ~ 40	8
$T_{dsh,r}$	Discharge superheat	30 ~ 70	55

Other Constant Parameters Required for Refrigerant Charge Fault

Two constant parameters, K_{sc} and K_{sh} are required for refrigerant charge detection model 1 and three constant parameters, A_{sc} , A_{sh} and A_{dsh} for required for refrigerant charge detection model 2. Those parameters are constant regardless of RTU system capacity, component type(e.g., compressor and expansion device), heat exchanger geometry, and manufacture. The subscript ‘sc’, ‘sh’, and ‘dsh’ indicate constant characteristic related to condenser subcooling, evaporator superheat and discharge superheat of compressor. To determine those default values for these constants, the available data sets (Kim and Braun 2012b and 2012c) were used and these are shown in Table 17 and Table 30. However, these parameters can be refined using the data from the field.

Table 17: Default Constants for Refrigerant Charge Model 1

K_{sc}	K_{sh}
0.17	0.35

Table 18: Default Parameters for Refrigerant Charge Algorithm Model 2

A_{sc}	A_{sh}	A_{dsh}
0.18	0.27	0.11

Refrigerant Fault Detection and Diagnostics Process

The primary goal of the refrigerant charge fault detection and diagnostic process is to determine if the RTU circuits are improperly charged. The fault detection and diagnostics process is broken down into several steps, so it is easy to embed in a controller.

Step 1. Assign the three rated constant values, four threshold values and seven default parameters to constant values.

(1-1) Three rated constant values: (1) $T_{sh,r}$, (2) $T_{sc,r}$, and (3) $T_{dsh,r}$ (Table 16).

(1-2) Seven default parameters: (4) K_{sc} and (5) K_{sh} (Table 17) for model 1, (6) A_{sc} , (7) A_{sh} , and (8) A_{dsh} (Table 18) for model 2, and (9) $Time_{st}$ and (10) n .

(1-3) Four threshold values: (11) Th_{sd} , (12) Th_{pa} , (13) $Th_{u,ch}$, and (14) $Th_{o,ch}$.

Step 2. Assign the five temperature measurements from the corresponding input channels from the controller.

The controller assigns in real-time five temperature measurements to corresponding input variables from the five temperature sensors ((1) condenser saturation [$T_{c,s}$], (2) evaporator saturation [$T_{e,s}$], (3) liquid line [T_{liq}], (4) compressor suction [T_{suc}], and (5) compressor discharge [T_{dis}]).

Step 3. Calculate T_{sc} , T_{sh} , and T_{dsh} .

Calculate the three derived input values using five surface-mounted temperature sensors from step 2. Once five temperature measurements are collected, the measured temperatures are used to calculate the three derived inputs, as shown in Table 19.

(3-1) Subcooling (T_{sc}) = $T_{c,s} - T_{liq}$.

(3-2) Suction superheat (T_{sh}) = $T_{suc} - T_{e,s}$.

(3-3) Discharge-superheat (T_{dsh}) = $T_{dis} - T_{e,s}$.

Table 19: Input for Model 1 and Model 2

Value	Description	Calculation	Range [°F]
T_{sc}	Subcooling	= $T_{c,s} - T_{liq}$	0 ~ 30
T_{sh}	Suction superheat	= $T_{suc} - T_{e,s}$	0 ~ 40
T_{dsh}	Discharge superheat	= $T_{dis} - T_{e,s}$	30 ~ 70

Step 4. Filter out the transient data using the steady-state detection process.

The refrigerant charge algorithm is based on the steady-state operating conditions. Therefore, the steady-state detection filter is needed to remove the transient data. The steady-state filter uses the standard deviation (SD) about the mean value of suction superheat (T_{sh}) as a basis to detect the steady-state condition. The SD is calculated using the equation (1).

$$SD = \sqrt{\frac{1}{n} \sum_{i=0}^{n-1} \left((T_{sh})_{t-i\delta} - \frac{1}{n} \sum_{i=0}^{n-1} ((T_{sh})_{t-i\delta}) \right)^2} \quad (1)$$

where n is the number of data points, t is the time of last reading. The time between readings is called the sampling intervals, δ ($\delta=10$ sec as default value).

Figure 12 shows the fixed-length sliding window of suction superheat (T_{sh}). The current time limit (**Time_{st}**) for steady-state condition is determined when seven sampling interval are taken. Initially, the predefined current time limit was set to 70 seconds (**Time_{st}** = 10 sec × 7) as default value, which will result in data point (n) of 8.

After the RTU system starting time (t_s) has reached ($t_s = 7$ minutes after system startup, which can be adjusted), the steady-state detector will confirm that the conditions are at steady-state or discard the measurement readings, as shown in Table 20. The threshold (**Th_{sd}**) for standard deviation (SD) about suction superheat (T_{sh}) were determined as 1.0.

A small threshold leads to more stable states, but less input data for refrigerant charge. On the other hand, large thresholds increase the uncertainty of the refrigerant charge prediction. Therefore, it is necessary to find thresholds (**Th_{sd}**) that minimize the uncertainty of the refrigerant charge prediction while maximizing the use of input data.

Table 20: State Condition after Steady-state Detection Process

State	Condition	Action
Steady-state	$SD < (\mathbf{Th}_{sd} = 1.0 \text{ as default value})$	Go to step 5
Unsteady-state (Dischard data)	$SD > (\mathbf{Th}_{sd} = 1.0 \text{ as default value})$	Go to step 2

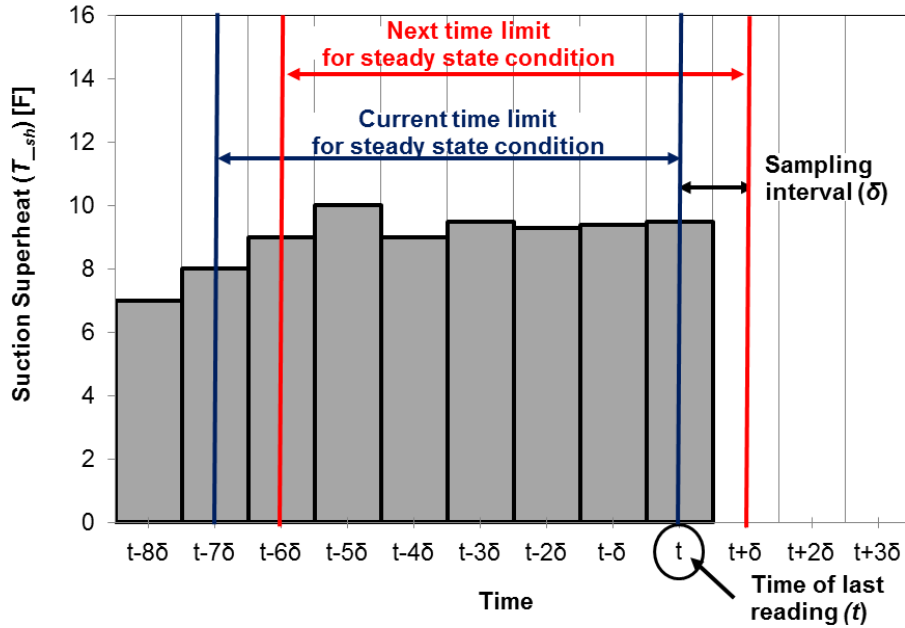


Figure 12: Fixed-length Sliding Window of Suction Superheat

Step 5. Calculate the refrigerant charge algorithm using model 1 (m_{r_ch1}).

The refrigerant charge algorithm uses: 1) three input measurements from Table 19, 2) rated constant values from Table 16, and 3) default constant parameters from Table 17. The refrigerant charge algorithm displays the current refrigerant charge level (m_{r_ch1}) at steady-state.

Refrigerant charge model 1 estimates the refrigerant charge level in terms of superheat and subcooling (T_{sh} and T_{sc}) as shown in Equation 2. The refrigerant charge level can be obtained by using two rated constant values (\mathbf{T}_{sh_r} and \mathbf{T}_{sc_r}) and two default parameters (\mathbf{K}_{sc} and \mathbf{K}_{sh}). The refrigerant charge level (m_{r_ch1}) is expressed as

$$m_{r_ch1} [\%] = \left(1 + \frac{\mathbf{K}_{sc}}{\mathbf{T}_{sc_r}} \cdot ((T_{sc} - \mathbf{T}_{sc_r}) - \mathbf{K}_{sh}(T_{sh} - \mathbf{T}_{sh_r})) \right) \times 100 \quad (2)$$

Step 6. Calculate refrigerant charge using model 2 (m_{r_ch2}).

The refrigerant charge algorithm uses: 1) three input measurements from Table 19, 2) rated constant values from Table 16, and 3) default parameters from Table 18.

Under low ambient temperature, the superheat (T_{sh}) and subcooling (T_{sc}) are almost zero. In these cases, model 1 cannot predict the accurate refrigerant charge level (m_{r_ch1}). Therefore, a refrigerant charge model 2 was developed to provide improved refrigerant charge level in these situations.

The refrigerant charge algorithm model 2 is a modification of the Equation 2 that includes a correlation for refrigerant charge in terms of the discharge superheat (T_{dsh}). The refrigerant charge level can be obtained by using three default parameters (A_{sc} , A_{sh} , and A_{dsh}) and three rated constant values (T_{sh_r} , T_{sc_r} , and T_{dsh_r}). The refrigerant charge level (m_{r_ch2}) is expressed as

$$m_{r_ch2} [\%] = \left(1 + \frac{A_{sc}}{T_{sc_r}} \cdot ((T_{sc} - T_{sc_r}) - A_{sh}(T_{sh} - T_{sh_r}) + A_{dsh}(T_{dsh} - T_{dsh_r})) \right) \times 100 \quad (3)$$

Step 7. Compare the difference between model 1 and model 2 with threshold (Th_{pa}), as shown Table 21. If the difference of charge level estimates from model 1 and 2 is less than the threshold, no action is needed. However, if the difference is greater than the threshold, a warning is issued (Wan_{c_p}). The recommended default value for the threshold (Th_{pa}) is 30%.

Table 21: Warning Condition for Default Parameters

State	Condition	Action
Normal	$ m_{r_ch1} - m_{r_ch2} < Th_{pa}$	No action is needed.
Parameter Warning	$ m_{r_ch1} - m_{r_ch2} \geq Th_{pa}$	Display Wan_{c_p}

Step 8. Compare m_{r_ch2} with the threshold ($Th_{u_ch} = 70\%$) for refrigerant undercharge fault (Error code: Err_{u_c}).

This step is used to determine if a refrigerant undercharge fault is present. The recommended default value for the threshold (Th_{u_ch}) for the refrigerant undercharge fault is 70% (Kim and Braun 2012b). The m_{r_ch2} is compared to Th_{u_ch} to identify whether a refrigerant undercharge fault is present as shown in Table 22.

Refrigerant undercharge fault is identified if m_{r_ch2} is lower than Th_{u_ch} and an error code is issued (Error code: Err_{u_c}). When a refrigerant undercharge fault is reported, the controller can also provide the refrigerant charge level (m_{r_ch2}) so the technician can add the correct amount of additional refrigerant charge to the RTU.

Table 22: Fault Condition for Refrigerant Charge Fault

State detection	Fault condition	Action
Refrigerant undercharge	$m_{r_ch2} \leq Th_{u_ch}$	Undercharge error (Error code: Err_{u_c})
No undercharge fault	$m_{r_ch2} > Th_{u_ch}$	Go to step 9.

Step 9. Compare m_{r_ch2} with the threshold ($Th_{o_ch} = 140\%$) for refrigerant overcharge fault (Error code: Err_{o_c}).

This step is used to determine if a refrigerant overcharge fault is present. The recommended default value for the threshold (Th_{o_ch}) is 140% (Kim and Braun 2012b). The value m_{r_ch2} is compared to Th_{o_ch} to identify if the refrigerant overcharge fault is present as shown in Table 23.

Refrigerant overcharge fault is identified if the refrigerant charge level is greater than Th_{o_ch} . When a refrigerant overcharge fault is reported, the controller can also provide the refrigerant charge level (m_{r_ch2}) so the technician can remove the correct amount of refrigerant charge to the RTU.

Table 23: Fault Condition for Refrigerant Charge Fault

State detection	Fault condition	Action
Normal (No fault)	$m_{r_ch2} < Th_{o_ch}$	No action is needed.
Refrigerant overcharge	$m_{r_ch2} \geq Th_{o_ch}$	Overcharge error (Error code: Err_{o_c})

The refrigerant charge approach presented in this section is better than most existing charge checking methods because it indicates the charging amount and not just whether the charge is high or low. Kim and Braun (2012a) developed this approach and showed that it is independent of the other faults. With the decoupling approach, it is not necessary to have a separate diagnostic classifier. The implementation details are shown in form of a flow chart in Figure 13.

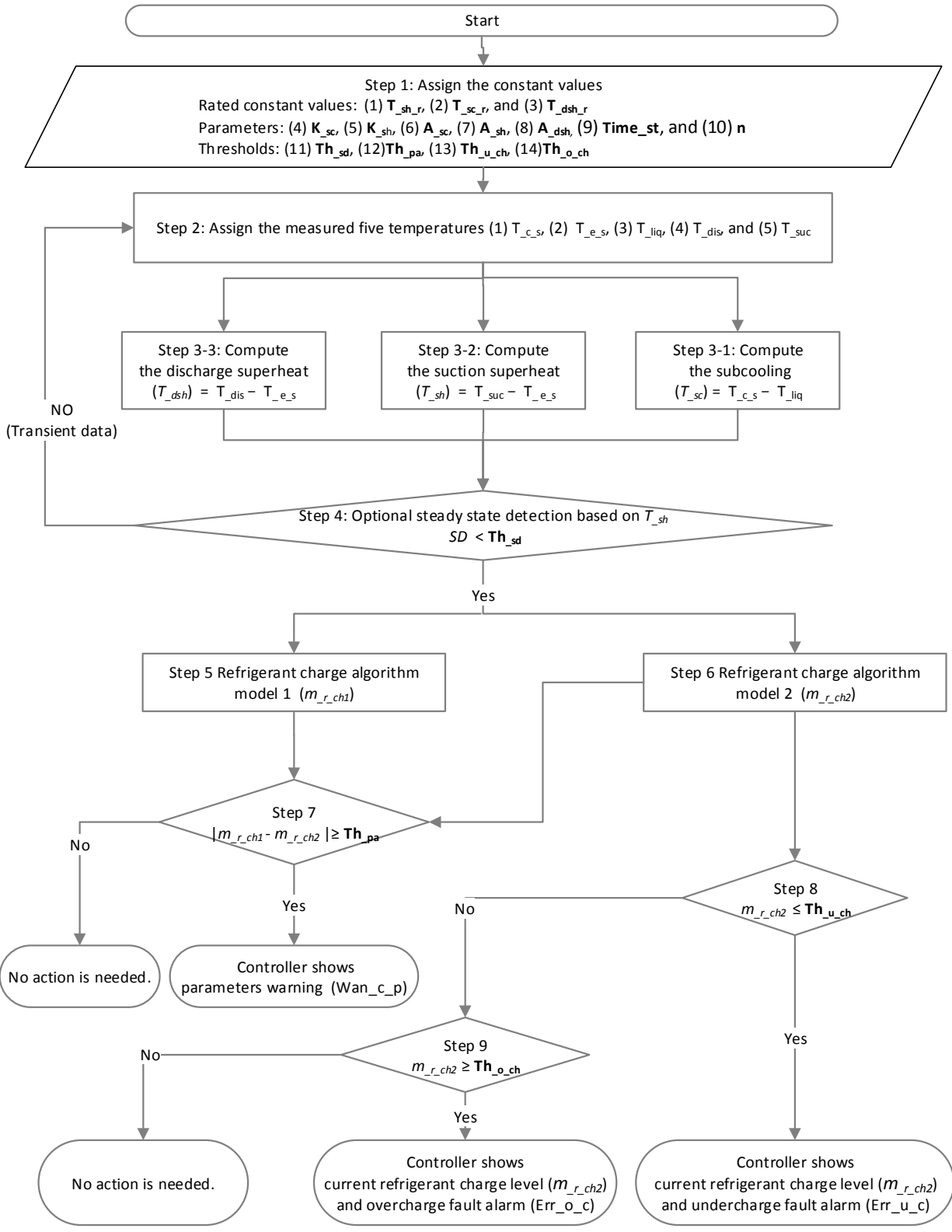


Figure 13: Implementation Details of Detect Improper Refrigerant Charge

B. Methodology to Estimate the Fault Impact

Once the fault is detected and the cause of the fault is identified, proper action should follow to correct the problem, adapt the control, or flag it for continued monitoring. The estimation of fault impact is useful information for diagnosing the severity of a fault before deciding if service is needed. To evaluate the impact of fault on performance, capacity and loss of energy efficiency are calculated and compared to expected reference values. In addition, this information can be used in real-time monitoring to support condition-based maintenance.

Input Parameters Required for Estimating the Fault Impact

The RTU controller needs five temperature measurements and compressor power to estimate the fault impact (Table 24). If there are multiple refrigerant circuits, these measurements have to be repeated for each circuit, as shown in Figure 10.

Table 24: Inputs Required for Estimating Fault Impact

Value	Description	Physical sensor location	Range [°F]/Btu/min
T _{c_s}	Condenser saturation temperature	Condenser tube band	95 ~ 135
T _{e_s}	Evaporator saturation temperature	Evaporator inlet line	5 ~ 65
T _{liq}	Liquid line temperature	Condenser exit line	90 ~ 130
T _{suc}	Compressor suction temperature	Compressor suction line	0 ~ 60
T _{dis}	Compressor discharge temperature	Compressor discharge line	95 ~ 135
W _{comp}	Compressor input power	Compressor input wire	>0

The condensing and evaporating saturated pressure can be estimated using the saturation temperature measurements and refrigerant saturated lookup table. The saturation lookup table of refrigerant R410A and R22 are shown in Appendix . The refrigerant saturated pressure can be calculated by a linear interpolation method. The linear interpolation is a method of calculating new data point, $P(T)$ within the range of a discrete set of known data points as shown in Equation 4. Because T is midway between T_a and T_b , the linear interpolation method takes two values, $P_a(T_a)$ and $P_b(T_b)$ in the lookup table.

$$P(T) = P_a + (P_b - P_a) \cdot \left(\frac{T - T_a}{T_b - T_a} \right) \quad (4)$$

For example, the R410A refrigerant saturation pressure $P(T=109.5^\circ F)$ can be obtained between $P(T=108^\circ F) = 369.7 \text{ psia}$ and $P(T=110^\circ F) = 379.6 \text{ psia}$, which yields 377.42 psia .

$$P(109.5^\circ F) = P(108^\circ F) + (P(110^\circ F) - P(108^\circ F)) \cdot \frac{(109.5 - 108)[F]}{(110 - 108)[F]} = 377.42 \text{ (psia)}$$

The next step is to calculate superheated vapor enthalpy of the refrigerant. The compressor discharge enthalpy and suction enthalpy can be estimated using the refrigerant saturation pressure, temperature measurement, and refrigerant superheated vapor enthalpy lookup table. The linear interpolation method takes two enthalpy points in superheated lookup tables of refrigerant R410A and R22 in Appendix .

As stated earlier, the linear interpolation is a method of calculating new data point $h(T, P)$ within the range of a discrete set of two known data points, as shown in Equation 5. The linear interpolation method takes two values ($h_a[T_a, P_a]$ and $h_b[T_b, P_a]$) from the lookup table. To estimate a new enthalpy $h(T, P)$, use the enthalpy value at pressure that is closest to P and then interpolate for the difference in temperatures. If P is closer to P_a then the new enthalpy will be estimated as follows:

$$h(T, P) = h(T, P_a) = h_a + (h_b - h_a) \cdot \left(\frac{T - T_a}{T_b - T_a} \right) \quad (5)$$

For example, the R410A refrigerant enthalpy at compressor discharge (h) at $P = 377.4 \text{ psig}$ and $T = 167.7 \text{ }^\circ\text{F}$ can be obtained using the lookup table where $h(370 \text{ psig}, 150^\circ\text{F}) = 138.2 \text{ Btu/lb}$ and $h(370 \text{ psig}, 180^\circ\text{F}) = 147.3 \text{ Btu/lb}$, which yields 143.56 Btu/lb .

$$h(167.7 \text{ }^\circ\text{F}, 377.4 \text{ psig}) = 138.2 + (147.3 - 138.2) \cdot \frac{(167.77 - 150)[^\circ\text{F}]}{(180 - 150)[^\circ\text{F}]} = 143.56 \text{ [Btu/lb]}$$

Similarly, refrigerant liquid line enthalpy can be estimated using the refrigerant saturated lookup table and liquid line temperature measurement. Because T is between T_a and T_b , the linear interpolation method takes two values ($h_a(T_a)$ and $h_b(T_b)$) from the lookup table to estimate the new enthalpy, as shown in the equation below. For example, the R410A discharge refrigerant enthalpy (h) at $T = 102.74^\circ\text{F}$ can be obtained between $h(102^\circ\text{F}) = 47.08 \text{ Btu/lb}$ and $h(104^\circ\text{F}) = 48.02 \text{ Btu/lb}$, which yields 47.43 Btu/lb .

$$h(102.74^\circ\text{F}) = 47.08 + (48.02 - 47.08) \cdot \frac{(102.74 - 102)[^\circ\text{F}]}{(104 - 102)[^\circ\text{F}]} = 47.43 \text{ Btu/lb}$$

The enthalpy (h_{dis}) at the compressor discharge, enthalpy (h_{suc}) at the compressor suction, and liquid line enthalpy (h_{liq}) can be calculated using the look table for the relevant refrigerant type (R410A, $\text{Ref}_{tp} = 1$ or R22, $\text{Ref}_{tp} = 0$) and five temperature measurements. Table 25 summarizes the inputs and calculated inputs necessary to estimate the three enthalpies.

Table 25: List of Inputs and Calculated Inputs Necessary for Estimating Enthalpies for Fault Impact

Value	Description	Input	Calculated Input	Range[Btu/lb]
h_{dis}	Compressor discharge enthalpy	T_{c_s} and T_{dis}	P_{c_s}	100 ~ 300
h_{suc}	Compressor suction enthalpy	T_{e_s} and T_{suc}	P_{e_s}	100 ~ 300
h_{liq}	Liquid line enthalpy	T_{liq}		0 ~ 200

Refrigerant mass flow rate is an important parameter for monitoring equipment performance and enabling fault detection and diagnostics. However, a traditional mass flow meter is expensive and difficult to install on RTU circuits. An alternative approach is to use an energy balance on the compressor to estimate refrigerant mass

flow rate (m_{ref_2}) as shown in Equation 6. The method provides refrigerant flow estimates based on the compressor power consumption (W_{comp}).

$$m_{ref_2} [lb/sec] = \frac{W_{comp} \cdot 0.95}{h_{dis}(T_{dis}, P_{c_s}) - h_{suc}(T_{suc}, P_{e_s})} \quad (6)$$

Estimating the Fault Impact

In this section, the process used to estimate the capacity and energy efficiency in real-time is broken down into several steps, so it is easy to implement in the RTU controller.

Step 1. Assign the constant values.

The assign the two rated constant values, three threshold values and refrigerant type.

(1-1) Two rated constant values: 1) **Q_{ref_r}** and 2) **COP_r**.

(1-2) Three default parameters: 3) **Ref_{tp}**, 4) **Time_{st}**, and 5) **n**.

(1-3) Three threshold values: 6) **Th_{sd}**, 7) **Th_{cp}**, and 8) **Th_{cop}**.

Step 2. Assign the compressor power measurements (W_{comp}).

The power meter provides the compressor power consumption (W_{comp}), as shown in Figure 10.

Step 3. Assign the five temperature measurements to the relevant variables: 1) T_{c_s} , 2) T_{e_s} , 3) T_{liq} , 4) T_{suc} , and 5) T_{dis} .

The controller assigns five temperature measurements from the corresponding input channels.

Step 4. Calculate T_{sc} , T_{sh} , and T_{dsh} .

Calculate the three derived input values using five surface-mounted temperature sensors from step 3. Once five temperature measurements are collected, the measured temperatures are used to calculate the three derived inputs.

(4-1) Subcooling (T_{sc}) = $T_{c_s} - T_{liq}$.

(4-2) Suction superheat (T_{sh}) = $T_{suc} - T_{e_s}$.

(4-3) Discharge-superheat (T_{dsh}) = $T_{dis} - T_{e_s}$.

Step 5. Filter out the transient data using the steady-state detection process.

The fault impact estimates are only reliable when the system is in the steady-state operating condition. Therefore, the steady-state detection filter is used to remove the transient data using the standard

deviation (SD) about T_{sh} as a basis as shown Equation 1. The state conditions after the steady-state detection process is complete are outlined in Table 26.

Table 26: State Condition after Steady-state Detection Process

State	Condition	Action
Steady-state	$SD < (Th_{sd} = 1.0 \text{ as default value})$	Go to step 6
Unsteady-state (Dischard data)	$SD > (Th_{sd} = 1.0 \text{ as default value})$	Go to step 2

Step 6. Read refrigerant enthalpy lookup table based on refrigerant type (**Ref_tp**).

The controller reads the enthalpy lookup table (Appendix) based on **Ref_tp**.

(6-1) R410A: **Ref_tp** = 1

(6-2) R22: **Ref_tp** = 0

Step 7. Calculate P_{c_s} and P_{e_s} .

The controller calculates the condenser saturation pressure (P_{c_s}) and evaporator saturation pressure (P_{e_s}) based on saturation lookup table, temperature measurements (T_{c_s} and T_{e_s}) and **Ref_tp**.

Step 8. Calculate the three enthalpies (h_{dis} , h_{suc} and h_{liq}).

The controller calculates two superheated vapor enthalpies (h_{dis} and h_{suc}) based on the superheated lookup table and four temperature measurements (T_{c_s} , T_{e_s} , T_{suc} , and T_{dis}) and liquid line enthalpy (h_{liq}) based on the saturation lookup table and liquid line temperature measurement (T_{liq}).

Step 9. Calculate the refrigerant mass flow rate (m_{ref_2}).

The refrigerant mass flow rate (m_{ref_2}) is estimated based on the h_{dis} , h_{suc} and W_{comp} , as shown in Equation 6.

Step 10. Calculate system capacity (Q_{ref}).

The capacity (Q_{ref}) is calculated based on m_{ref_2} with h_{suc} and h_{liq} , shown in Equations 7.

$$Q_{ref} [Btu / sec] = m_{ref_2} \cdot (h_{suc}(P_{e_s}, T_{suc}) - h_{liq}(T_{liq})) \quad (7)$$

Step 11. Compare difference between Q_{ref} and Q_{ref_r} with Th_{cp} to flag capacity degradation (Error code: ERR_{cap}).

The rated system capacity (Q_{ref_r} , Btu/sec) can be obtained from the manufacturer data or rated test data. If the actual capacity is severely degraded, then it warrants a visit from the technician to correct the fault.

If the percent difference between Q_{ref} and Q_{ref_r} is within threshold ($Th_{cp} = 40\%$), then no action is need. However, if the difference exceeds the threshold, it is flagged as an error and a technician visit is recommended (Table 27).

Table 27: Rules to Flag Capacity Degradation

State	Condition	Action
Normal	$\frac{(Q_{ref} - Q_{ref_r})}{Q_{ref_r}} \cdot 100 < (Th_{cp} = 40\%)$	Normal operation
Capacity degradation fault	$\frac{(Q_{ref} - Q_{ref_r})}{Q_{ref_r}} \cdot 100 \geq (Th_{cp} = 40\%)$	Display the capacity degradation fault (Error code: ERR_{cap})

Step 12. Calculate system energy efficiency (COP_{ref}).

The energy efficiency (COP_{ref}) is calculated based on Q_{ref} and W_{comp} , shown in Equation 8.

$$COP_{ref} = \frac{Q_{ref}}{W_{comp}} \quad (8)$$

Step 13. Compare difference between COP_{ref} and its COP_r with Th_{cop} to flag energy efficiency degradation (Error code: ERR_{cap}).

The rated system energy efficiency (COP_r) can be also obtained from the manufacturer data or rated test data. If the difference between COP_{ref} and its COP_r is within efficiency threshold ($Th_{cop}=40\%$), no action is recommended. However, if the difference is greater than the threshold, it is flagged as an error and a technician visit is recommended (Table 28).

Table 28: Rules to Flag Energy Efficiency Degradation

State	Condition	Action
Normal	$\frac{(COP_{ref} - COP_r)}{COP_r} \cdot 100 < (Th_{cop} = 40\%)$	Normal operation
Energy efficiency degradation fault	$\frac{(COP_{ref} - COP_r)}{COP_r} \cdot 100 \geq (Th_{cop} = 40\%)$	Display the efficiency degradation fault (Error code: ERR_{cop})

The current approach based on an energy balance model has the limitation of not being valid when subcooling (T_{sc}) at the outlet of the condenser is zero. This condition is typically associated with low refrigerant charge (m_{rch2}), which can be diagnosed using the refrigerant charge algorithm model 2. The implementation detail of the fault impact process is shown as a flow chart in Figure 14.

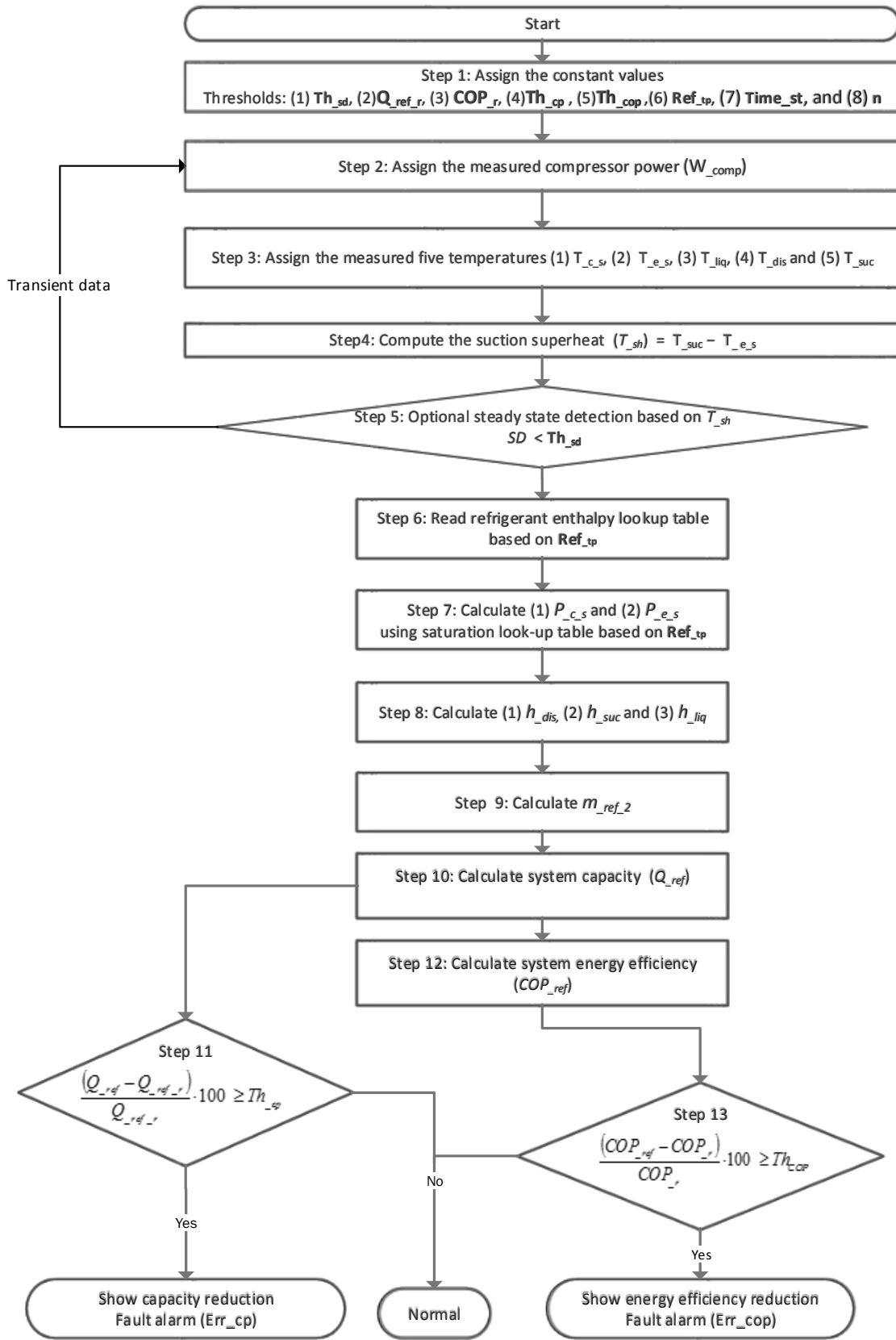


Figure 14: Fault Impact Estimation Process

C. Condenser Fouling Fault Detection

The purpose of this diagnostic measure is to identify and isolate condenser fouling. Fouling of air-side heat exchanger (e.g., the deposit of dust and other particulate matter) increases system pressure drop, decreases heat transfer rate and, correspondingly, decreases system air flow and RTU performance. The condenser can become dirty if it is not periodically cleaned, inhibiting heat transfer from the refrigerant-side to the air-side. Sometimes, the outdoor air flow may also decrease because of a defective fan motor. Based on a survey and analysis of 215 RTU (New Buildings Institute 2003), 39% of the units had very low condenser air flow rate. The average flow rate of all systems was about 20% less than the rated value. This study reported that reduced air flow increased annual cooling energy by about 9%.

The air flow measurements are generally very expensive and unreliable for application in the field. The air flow rates can be estimated using energy balances between air-side and refrigerant-side on the condenser.

Input Parameters Required for Condenser fouling Fault

The RTU controller needs five temperature measurements and the compressor power listed in Table 24 to implement the condenser fouling fault. In addition to the five temperatures, two additional air-side temperatures are also needed (Table 29). If there are multiple refrigerant circuits, these measurements have to be repeated for each circuit as shown in Figure 10, with the exception to the two temperatures listed in Table 29.

Table 29: Input Parameter Required for Condenser Fouling Fault

Value	Description	Physical sensor location	Range (°F)
T_c_a_i	Ambient temperature	Ambient	50 ~ 110
T_c_a_o	Condenser air-side outlet temperature	Condenser air-side outlet	70 ~ 130

The condensing and evaporating saturation pressure can be estimated using the saturation temperature measurements and refrigerant saturated lookup table, as described previously (Methodology to Estimate the Fault Impact). Next, the superheated vapor enthalpy and the liquid line enthalpy of the refrigerant can also be calculated as described previously (Methodology to Estimate the Fault Impact). The mass flow rate (m_{ref_2}) of the refrigerant can be estimated using the Equation 66666. That method estimates the refrigerant flow based on the compressor power consumption (W_{comp}) and suction and discharge refrigerant enthalpies.

Condenser Fouling Fault Detection and Diagnostics Process

The primary goal of the condenser fouling fault detection and diagnostic process is to determine if the condenser is fouled. The fault detection and diagnostics process is broken down into several steps, so it is easy to embed in a controller.

Step 1. Assign one rated constant value, three default parameters to constant values and two thresholds.

(1-1) Rated constant values: (1) V_{a_r} .

(1-2) Three default parameters: (2) Ref_{tp} , (3) $Time_{st}$, and (4) n .

(1-3) Two threshold values: (5) Th_{sd} and (6) Th_{cond} .

Step 2. Assign the compressor power measurements (W_{comp}) from the corresponding input channel.

The controller assigns in real-time the power consumption of the compressor (W_{comp}).

Step 3. Assign the seven temperature measurements from the corresponding input channels from the controller.

The controller assigns in real-time the seven temperature measurements to corresponding input variables (condenser saturation [T_{c_s}], evaporator saturation [T_{e_s}], liquid line [T_{liq}], compressor suction [T_{suc}], compressor discharge [T_{dis}], ambient temperature [$T_{c_a_i}$] and condenser air-side outlet temperature [$T_{c_a_o}$]).

Step 4. Calculate T_{sc} , T_{sh} , and T_{dsh} .

Calculate the three derived input values using five surface-mounted temperature sensors from step 2. Once five temperature measurements are collected, the measured temperatures are used to calculate the three derived inputs.

(3-1) Subcooling (T_{sc}) = $T_{c_s} - T_{liq}$.

(3-2) Suction superheat (T_{sh}) = $T_{suc} - T_{e_s}$.

(3-3) Discharge-superheat (T_{dsh}) = $T_{dis} - T_{e_s}$.

Step 5. Filter out the transient data using the steady-state detection process.

The fault impact estimates are only reliable when the system is in the steady-state operating condition. Therefore, the steady-state detection filter is used to remove the transient data using the standard deviation (SD) about T_{sh} as a basis as shown Equation 1. The state conditions after steady-state detection process is complete are outlined in Table 30.

Table 30: State Condition after Steady-state Detection Process is Complete

State	Condition	Action
Steady-state	$SD < (Th_{sd} = 1.0 \text{ as default value})$	Go to step 6
Unsteady-state (discard data)	$SD > (Th_{sd} = 1.0 \text{ as default value})$	Go to step 2

Step 6. Read refrigerant enthalpy lookup table based on refrigerant type (**Ref_tp**).

The controller reads the enthalpy lookup table (Appendix A) based on **Ref_tp**.

(6-1) R410A: **Ref_tp** = 1

(6-2) R22: **Ref_tp** = 0

Step 7. Calculate P_{c_s} and P_{e_s}

The controller calculates the condenser saturation pressure (P_{c_s}) and evaporator saturation pressure (P_{e_s}) based on saturation lookup table, temperature measurements (T_{c_s} and T_{e_s}) and **Ref_tp**.

Step 8. Calculate the three enthalpies (h_{dis} , h_{suc} and h_{liq}).

The controller calculates two superheated vapor enthalpies (h_{dis} and h_{suc}) based on the superheated lookup table and four temperature measurements (step 3) and liquid line enthalpy (h_{liq}) based on the saturation lookup table and liquid line temperature measurement (step 3).

Step 9. Calculate the refrigerant mass flow rate (m_{ref_2}).

The refrigerant mass flow rate (m_{ref_2}) is estimated based on the h_{dis} , h_{suc} and W_{comp} , as shown in Equation (7).

Step 10. Calculate the condenser air flow rates (V_{a_cd}).

The condenser air flow rates (V_{a_cd}) can be estimated using energy balances between air-side and refrigerant-side using Equation 9. Refrigerant-side capacity can be obtained using Equation 7. The specific volume of air (v_{c_a}) can be calculated using the two air-side temperature measurements using Equation 10.

$$V_{a_cd} \left[ft^3 / sec \right] = \frac{m_{ref_2} \cdot (h_{dis}(P_{c_s}, T_{dis}) - h_{liq}(T_{liq}))}{(T_{c_a_o} - T_{c_a_i})} \cdot \frac{v_{c_a}}{1.013} \quad (9)$$

$$v_{c_a} \left[ft^3 / lb \right] = 0.04512 \cdot \left(\frac{T_{c_a_i} + T_{c_a_o}}{2} + 273.15 \right) \quad (10)$$

Step 11. Compare the difference between V_{a_cd} and its V_{a_r} , with Th_{cond} to flag condenser fouling fault (Error code: *ERR_cd*).

The condenser air flow rate is constant for RTU with fixed-speed fan. The estimated V_{a_cd} can be compared with its rated condenser air flow rate (V_{a_r} , unit: ft^3/sec). If the percent difference between V_{a_cd} and V_{a_r} is within condenser fouling threshold ($Th_{cond} = 30\%$), no action is required. However, if the difference exceeds the threshold, it is flagged as an error as shown in Table 31.

Table 31: Fault Condition for Capacity Impact

State	Condition	Action
Normal	$\frac{ V_{-a_cd} - V_{-a_r} }{V_{-a_r}} \cdot 100 > (Th_{cond} = 30 [\%])$	Normal operation
Condenser fouling fault	$\frac{ V_{-a_cd} - V_{-a_r} }{V_{-a_r}} \cdot 100 \leq (Th_{cond} = 30 [\%])$	Identify the condenser fouling fault (Error code: <i>ERR_cd</i>)

The current approach based on an energy balance model has the limitation of not being valid when subcooling at the outlet of the condenser is zero. This condition is typically associated with low refrigerant charge and can lead to inaccurate estimate of the condenser air flow rate (V_{-a_cd}). The implementation details of the condenser fouling fault detection and diagnostic process is outlined as a flow chart in Figure 15.

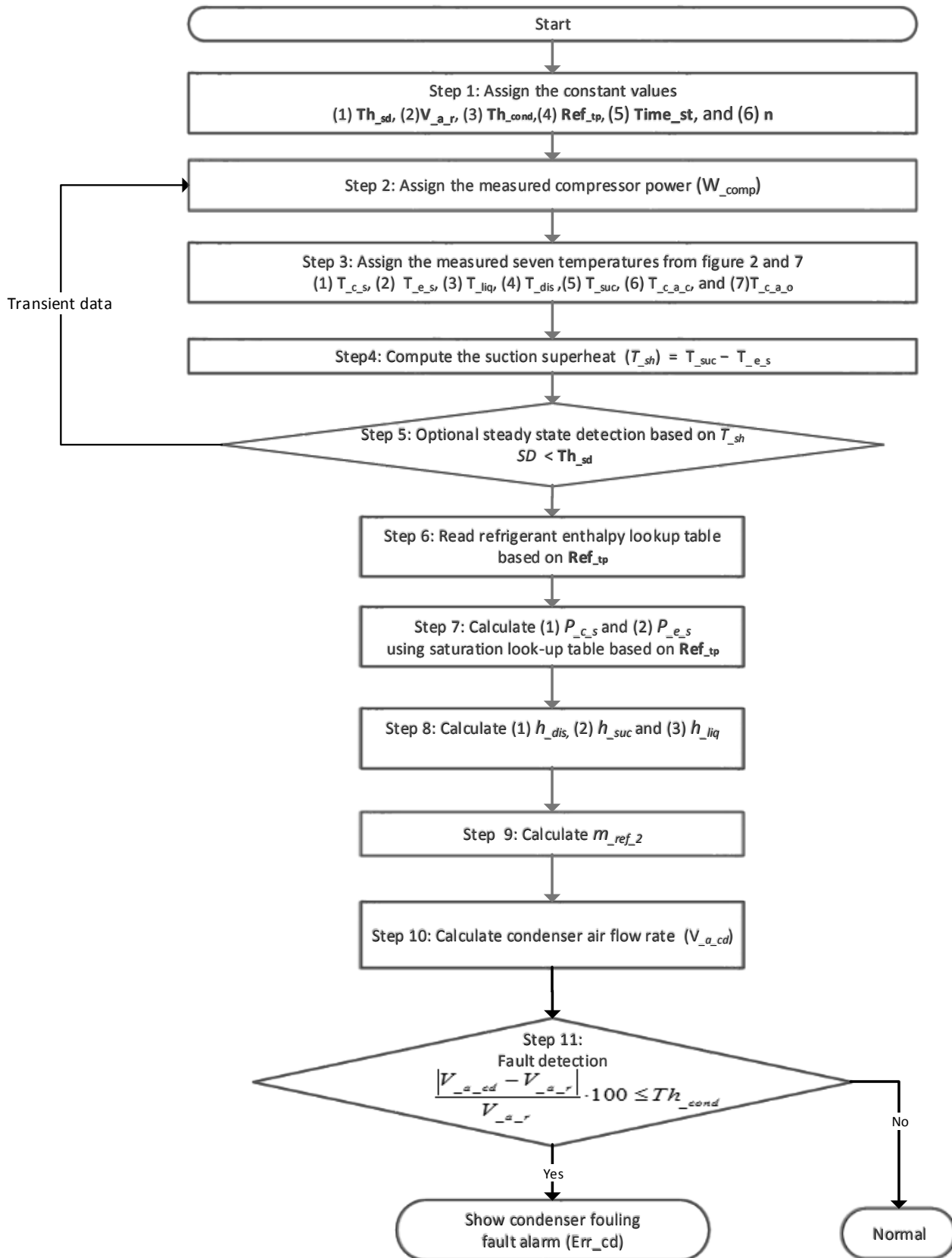


Figure 15: Condenser Fouling Fault Detection and Diagnostic Process

D. Liquid Line Restriction Fault Detection and Diagnostics

The purpose of this fault detection and diagnostic feature is to identify and isolate liquid line restriction fault. This fault generally results from clogged or dirty filter/dryer. The filter/dryer is installed in the liquid line to remove moisture and tiny particles introduced during refrigerant charging or metal parts from the piping connections. Accumulation of these substances overtime can block the filter/dryer, causing a reduction in the refrigerant mass flow. When the restrictions are severe, the TXV (thermostatic expansion valve) with variable opening may be fully open and behave like a fixed orifice.

The RTU controller needs six temperature measurements to implement the liquid line restriction fault detection and diagnostic (Table 32). If there are multiple circuits, these measurements have to be repeated for each circuit, as shown in Figure 10.

Table 32: Input Parameters Required to Detect and Diagnosis Liquid Line Restriction

Value	Description	Physical sensor location	Range (°F)
T _{c_s}	Condenser saturation temperature	Condenser tube band	95 ~ 135
T _{e_s}	Evaporator saturation temperature	Evaporator inlet line	5 ~ 65
T _{suc}	Compressor suction temperature	Compressor suction line	0 ~ 60
T _{liq}	Liquid line temperature	Condenser exit line	
T _{dis}	Compressor discharge temperature	Compressor discharge line	
T _{TXV_i}	Expansion valve inlet temperature	Expansion valve inlet line	95 ~ 135

Liquid Line Fault Detection and Diagnostic Process

The primary goal of the liquid line fault detection and diagnostic is to determine if there is liquid line restriction in the RTU refrigeration circuit. The implementation details of liquid line restriction fault detection are given in Figure 16. The process of detection and diagnostics is broken down into several steps, so it is easy to implement in a controller.

Step 1. Assign one the rated constant value, two default parameters and two threshold values.

- (1-1) Rated constant values: (1) T_{1d} .
- (1-2) Two default parameters: (2) Time_{st} , and (3) n .
- (1-3) Two threshold values: (4) Th_{sd} and (5) Th_{liq} .

Step 2. Assign the six temperature measurements from the corresponding input channels from the controller.

The controller assigns six temperatures measurements to corresponding input variables (condenser saturation [T_{c_s}], evaporator saturation [T_{e_s}], compressor suction [T_{suc}], liquid line [T_{liq}], compressor discharge [T_{dis}], and expansion valve inlet [T_{TXV_i}]).

Step 3. Calculate T_{sc} , T_{sh} , and T_{dsh} .

Calculate the three derived input values using five surface-mounted temperature sensors from step 2. Once five temperature measurements are collected, the measured temperatures are used to calculate the three derived inputs.

- (3-1) Subcooling (T_{sc}) = $T_{c_s} - T_{liq}$.
- (3-2) Suction superheat (T_{sh}) = $T_{suc} - T_{e_s}$.
- (3-3) Discharge-superheat (T_{dsh}) = $T_{dis} - T_{e_s}$.

Step 4. Filter out the transient data using the steady-state detection process.

The liquid line fault detection and diagnostic is only reliable when the system is in the steady-state operating condition. Therefore, the steady-state detection filter is used to remove the transient data using the standard deviation (SD) about T_{sh} as a basis as shown Equation 1. The state conditions after steady-state detection process is complete are outlined in Table 33.

Table 33: State Condition after Steady-state Detection Process

State	Condition	Action
Steady-state	$SD < (Th_{sd} = 1.0 \text{ as default value})$	Go to step 1
Unsteady-state (discard data)	$SD > (Th_{sd} = 1.0 \text{ as default value})$	Go to step 5

Step 5. Compute the liquid line temperature difference (T_{l_d})

The liquid line temperature difference (T_{l_d}) between T_{liq} and T_{TXV_i} is used to detect liquid-line restriction fault conditions as shown in Equation (11).

$$T_{l_d} = T_{liq} - T_{TXV_i} \tag{11}$$

Step 6. Compare difference of T_{l_d} and its T_{l_r} with Th_{liq} to flag liquid line error (Error code: ERR_{liq}).

If the computed liquid line percent difference T_{l_d} is less than reference difference (T_{l_r}), then no action is needed. However, if the computed percent difference is greater than the reference difference, a liquid line fault is flagged (Table 34).

Table 34: Rules to Flag Liquid Line Restriction Fault Condition

State	Condition	Action
Normal	$\frac{ T_{l_d} - T_{l_r} }{T_{l_r}} \cdot 100 < Th_{liq} (= 100 \%)$	Normal operation
Liquid line restriction fault	$\frac{ T_{l_d} - T_{l_r} }{T_{l_r}} \cdot 100 \geq Th_{liq} (= 100 \%)$	Identify the condenser fouling fault (Error code: ERR_{liq})

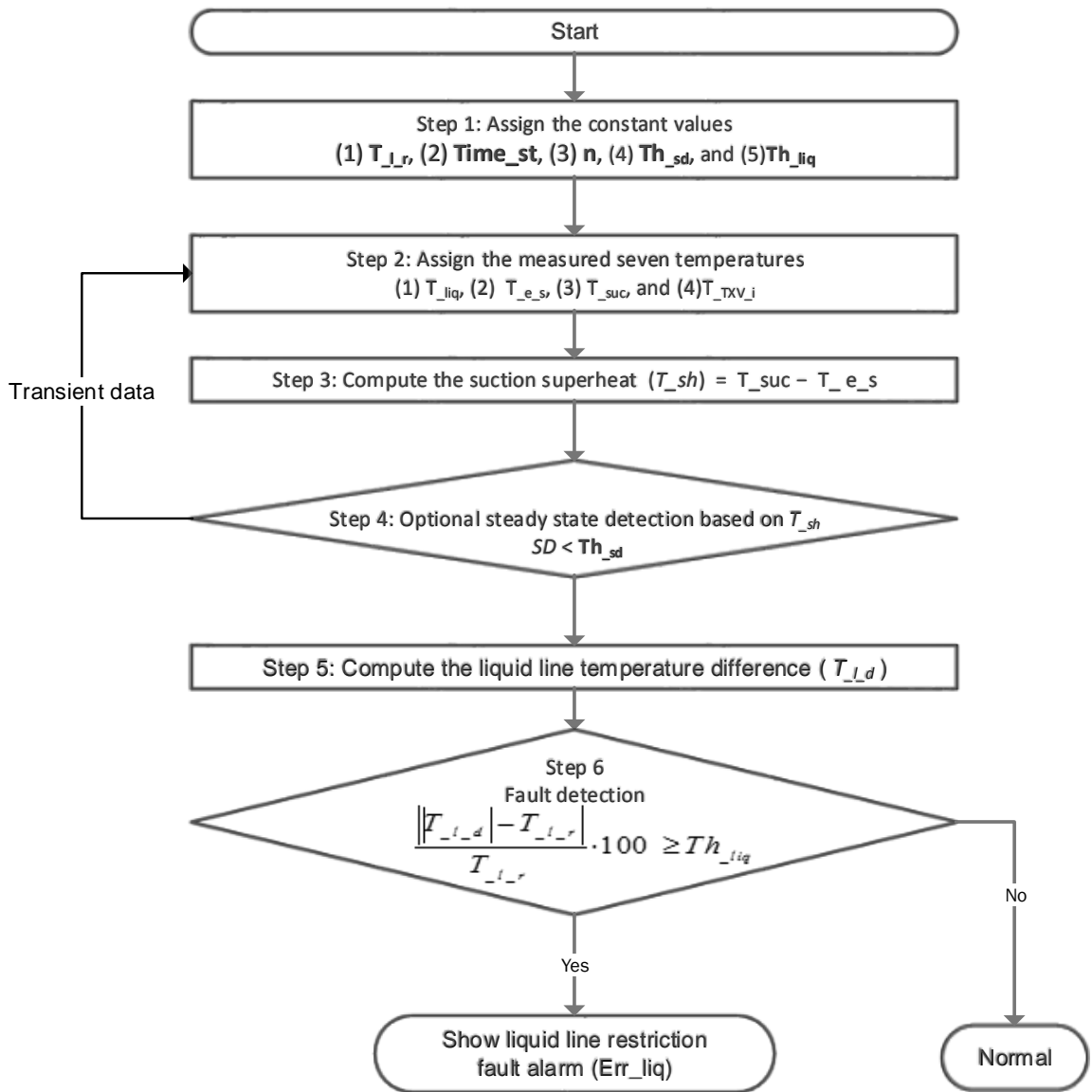


Figure 16: Liquid Line Restriction Fault Detection and Diagnostic Process

VI. Testing and Validation Methodology for both Air- and Refrigerant-side Embedded Diagnostics

The air-side and refrigerant-side diagnostics described previously were embedded on to an advanced RTU controller.

The validation of the embedded diagnostics was done in two steps: 1) comparison of various outputs generated by the algorithms embedded in the controller with outputs generated from programming the algorithm in an Excel spreadsheet and 2) validating the diagnostic results generated by the algorithms embedded in the controller with offline analysis of the raw data.

For the first comparison, the controller was programmed to output various “debug” data. The same “debug” data was also generated by programming the algorithm in an Excel spreadsheet. By comparing the two sets of results, it was confirmed that the algorithms programmed in the controller were generating accurate results. The second set of validation was done by comparing the diagnostic results generated by the controller to results generated by offline analysis of the same input data. This validation is described in the next section.

A. Demonstration Site Description

The refrigerant-side testing conducted on five RTUs at an office building in Kent, WA and on four RTUs at a grocery store in Phoenix, AZ. The air-side diagnostics were tested on the same five RTUs in Kent, WA and 2 RTUs on a retail store in Seattle, WA. Each RTU was instrumented to provide all the data needed for the controller to conduct the fault detection and diagnostics in online and in real-time. The field tests were conducted in the summer of 2014 (June through September). Figure 17 show the external view for office building, located in Kent, WA. The five RTUs located on the roof of that building are shown in Figure 18. The details of the five RTUs are listed Table 35. These five units were used to validate both the air-side and refrigerant diagnostics. Figure 19 shows an external view of grocery store in Phoenix, AZ. The four RTUs located on the roof of that building are shown in Figure 20. The details of the four RTUs are listed Table 36, these units were only used to validate the refrigerant-side diagnostics. Two RTU were used at the third site to validate just the air-side diagnostics (Table 37).



Figure 17: External View for Office Building, Kent, WA



Figure 18: Locations of RTUs on the Office Building

Table 35: Details of the RTUs on the Office Building in Kent, WA (FXO: Fixed Orifice and TXV: Thermal Expansion Valve)

Equipment ID	RTU Model	System Type	Number of Circuit	Refrigerant Type	Capacity [tons]	Number of Condenser Fan	Type of Expansion Device	Rated Refrigerant Charge [lbm]
Unit 425	48GS-030	Air Conditioner	1	R22	3	1	FXO	4.2
Unit 1327	48TJE014	Air Conditioner	2	R22	12.5	2	FXO	8.6
Unit 1328								8.4
Unit 1329	50TC050	Heat Pump	1	R410A	4	1	TXV	5.2
Unit 1330	48TFD014	Air Conditioner	2	R22	12.5	2	FXO	8.6
Unit 1331								8.4
Unit 1332	50EZA24	Heat Pump	1	R410A	2	1	TXV	4.3



Figure 19: External View for Grocery Store in Phoenix, AZ

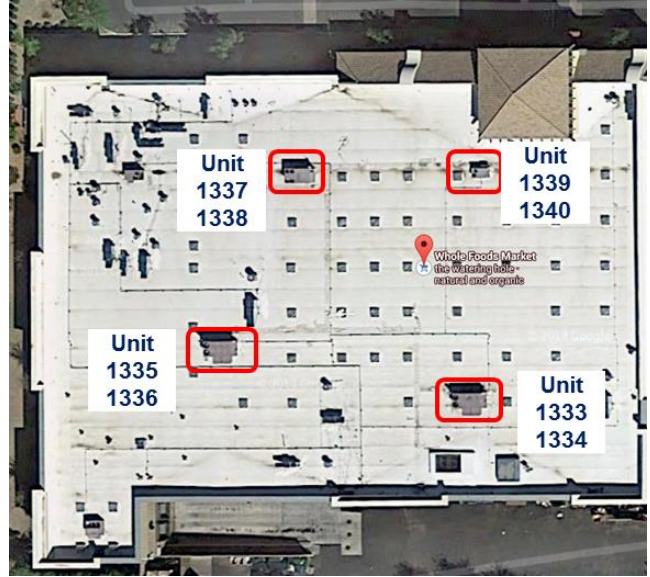


Figure 20: Locations of RTUs on the Grocery Store

Table 36: Details of the RTUs on the Grocery Store Building in Phoenix, AZ (FXO: Fixed Orifice and TXV: Thermal Expansion Valve)

Equipment ID	RTU Model	System Type	No. of Circuit	Refrigerant Type	Capacity [tons]	No. of Condenser Fan	Type of Expansion Device	Rated Refrigerant Charge [lbm]
Unit 1333	48HJF01	Air conditioner	2	R22	15	3	TXV	20.7
Unit 1334	7							13.4
Unit 1335	48HJF02	Air conditioner	3	R22	18	4	TXV	13.1
Unit 1336	0							12.7
Unit 1337	48HJF01	Air conditioner	2	R22	10	2	FXO	9.4
Unit 1338	2							10.6
Unit 1339	48HJF00	Air conditioner	2	R22	7.5	2	FXO	7.6
Unit 1340	8							8.1

Table 37: Details of the RTUs at a Retail Site in Seattle, WA

Equipment ID	No. of Compressors	Cooling Capacity (tons)	System Type
37	2	10	AC w/gas heat
38	2	10	AC w/gas heat

B. Metering and Monitoring Plan

This effort involves integrating and testing refrigerant-side and air-side diagnostics into an advanced RTU controller. Although the same RTU controller is used to deploy both the refrigerant-side and air-side

diagnostics, the metering and monitoring requirements for the two sets of diagnostics are different. Therefore, the metering and monitoring plans are discussed separately. The data required for both sets of diagnostics are recorded at 1-minute interval (instantaneous values). The recorded data is used to validate the diagnostic results reported by the RTU controller. The details of the metering for the air-side and the refrigerant side were discussed previously in Development of Refrigerant-side RTU Diagnostics and Development of Air-side RTU Diagnostics, respectively.

The monitoring plan consisted of collection of data (both raw sensor and diagnostic output) at each RTU at 1-minute intervals, storing it locally on the roof, and streaming the data in real-time to the Cloud for further analysis. The cellular network was used to upload data from each site to the Cloud. In case of loss of communication between the site and Cloud, the logged data stored locally at each site had a maximum storage capacity to store data for couple of days. Figure 21 schematically shows the entire monitoring process.

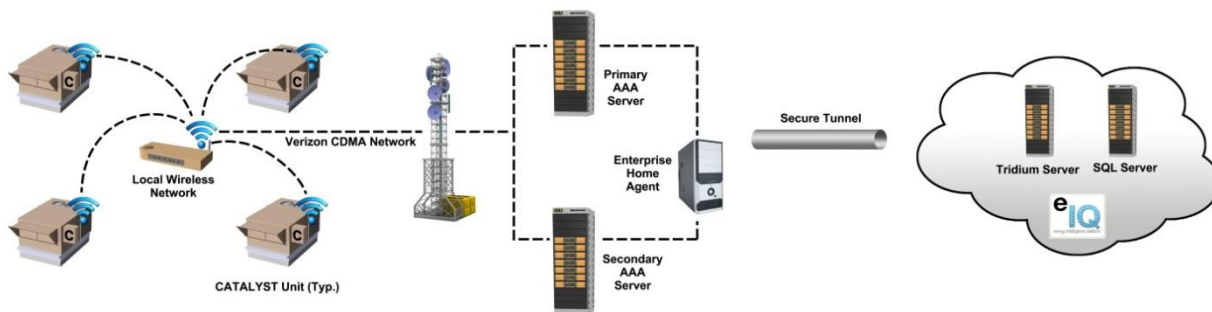


Figure 21: Schematic of the RTU Monitoring

VII. Validation of Air-side Embedded Diagnostics

As noted previously seven AFDD algorithms were developed and deployed on the RTU controller for detecting and diagnosing faults with the RTU economizer and ventilation operations using sensors that are commonly installed for advanced control purposes. In this section, the embedded air-side diagnostics implemented in the RTU controller was validated through offline analysis of sensor data from the RTU controller. The algorithms utilize rules derived from engineering principles of proper and improper RTU operations, including:

- Compare DAT with MAT for consistency (AFDD0)
- Check if the OAD is modulating (AFDD1)
- Detect RTU sensor faults (OAT, RAT and MAT sensors) (AFDD2)
- Detect if the RTU is not economizing when it should (AFDD3)
- Detect if the RTU is economizing when it should not (AFDD4)
- Detect if the RTU is using excess outdoor air (AFDD5)
- Detect if the RTU is bringing in insufficient ventilation air (AFDD6).

The diagnostics are available as a proactive test that can be run on demand, and as a passive test that continuously monitors the RTUs sensor readings and command outputs. The passive tests do not alter the RTU's control sequence in any way. During the passive diagnostics, all seven diagnostics run concurrently and diagnostic results are generated as operational conditions permit. Table 38 shows a summary of the RTUs cooling and ventilation operations.

Table 38: Summary of RTU Cooling Operations

Mode	OAT 58°F and Below	OAT Between 58°F and 70°F	OAT 70°F and Above
Ventilation (No call for cooling)	Supply fan speed at 40%; minimum OAD at 13%	Supply fan speed at 40%; minimum OAD at 13%	Supply fan speed at 40%; minimum OAD at 13%
1st Stage Cooling	Economizer only operation; supply fan speed at 75%; no mechanical cooling; OAD at 100%	Economizer only operation; supply fan speed at 90%; no mechanical cooling; OAD at 100%	1 st stage mechanical cooling and integrated economizing; supply fan speed at 75%; minimum OAD at 7%
2nd Stage Cooling	Economizer only operation; supply fan speed at 90%	1 st stage mechanical cooling and integrated economizing; supply fan speed at 90%	2 nd stage mechanical cooling and integrated economizing; supply fan speed at 90%; minimum OAD at 6%

The first diagnostic check (AFDD0) is designed to compare the DAT and MAT sensor readings with each other. The purpose of this proactive diagnostic test is not to identify which sensor is "faulty," but to establish whether

there is a lack of confidence in one or both sensors and their accuracy. RTU 451 showed inconsistencies between the MAT and DAT (AFDD0 returned a fault during the diagnostic).

The validation process involved using the raw sensor data from the RTUs, conducting an offline analysis and generating diagnostics results. The offline diagnostics results were then compared to the diagnostics results output by the controller. Figure 22 shows that there is a significant deviation in the MAT and DAT sensor readings when the OAD is open to 100%. AFDD0 does not isolate the cause of the problem but draws attention to the fact that a fault may exist. The results from the embedded diagnostics also reported this fault for that period of time.

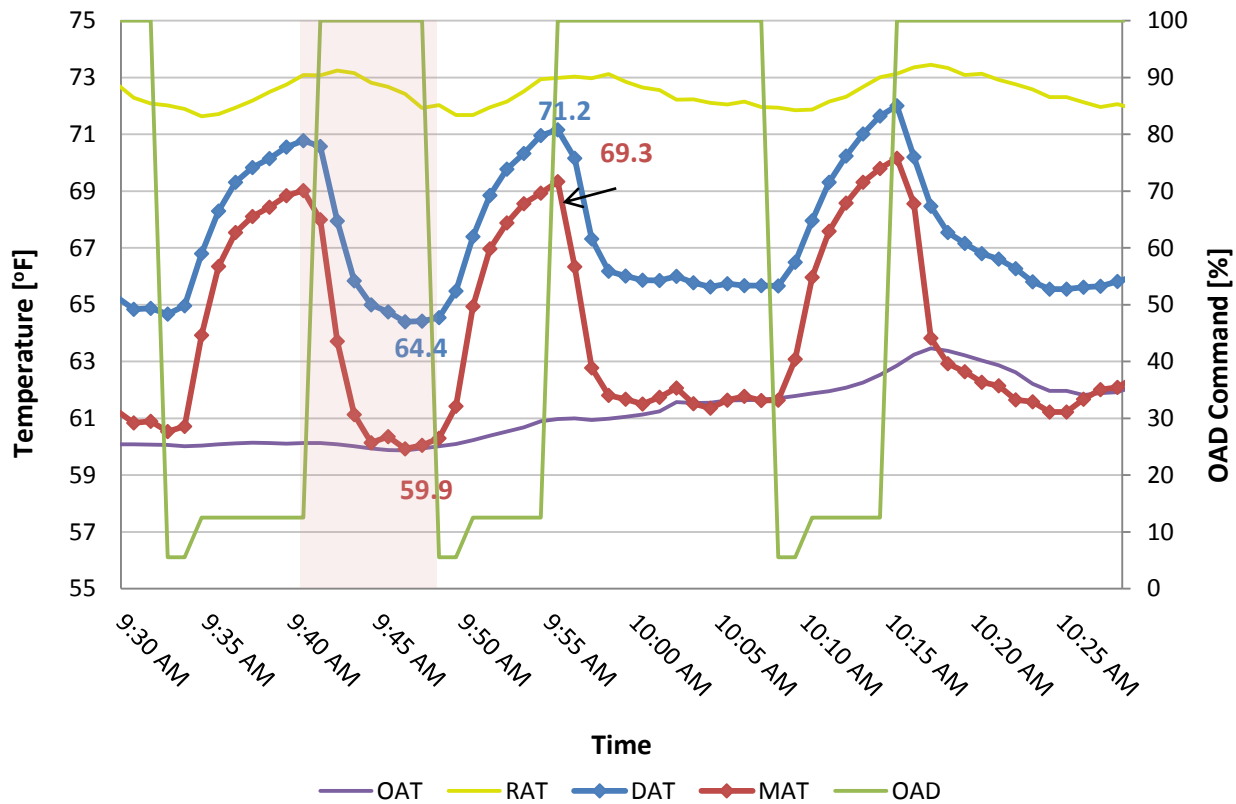


Figure 22: Validation of Embedded AFDD0 Air-side Diagnostics

Figure 22 shows that when the OAD is fully open, the unit is economizing (see Table 38 for operational details), there was a significant deviation between the MAT and DAT. The MAT was 59.9°F and the DAT was 64.4°F, a difference of 4.5°F (the threshold for calling a fault on AFDD0 was 4°F). Figure 22 shows that a short time later, when the OAD is in the minimum position this difference is much smaller, less than 1°F.

The second diagnostic (AFDD1) determines if the OAD is modulating properly. This diagnostic was initiated both as a passive and proactive diagnostic on the RTU controller. For the proactive diagnostics, AFDD1 will use the OAD command to create two analytical redundancies to detect and diagnose the OAD modulation fault. The first condition is obtained by commanding the OAD to a fully open position (100% outdoor air). The second

condition is obtained by commanding the OAD to a fully closed position (0% outdoor air). If the damper is fully open, the difference between the OAT and the MAT should be minimal (between 2°F and 4°F). If the damper is closed, the difference between the RAT and the MAT should be minimal.

Unlike the proactive diagnostic, the passive diagnostic does not modify the RTU’s controls but instead waits for the right conditions (RTU operations) to evaluate this fault. The required difference between the OAT and RAT for the passive diagnostic was chosen to be 10°F, although this value could be adjusted. None of the RTUs in the field exhibited AFDD1 problem. The offline analysis of the data also confirmed that finding by the embedded diagnostics. Figure 23 shows the passive diagnostic process where the MAT and OAT temperatures are nearly equal when the OA damper was fully open (100%) and MAT and RAT temperatures were nearly equal when the OA damper fully closed (minimum OA position).

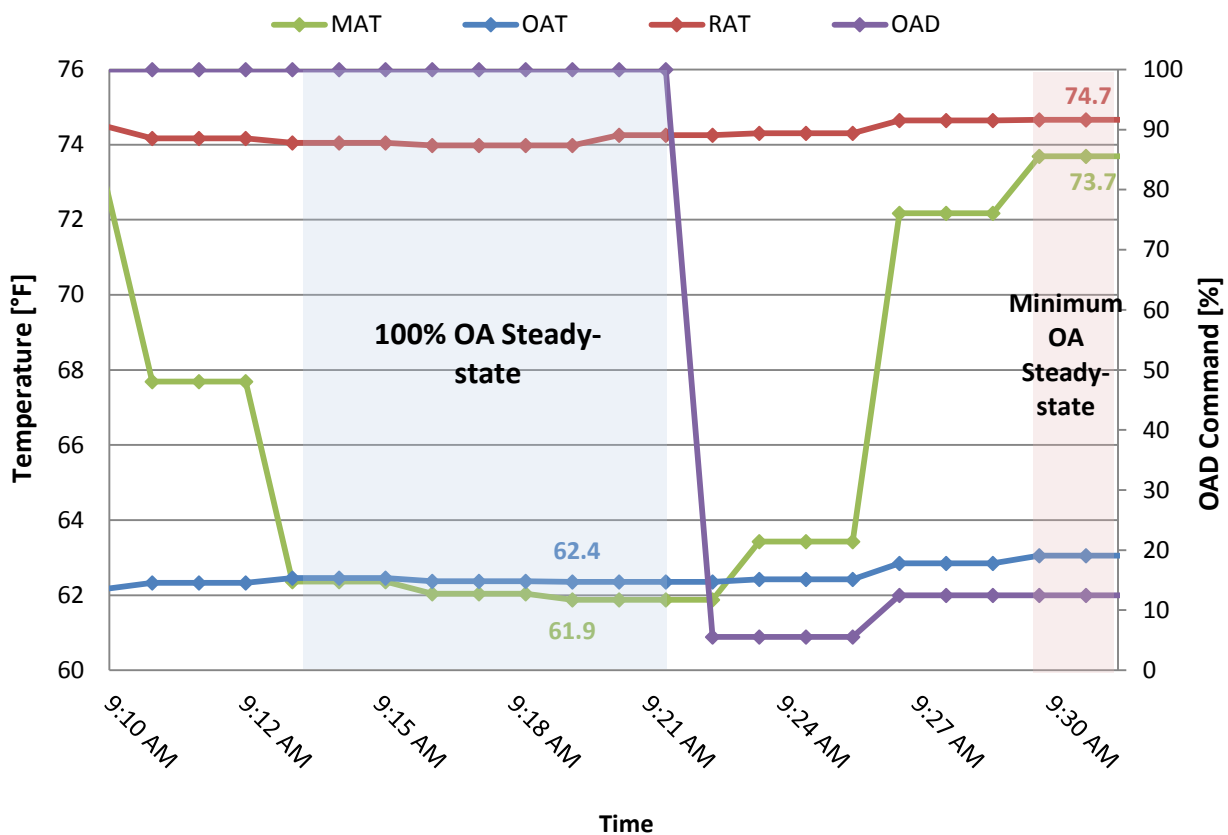


Figure 23: Validation of Embedded AFDD1 Air-side Diagnostics

The third diagnostic determines if there is a temperature sensor problem. The initial step in the temperature sensor diagnostic is to identify if a temperature sensor problem is present. Because the mixed-air is a mixture of the outdoor-air stream and the return-air stream the MAT reading should always fall between the RAT and OAT sensor readings. When the MAT sensor reading is significantly larger than both the OAT and RAT or if the MAT sensor reading is significantly less than both the OAT and RAT, a temperature sensor problem exists. No air-temperature sensor faults (AFDD2) were detected for any of the RTUs at the two sites. Figure 24 shows the

temperature sensor readings during operational hours for one RTU. The MAT is consistently between the OAT and RAT. This behavior was consistent for all the RTUs monitored.

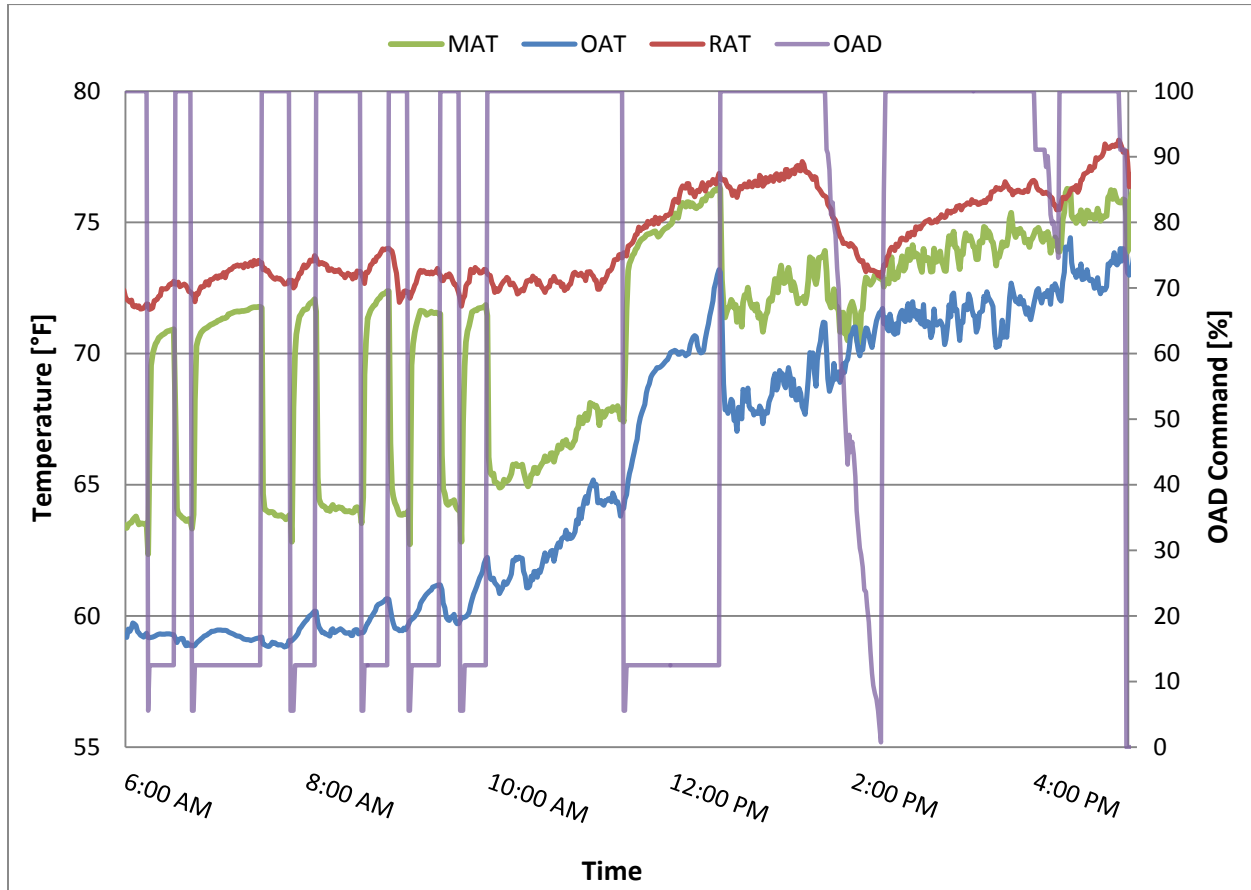


Figure 24: Validation of Embedded Air-side Diagnostics AFDD2

The purpose of AFDD3 diagnostic is to identify conditions when the economizer controls are not working properly or when the economizer is not being fully utilized when outdoor conditions are favorable for economizing. The RTU controller enables economizing whenever there is a call for cooling and the OAT is less than 70°F. When the OAT is greater than 70°F and there is a call for cooling, the RTU controller uses differential dry-bulb economizer logic. The RTUs at both sites consistently executed the control logic for the economizer correctly. When there was a call for cooling from the space served by the RTU and outdoor conditions were favorable for economizing, the OAD was fully opened to allow the maximum outdoor air into the RTU. Although the controller executed the control logic correctly and modulated the damper accordingly, AFDD3 did detect that all RTUs at both sites consistently provided far less than 100% outdoor air, even when the OAD was command to be fully open (100% open). Figure 25 illustrates that problem using the data from one RTU. When the OAD is fully open, the OAF should be 100%, but it is only 60%. This condition is a result of leakage of air from the return air damper, because the return-air temperature is much warmer than the outdoor-air temperature the OAF is less than 100%.

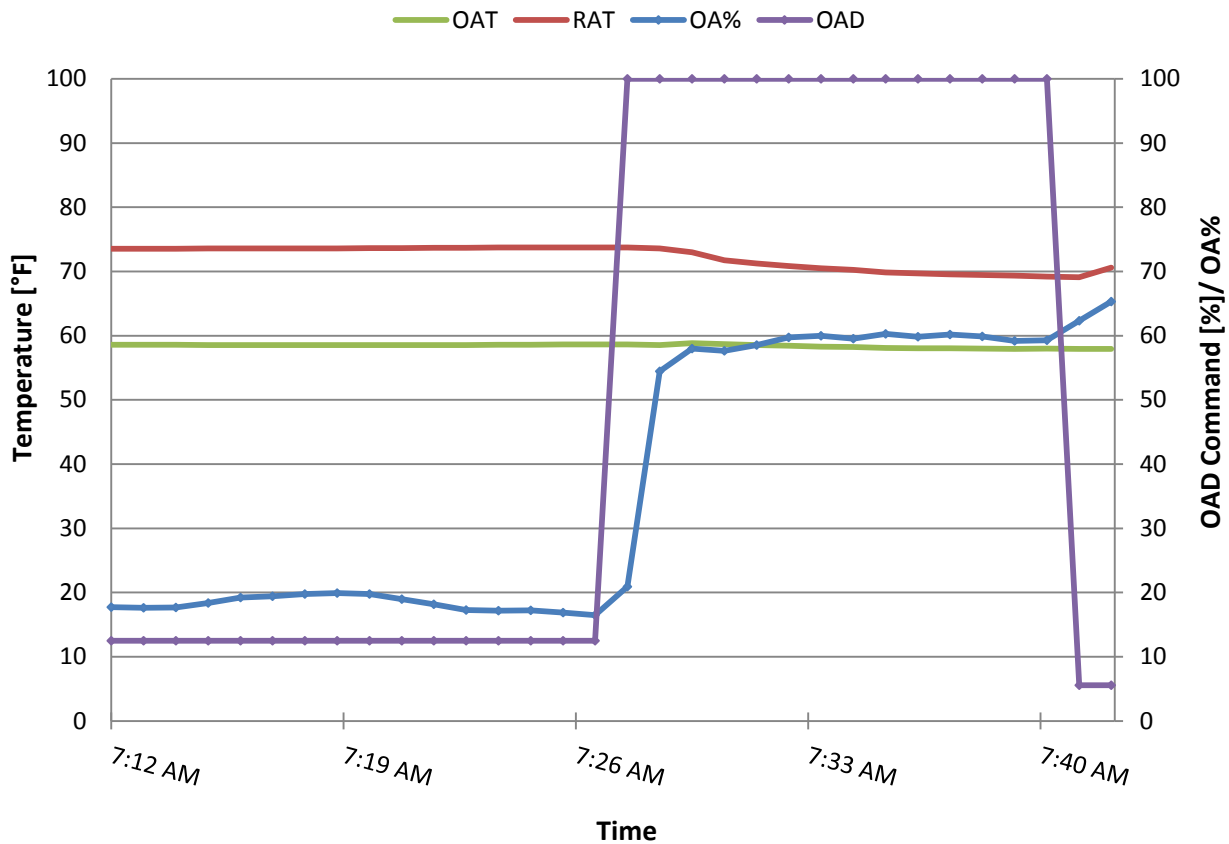


Figure 25: Validation of Embedded Air-side Diagnostics for AFDD3

The purpose of AFDD4 diagnostic measure checks if the RTU controls are commanding the OAD to (or near) the minimum damper command position when conditions are not favorable for economizing. All RTUs at both sites executed the economizer control logic correctly. Figure 26 shows the operation of one RTU when there is a call for cooling and the OAT is less than the RAT. The OAD correctly opens to 100%, the RTU is economizing, using the cool outdoor air to help maintain space temperatures. When the call for cooling ends, the OAD modulates to the minimum position required to meet the ventilation needs. When there is a call for cooling but the OAT is greater than the RAT, the OAD stays at the minimum position.

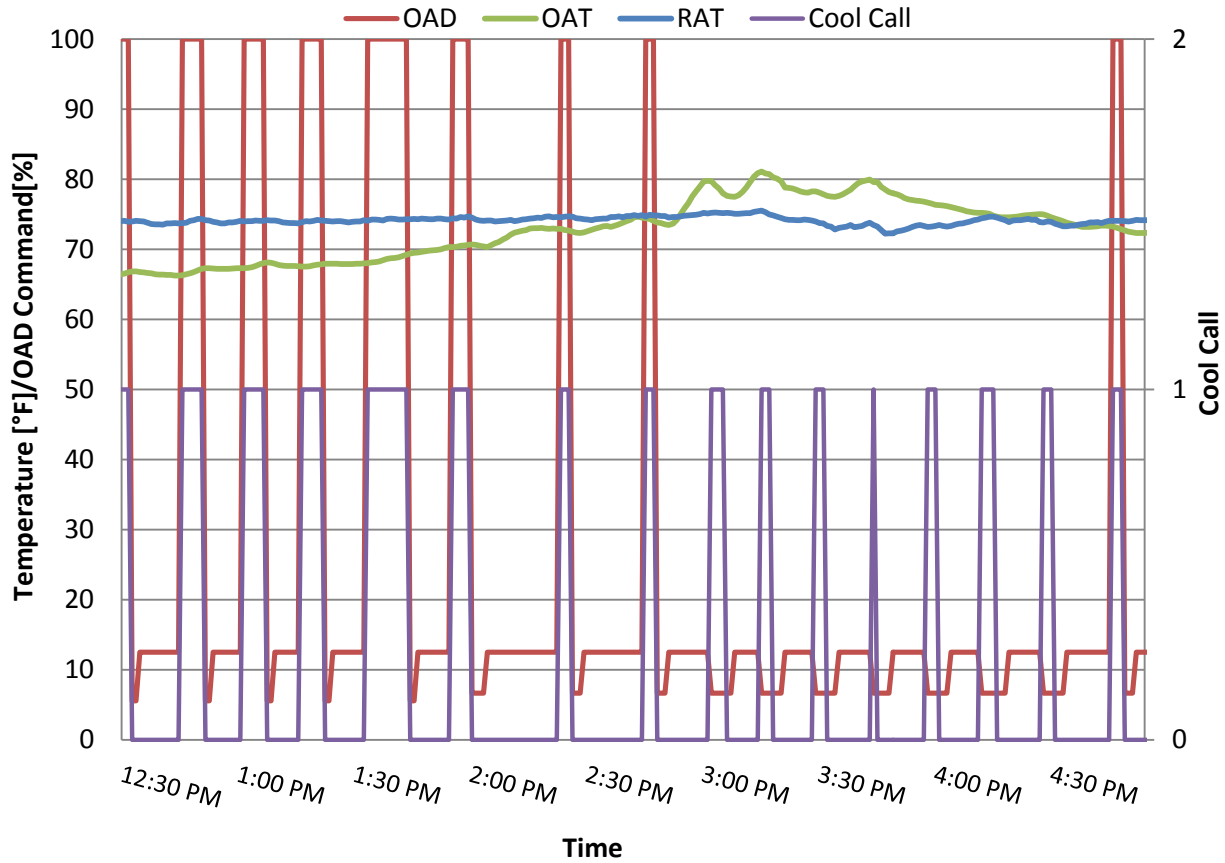


Figure 26: Execution of Economizer Control Logic (AFDD3 and AFDD4) for RTU 449

The sixth diagnostic (AFDD5) validates if the RTU is introducing excess outside air beyond the value required to provide minimum ventilation. When the damper is closed or at the minimum position, the OAF also should be equal to the minimum value. If the calculated OAF (or OA as percent) is above the minimum value by more than 10% (adjustable), a fault is generated for AFDD5. The data for one RTU is plotted in Figure 27. For this particular RTU, the minimum OA intake is configured by the building owner as 20%. Therefore, there is no AFDD5 fault during this period or at any other period.

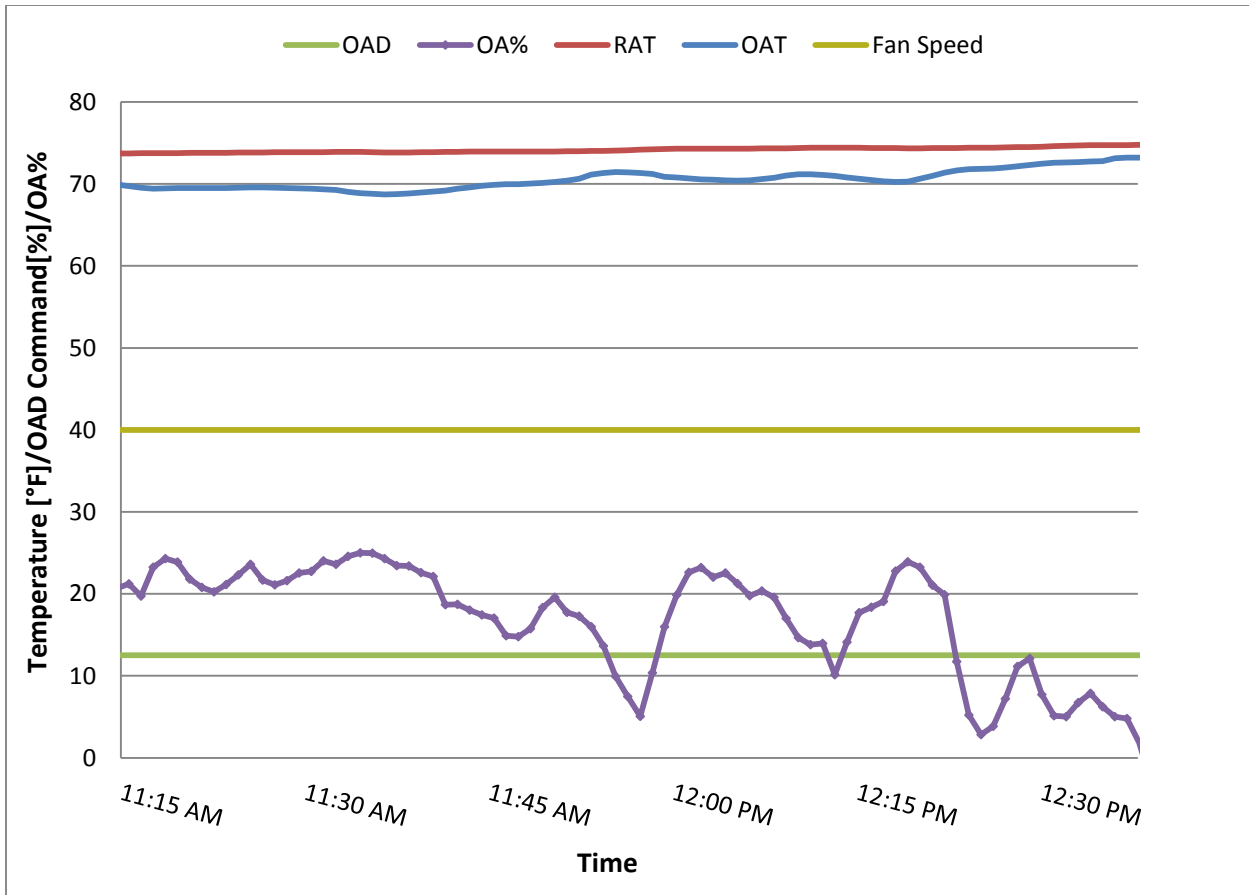


Figure 27: Validation of Embedded Air-side Diagnostics AFDD5

The seventh and final diagnostic check determines if the RTU is introducing insufficient outdoor air below the minimum ventilation requirement. The calculated OAF is compared to a minimum OAF threshold to determine if insufficient ventilation air is being introduced into the space. The minimum OAF threshold used for this diagnostic was 5% (adjustable parameter). Figure 28 shows the OA intake (as percent) during typical ventilation only operations for one RTU. If the calculated OA intake falls below 5% a fault is generated. However, for this RTU, AFDD6 fault did not occur.

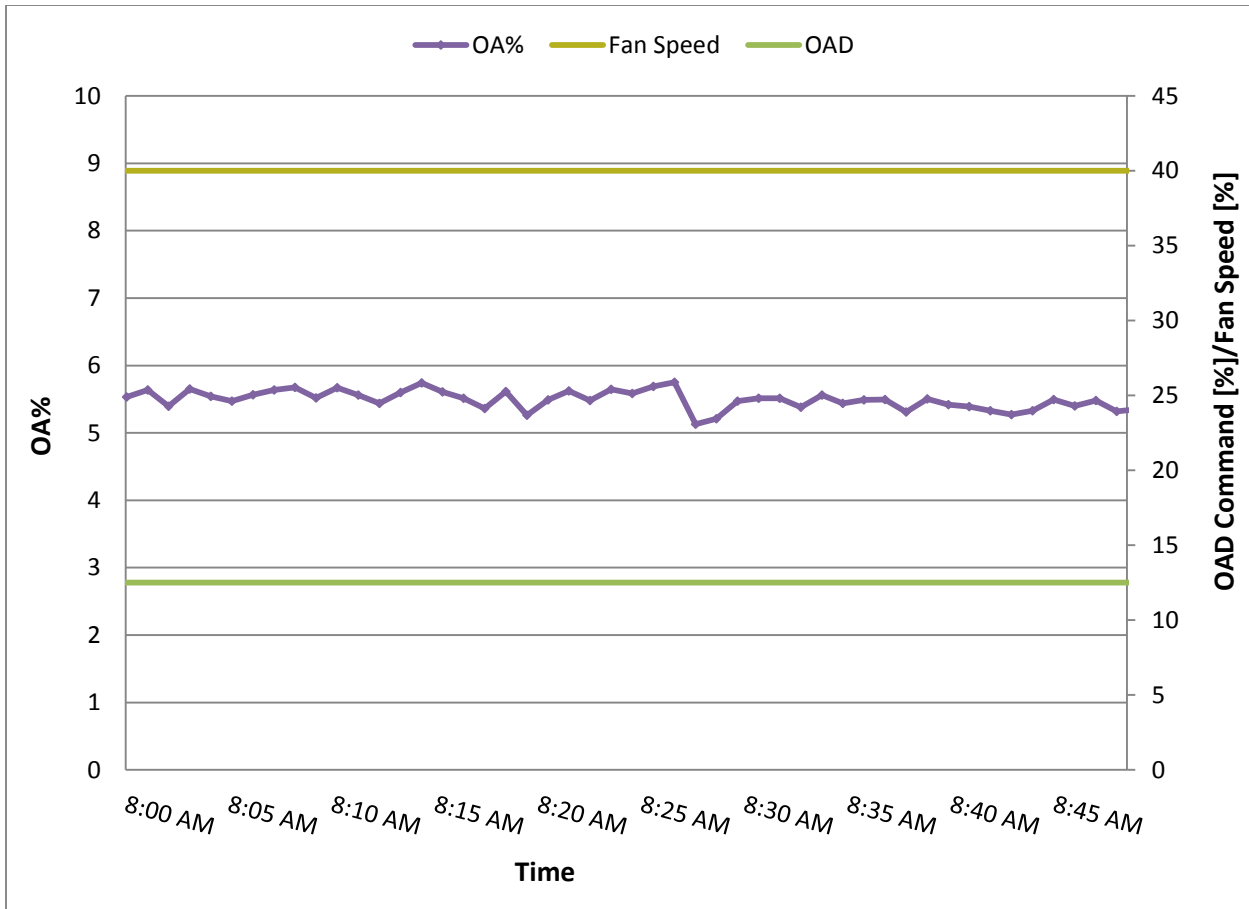


Figure 28: Validation of Embedded Air-side Diagnostic AFDD6

VIII. Validation of Refrigerant-Side Embedded Diagnostics

In this section, implementation of the embedded refrigerant-side diagnostics in the RTU controller is validated. Because all the RTUs in the field tests did not exhibit significant refrigerant-side fault conditions, it was decided that faults would be artificially instigated in two RTUs in the field to validate the diagnostics. Therefore in this section, first the validation of diagnostics using “faulty” data is described followed by the offline analysis of the data from the field.

A. Validation of Refrigerant-side Diagnostics using Artificial “Faults” in the Field

The refrigerant charge and condenser blockage faults were artificially introduced in two RTUs in the field. Table 39 shows the details of the two air conditioners that are located on the rooftop of an office building in Kent, WA. Each system has two separate circuits which are connected to a separate compressor. The RTUs used R-22 as the refrigerant with a fixed orifice expansion device. The rated condenser air flow rate, capacity and coefficient of performance (COP) were obtained from estimated values when the AFDD approach was implemented assuming that there is no fault. The rated refrigerant charge amount was obtained from technical specification provided by manufacturers.

Table 39 Details of the RTUs used for AFDD Validation

System	Unit	Refrigerant	Expansion valve	Rated Condenser Air Flow Rate (CFM)	Rated Refrigerant Charge Amount (lbs)	Rated Capacity (Btu/min)	Rated COP
I	1327	R22	Fixed orifice	880	8.6	1345	4.7
	1328			960	8.4	1500	4.7
III	1331			1050	8.6	1700	4.8
	1332			900	8.4	1450	4.8

The tests were run under a wide range of outdoor conditions with seven actual refrigerant charge levels and three different condenser blocking levels (Table 40). During the field test period, the outdoor-air temperature varied between a high of 92°F and a low of 62°F. The condenser fouling (improper outdoor-air-flow rate) fault was implemented by blocking the heat exchanger with paper towels. The condenser fouling fault level is defined as the ratio of blocked face area with paper divided by the total face area of the outdoor heat exchanger. Three fouling levels were considered 0%, 50% and 75%. A refrigerant charge fault was simulated by reducing or increasing the total amount of refrigerant charge. The refrigerant charge level is determined as a ratio of the charge to the rated charge. The simulated charge level ranged between 50% and 140%.

Table 40 Validation Tests for Refrigerant-Side Diagnostics

Unit	Outdoor-Air Dry Temperature (°F)	Condenser Fouling Fault Levels (%)	Damper Opening	Refrigerant Charge Level (%)
1327	62 ~ 89	0, 50, 75	0 or 100	50, 60, 70, 85, 100, 115, 130
1328	65 ~ 89			100
1331	65 ~ 92			50, 60, 70, 85, 100, 115, 130
1332	66 ~ 92			100

B. Refrigerant Undercharge and Overcharge Tests

Improper refrigerant charge causes problems in the field (such as compressor damage) and could lead to a significant energy consumption increase. The refrigerant charge fault was simulated by removing or adding charge to the two units in the field, as shown in Figure 29. For the overcharge condition, the refrigerant was added from an R-22 refrigerant tank using a manifold gauge. The tank was initially weighed using a digital scale to ensure that the system was correctly charged, and then the charge was added or removed based on the test. For the undercharge tests, refrigerant was recovered from the system into a tank connected to the manifold gauge. The recovered refrigerant amounts were also weighed using a digital scale.



Figure 29 Refrigerant Charging Method: Adding Refrigerant (left) and Removing Refrigerant (right)

Figure 30 shows the comparison of the predicted and actual refrigerant charge level for the two RTUs. The charge predictions were made using the algorithms described previously (Refrigerant Charge (undercharge/overcharge) Fault Detection and Diagnostics) of the under/over charge detection. The parameters for refrigerant charge detection were tuned using historical data points. Overall, the predicted charge levels were within 10% of the measured charge level covering a wide range of outdoor conditions. Based on the data analyzed by Kim and Braun (2102), it appears that undercharging a unit by 10% would result in less than a 5% impact on capacity and

overcharging by 10% would have a minimal impact. Therefore, a prediction accuracy that is within 10% is acceptable.

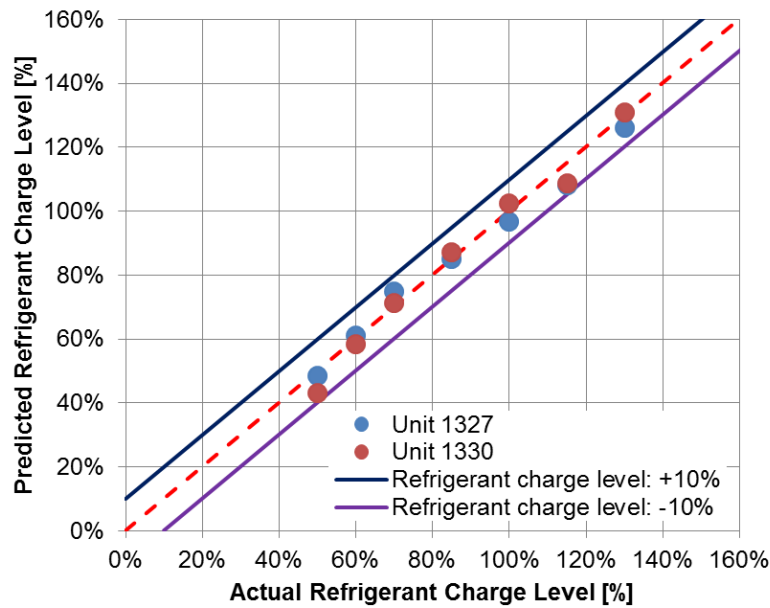


Figure 30 Comparison of Predicted Refrigerant Charge Amount with Actual Charge Level

Once the refrigeration charge is estimated from the FDD, the next step in the diagnostics is to estimate its impact on the cooling capacity. Figure 31 shows the cooling capacity reduction from refrigerant-undercharge fault as a function of the refrigerant charge level. The refrigerant undercharge level is defined as the ratio of the actual refrigerant charge to that of the rated charge under fault-free condition. The capacity reduction is the ratio of the actual capacity to the rated capacity under fault-free operation. The intersection of the vertical line for the refrigerant-undercharge fault threshold and the horizontal line for the capacity threshold can separate fault, warning, and normal regions in the Figure 31. Note that the fault threshold for undercharge fault was set at 40% capacity reduction. It appears that at approximately 30% undercharge condition, there is a 40% degradation in cooling capacity.

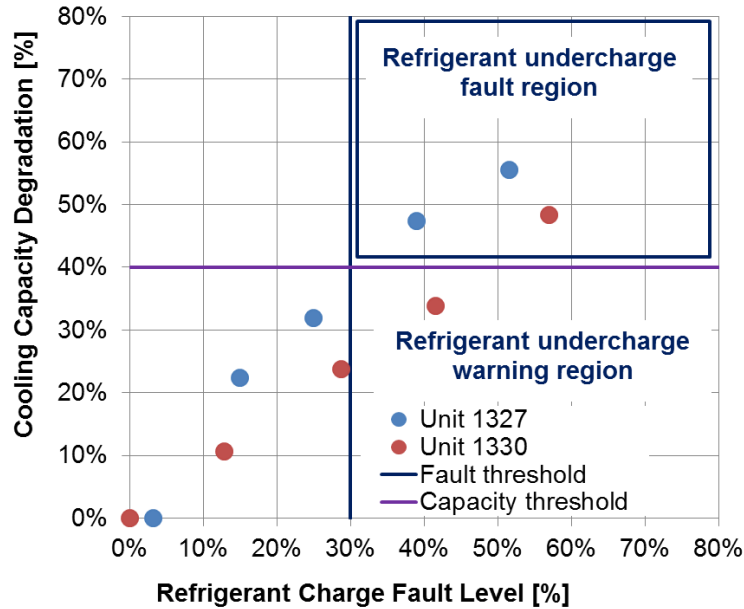


Figure 31 Validation of Embedded Refrigerant Undercharge Diagnostics

Figure 32 shows the screen shots from the RTU controller showing the results from the embedded diagnostics for 60% and 100% refrigerant charge level testing for unit 1330. The display shows various temperatures and power measurement under the 'STATUS' column, number of diagnostic results under the 'FAULTS' column and a number of calculated values under the 'CALCULATED VALUES'.

To validate the charge diagnostics, the RTU system was charged with 60% refrigerant charge level to simulate the undercharged condition. Figure 32 (left side) shows the estimated charge level ('M_r_ch2') at 61%, which is close to the actual charge. Both the estimated cooling capacity ('Q_ref') and the efficiency ('COP_ref') are at 53% and 57% of the rated values, respectively. It is clear from the results generated by the embedded charge diagnostics correctly identified the undercharge fault.

After completing the 60% undercharge test, the system was recharged to 100% charge level (rated charge). Figure 32 (right side) shows the estimated charge level ('M_r_ch2') of 97%, which is close to the actual charge level of 100%. Both the estimated cooling capacity (Q_ref) and the efficiency (COP_ref) are at 94 % and 100%, respectively, close to the rated value of 100%, indicating normal conditions. The display also correctly shows that there are no other faults ('V_a_cd' and 'T_l_d').

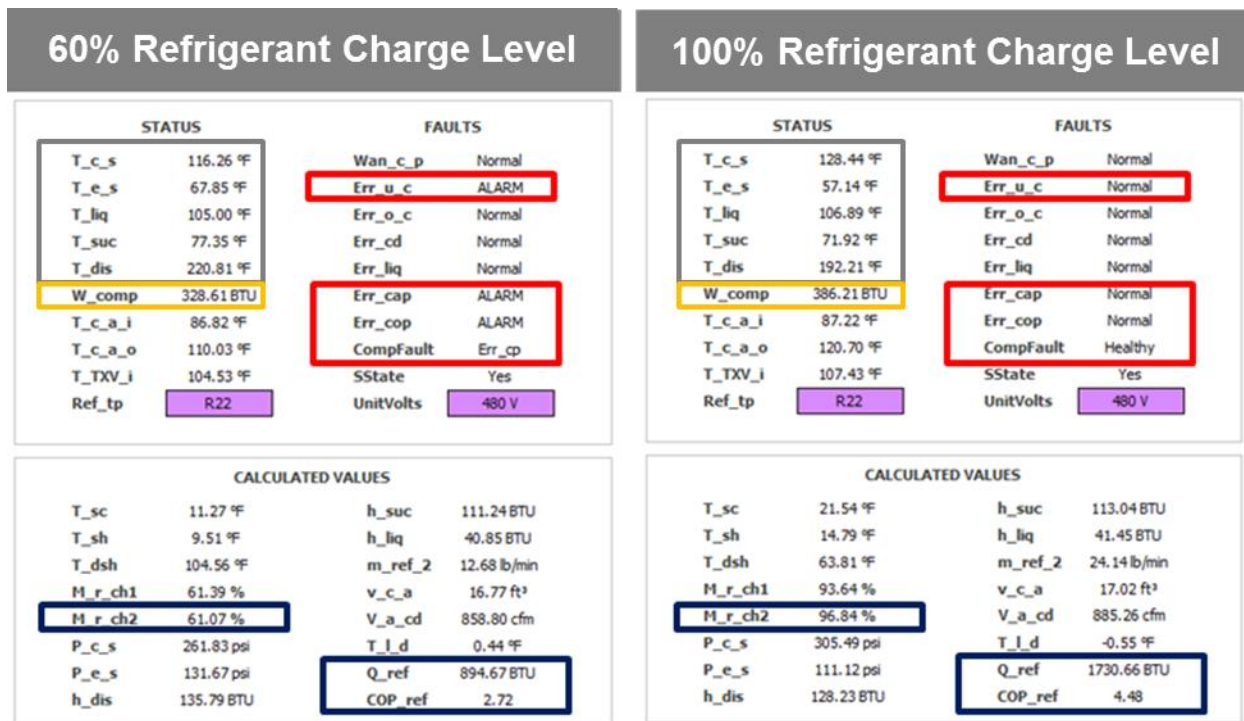


Figure 32: Screen Shots of Undercharge Refrigerant-side AFDD Results Generated by the RTU Controller: 60% Charge (left) and 100% Charge (right)

Improper Condenser Air Flow (condenser blockage) Tests

The condenser can be easily clogged by debris and dust. A clogged condenser without service for several years may become dirty, inhibiting heat transfer from the refrigerant-side to the air-side. Sometimes, the outdoor-air flow degradation can also be caused by a defective fan motor. To simulate condenser fouling or a defective fan motor fault for the RTU system, the heat exchanger area was blocked by one layer of paper towel as shown in Figure 33.

Figure 34 shows the estimated condenser air flow rate as a function of the condenser blockage for the two test RTUs. The estimated air flow rates based on an energy balance between air-side and refrigerant-side can be compared to the rated condenser air flow rate to detect condenser fouling. The AFDD approach predicted the rated condenser air flow rate within 15% under normal condition. Based on a survey and analysis of 215 RTUs (New Buildings Institute, 2003), the 15% reduced condenser air flow rate increases annual energy efficiency by about 5%. Therefore, the accuracy of the AFDD method to estimate the air flow rate within 15% is acceptable. As the severity of the condenser fouling increases, the estimated air flow rate decreases. A 75% blockage of the condenser area resulted in the air flow rate that was 60% of the rated air flow rate.

50% Condenser Fouling



75% Condenser Fouling



Figure 33 Simulation of Condenser Blockage: 50% (Left) and 75% (Right)

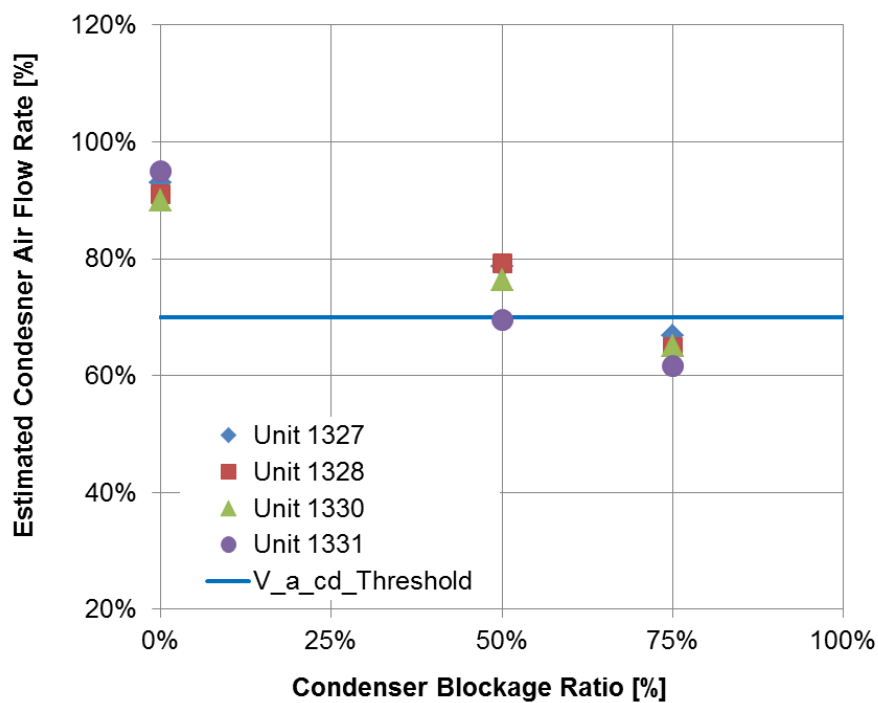


Figure 34 Estimated Condenser Air Flow Rate as a Function of Condenser Blockage

Figure 35 shows percent reduction in COP as a function of percent condenser air flow reduction for the two test RTUs. The percent condenser air flow reduction is computed as a ratio of the estimated condenser air flow and the rated condenser air flow under fault-free conditions. COP was chosen as the performance index because of its greater sensitivity to condenser fouling compared to cooling capacity. The percent reduction in the COP is estimated as a ratio of the estimated COP and the COP at the rated conditions and fault-free operation.

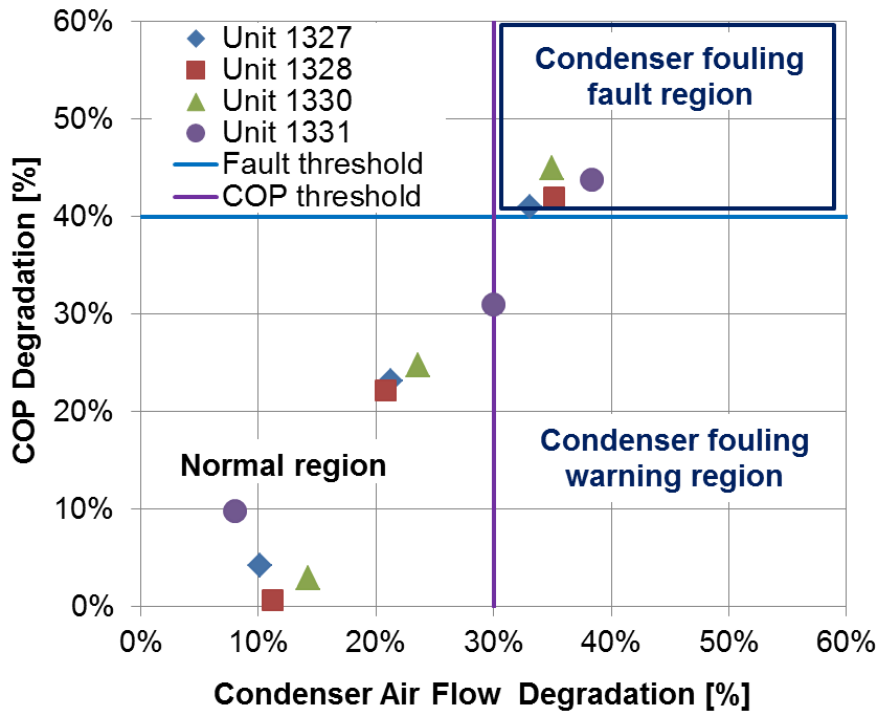


Figure 35 Percent Reduction in COP as a Function of Percent Condenser Air Flow Reduction

A COP reduction threshold of 40% is used to report the condenser fouling fault. When the air flow rate decreased by 30%, the resulting reduction in COP was over 40%. The embedded diagnostic reports a fault when there is a 40% reduction the COP and a warning when the percent air flow rate reduces by 30% but the COP reduction is less than 40% as shown in Figure 35.

Figure 36 shows the screen shots of results generated by the embedded diagnostics on the RTU controller for 0% and 75% blockage for one of the test RTU. The condenser fouling fault detection requires three refrigerant-side temperature inputs: (1) condensing (T_{c_s}), (2) discharge line (T_{dis}), and (3) liquid line (T_{liq}) and two air-side temperature inputs: (1) condenser air inlet ($T_{c_a_i}$) and (2) condenser air outlet ($T_{c_a_o}$).

When 75% of the face area of the heat exchange is blocked, the condenser air flow rate (V_{a_cd}) drops to 35% of a rated value. A condenser fouling fault was detected by comparing this estimated air flow rate with the rated condenser air flow rate. The COP_{ref} was also reduced to 60% by a condenser fouling fault. The results demonstrate that the impact of condenser fouling on energy efficiency is large for the 75% condenser fouling level at this operating condition. Based on the readings, the diagnostic outputs indicate that service is needed for this condenser fouling fault. When the condenser blockage was removed, the AFDD results indicated the normal operation.

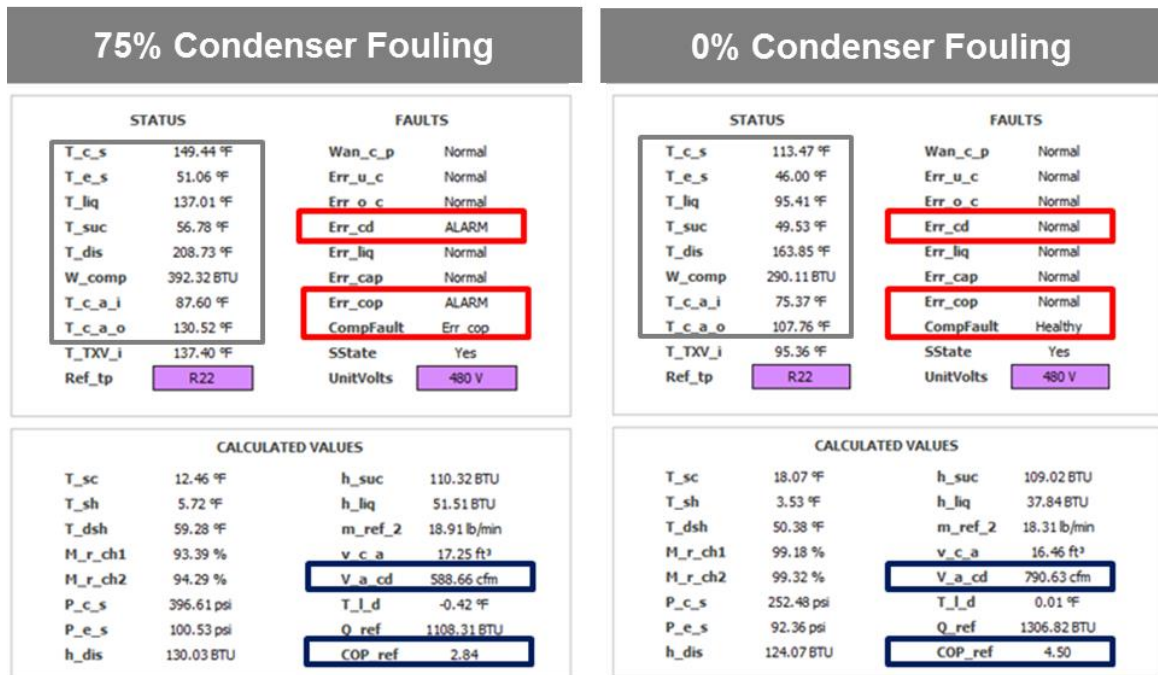


Figure 36 Screen Shots of Condenser Fouling Refrigerant-Side AFDD Results Generated by the RTU Controller: 75% Condenser Fouling (left) and 0% Condenser Fouling (right)

Simultaneous Refrigerant Undercharge and Condenser Fouling Fault Tests

In addition to independently validating the refrigerant charge fault and condenser fouling fault, a test with combined charge and condenser fouling was conducted. When a refrigerant charge fault and condenser fouling fault exist at the same time, the subcooling at the liquid line is decreased. The increasing condenser fault levels could lead to large errors in refrigerant charge predictions. Occasionally, the faulty component causes faults in other system components. The AFDD algorithms must be able to diagnose both fault sources. If only one fault is diagnosed and repaired, the system will continue to operate with an undiagnosed fault, which could cause the repaired component(s) to fail again.

Therefore, a fault diagnostics system should be able to analyze a given set of fault levels and identify which faults are affecting the system at any given point in time. For the combined fault, a 70% refrigerant charge-fault level was simulated with 50% and 75% condenser-fouling level faults, simultaneously, as shown in Figure 37.

Figure 38 shows the screen shots of results generated by the embedded diagnostics on the RTU controller for the combined charge and condenser-fouling faults for one of the test RTU. When the condenser blockage levels were 50% and 75%, the condenser air flow rate ('V_a_cd') decreased by 28% and 42%, respectively, compared to the rated value. The reduction of condenser air flow rate is proportional to the condenser-fouling fault level and is independent of refrigerant-charge level. The refrigerant-charge level ('M_r_ch2') of 69% and 67% was reported. The refrigerant charge level prediction was within 5% of the actual charge level regardless of the existence of condenser-fouling fault. Even though the unit had two simultaneous faults, the embedded refrigerant-side diagnostics detected both of them correctly.

**70% Refrigerant Charge Level
50% Condenser Fouling**



**70% Refrigerant Charge Level
75% Condenser Fouling**



Figure 37 Refrigerant-Charge Fault and Condenser-Fouling Fault: 70% Charge and 50% Blockage (left) and 70% Charge and 75% Blockage (right)

**75% Refrigerant Charge Level
50% Condenser Fouling**

STATUS		FAULTS	
T_c_s	126.54 °F	Wan_c_p	Normal
T_e_s	63.08 °F	Err_u_c	ALARM
T_liq	110.79 °F	Err_o_c	Normal
T_suc	73.19 °F	Err_cd	Normal
T_dis	212.38 °F	Err_liq	Normal
W_comp	293.19 BTU	Err_cap	Normal
T_c_a_i	68.75 °F	Err_cop	Normal
T_c_a_o	100.42 °F	CompFault	Err_u_c
T_TXV_i	109.66 °F	SState	Yes
Ref_tp	R22	UnitVolts	480 V

CALCULATED VALUES			
T_sc	15.74 °F	h_suc	113.27 BTU
T_sh	10.10 °F	h_liq	42.70 BTU
T_dsh	85.83 °F	m_ref_2	14.29 lb/min
M_r_ch1	89.00 %	v_c_a	16.14 ft³
M_r_ch2	68.69 %	V_a_cd	647.47 cfm
P_c_s	298.48 psi	T_l_d	1.14 °F
P_e_s	122.22 psi	Q_ref	1008.00 BTU
h_dis	132.77 BTU	COP_ref	3.44

**100% Refrigerant Charge Level
75% Condenser Fouling**

STATUS		FAULTS	
T_c_s	130.81 °F	Wan_c_p	ALARM
T_e_s	62.44 °F	Err_u_c	ALARM
T_liq	112.93 °F	Err_o_c	Normal
T_suc	73.96 °F	Err_cd	ALARM
T_dis	219.91 °F	Err_liq	Normal
W_comp	297.95 BTU	Err_cap	Normal
T_c_a_i	67.26 °F	Err_cop	Normal
T_c_a_o	105.18 °F	CompFault	Err_u_c
T_TXV_i	112.06 °F	SState	Yes
Ref_tp	R22	UnitVolts	480 V

CALCULATED VALUES			
T_sc	17.88 °F	h_suc	113.40 BTU
T_sh	11.51 °F	h_liq	43.39 BTU
T_dsh	89.11 °F	m_ref_2	13.42 lb/min
M_r_ch1	97.38 %	v_c_a	16.21 ft³
M_r_ch2	66.77 %	V_a_cd	516.25 cfm
P_c_s	314.88 psi	T_l_d	0.88 °F
P_e_s	120.95 psi	Q_ref	941.02 BTU
h_dis	134.49 BTU	COP_ref	3.15

Figure 38 Screen Shots of Combined Charge and Condenser Fouling Refrigerant-Side AFDD Results Generated by the RTU Controller: 70% Refrigerant Charge Level + 50% Condenser Fouling (left) and 70% Refrigerant Charge + 75% Condenser Fouling (right)

C.Summary of Validation of the Embedded Refrigerant-side Diagnostics with Artificial Faults

The embedded AFDD algorithms on the RTU controller were tested under various refrigerant charge levels and condenser blockages. The AFDD algorithms successfully identified the charge faults when the system was undercharged by 30% or more, and when the condenser blockage exceeded 50%. The AFDD algorithms were also successful in identifying simultaneous charge and condenser-fouling faults.

Validation of the Embedded Refrigerant-side Diagnostics with Offline Analysis

The embedded refrigerant-side diagnostics included detection of three commonly faults in the vapor compression systems:

1. Refrigerant charge
2. Condenser fouling
3. Liquid line restriction.

To validate the embedded refrigerant-side diagnostics, the same data used by the RTU controller was used to conduct an offline analysis. The same diagnostic algorithms that were embedded in the RTU controller were also implemented in the spreadsheet to validate the algorithms embedded on the controller.

Parameters needed for the Refrigerant-Side Fault Detection and Diagnostics

Nine parameters are needed to implement the refrigerant-side AFDD algorithms. Because some of these parameters are not known for the RTUs initially, defaults were assigned based on past experience of the authors. After the data collection from RTUs was initiated, the default parameters were refined. The approach used to update the default parameters is explained in a companion report. Table 41 shows the default parameter and “tuned” (updated) parameters for each RTU. To determine reasonable default parameters, existing test data available from Kim (2013) was used to estimate values for the nine parameters. However, the default parameters may not be reliable because each RTU system has different capacity, configurations (e.g., heat pump and air conditioner) and components (e.g., expansion device and compressor).

The three parameters, $T_{sc,r}$, $T_{sh,r}$ and $T_{dsh,r}$ were readily obtained from the test data of each RTU. The three parameters are determined in the absence of faults at the “rated” indoor and outdoor driving conditions. The “rated” condition is not that critical as long as the values of $T_{sc,r}$, $T_{sh,r}$ and $T_{dsh,r}$ are available for the same driving condition.

The three parameters for A_{sc} , A_{sh} , and A_{dsh} were “tuned” to improve accuracy using the data that was available over a range of operating conditions. The parameter tuning is accomplished using the linear regression technique and can minimize the errors between predicted and known refrigerant-charge levels.

The three tuned parameters, $V_{a,r}$, $Q_{ref,r}$, and COP_r can be determined by the estimated average values based on the “rated” data set.

Table 41 Comparison of Default Parameter and “Tuned” Parameter (first row below the

labels represents the default parameter for all units)

RTU system			$T_{sc,r}$	$T_{sh,r}$	$T_{dsh,r}$	A_{sc}	A_{sh}	A_{dsh}	$V_{a,r}$	$Q_{ref,r}$	COP_r
Default parameters			10.0	8.0	55.0	0.18	0.10	0.11	1000	675	4.5
WA Site	48GS-030	Unit 425	3.7	4.8	72.7	0.25	-0.15	-0.35	1930	670	5.0
	48TJE014	Unit 1327	18.8	3.0	49.0	0.05	-1.26	-3.36	880	1350	4.7
		Unit 1328	17.3	2.4	53.9	0.05	-1.26	-3.36	980	1520	4.5
	50TC050	Unit 1329	8.2	0.0	36.4	0.25	-0.15	-0.35	650	630	4.8
	48TFD014	Unit 1330	23.3	12.1	56.4	0.05	-1.26	-3.36	1050	1700	4.8
		Unit 1331	12.9	3.1	46.2	0.05	-1.26	-3.36	820	1430	4.7
	50EZA24	Unit 1332	6.4	2.9	28.7	0.25	-0.15	-0.35	2300	840	7.6
AZ Site	48HJF017	Unit 1333	15.2	12.6	61.9	0.34	-0.27	-0.43	1950	2140	4.1
		Unit 1334	13.8	10.5	65.4	0.34	-0.27	-0.43	1000	1180	3.7
	48HJF020	Unit 1335	17.9	23.1	55.2	0.34	-0.27	-0.43	1920	1490	5.6
		Unit 1336	18.7	21.3	60.7	0.34	-0.27	-0.43	1770	1360	5.2
	48HJF012	Unit 1337	17.7	12.4	58.5	0.05	-1.26	-3.36	1930	1450	4.9
		Unit 1338	17.9	12.2	55.9	0.05	-1.26	-3.36	1670	1250	4.9
	48HJF008	Unit 1339	18.5	0.7	35.7	0.05	-1.26	-3.36	2270	1230	6.3
		Unit 1340	15.6	9.8	43.9	0.05	-1.26	-3.36	2170	1180	6.1

Validation of Refrigerant-Side Embedded Diagnostics with Offline Analysis

In this section the results from the embedded diagnostics are compared to the results generated by the offline analysis. Table 42 shows the fault detection thresholds used by the AFDD algorithms (refer to Development of Refrigerant-side RTU Diagnostics for more details on the thresholds). The thresholds were determined from previous laboratory and field data (Kim, 2013). The selection of thresholds is critical because if the thresholds are too aggressive, it may lead to false alarms. On the other hand, if thresholds are conservative, the AFDD algorithms may miss faults that potentially reduce system performance. Therefore, it is very important to define reasonable thresholds for appropriate fault detection.

Table 42 Fault Detection Thresholds used by the AFDD Algorithms

	Refrigerant Overcharge Fault	Refrigerant Undercharge Fault	Condenser Fouling Fault	Liquid Line Restriction Fault
Threshold	30%	30%	30%	100%

Figure 39 shows the outputs from the embedded diagnostics for the four refrigerant-side faults for one unit in the field. The outdoor temperature during this period ranged between 86°F and 93°F. For the refrigerant-charge fault diagnostics, the parameter used to detect a fault is the charge level. If the estimated charge degradation exceeds 30% (i.e., if the actual charge is less than 70% of the rated charge), then a charge fault is reported. For

this unit, the refrigerant-charge degradation was mostly less than 10%, which was significantly below the 30% threshold, so the embedded diagnostics did not report a charge fault for this unit. Similarly, the charge for the rest of the units was also normal and therefore, no charge faults were reported of any of the nine units.

For the condenser-fouling fault, degradation in condenser air flow rate is used to detect a presence of the fault. If the estimated air flow degradation exceeds 30% (i.e., if the actual condenser air flow rate is less than 70% of the rated air flow rate), then a condenser fouling fault is reported. For this unit (Figure 39), the condenser air-flow degradation estimated by the embedded diagnostics never exceeded more than 20%. Although for the most part the air flow degradation was less than 10%, the degradation shows relatively larger deviations compared to other parameters primarily as a result of inaccuracy in measuring the condenser outlet air temperature. When the air temperature distribution in the condenser is non-uniform, the outlet air measurement becomes inaccurate when a single-point measurement is used. Depending on the placement of the RTD temperature sensor, the inaccuracy can become significant. An averaging probe might reduce the uncertainty of the measurement but placement of the averaging sensor could be a challenge.

The liquid line restriction fault is meant to represent a dirty filter/dryer. For this fault, the pressure drop across the filter/dryer is used to detect the presence of the fault. For this unit (Figure 39), the increase in the pressure drop across the filter/dryer between 0% and 10%, is significantly lower than the threshold. This method was insensitive to variations in operating conditions.

To validate the degradation parameters estimated by the embedded diagnostics, the diagnostics were implemented in a spreadsheet and analyzed using the same sensor input data from the RTU controller. The results from the offline analysis were almost identical to the results from the embedded algorithms, as shown in Figure 40.

In addition to estimating the degradation of the various parameters, the embedded diagnostics also estimate the performance impact (degradation in cooling capacity and COP). Figure 41 shows the degradation of capacity or COP for a unit in WA. Unless a fault leads to a capacity or COP reduction of 40%, it is not reported as a fault. There is a relatively large deviation in the estimated capacity and COP primarily because of a large variation of indoor and/or outdoor conditions. At low outdoor temperatures (below 70°F), the method used to estimate the capacity and COP have a large uncertainty. Therefore, as the outdoor temperature decreased, capacity and COP degradation estimates increased to 15% and 25%, respectively. These values are still below the fault threshold of 40%.

To validate the capacity and COP degradation estimated by the embedded diagnostics, these parameters were estimated using the offline analysis. The results from the offline analysis were almost identical to the results from the embedded algorithms, as shown in Figure 42.

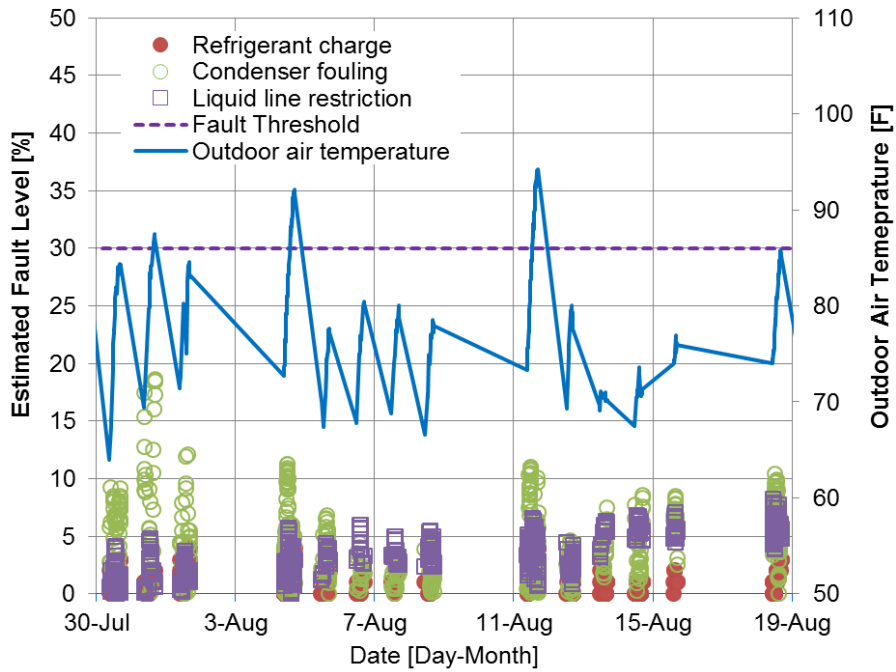


Figure 39: Outputs Showing the Estimated Fault Level from the Embedded Diagnostics for Refrigerant Charge, Liquid line Restriction, and Condenser Fouling for one Unit in WA

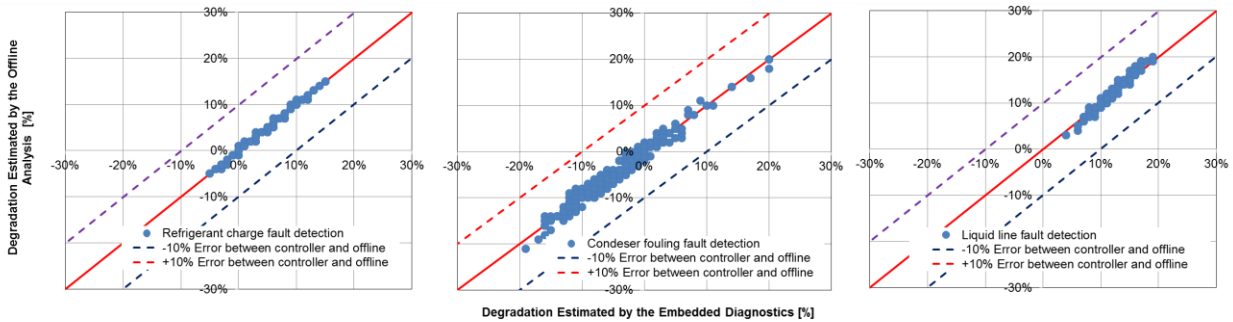


Figure 40: Comparison of Degradation Parameters Estimated by the Embedded Diagnostics

and Offline Analysis

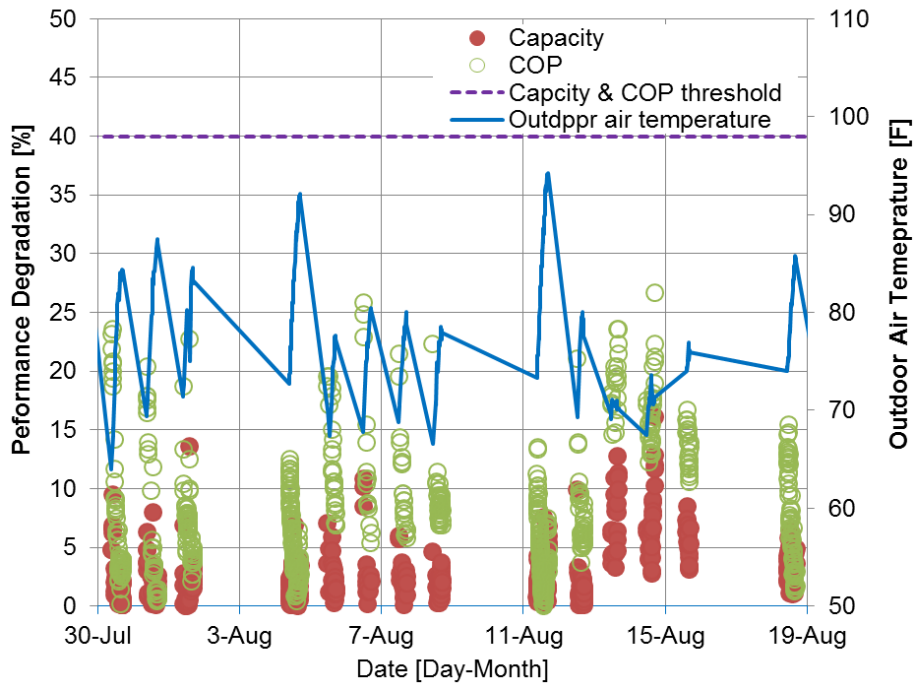


Figure 41 Outputs Showing the Performance Impact Estimated by the Embedded Diagnostics for Refrigerant Charge, Liquid line Restriction, and Condenser Fouling for one Unit in WA

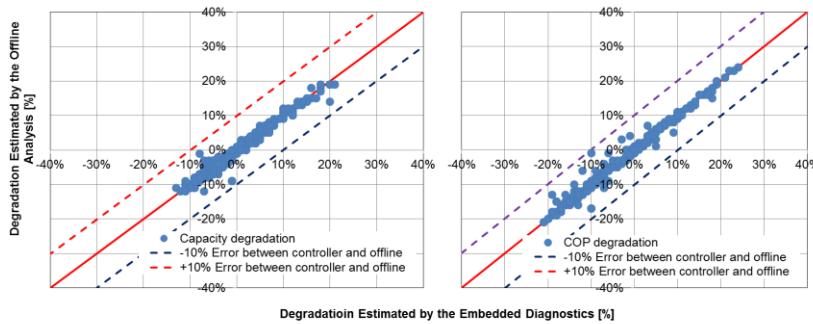


Figure 42: Comparison of Capacity and COP Degradation Estimated by the Embedded Diagnostics and Offline Analysis

Figure 43 shows the outputs from the embedded diagnostics for the four refrigerant-side faults for another unit in the field in AZ. For this unit, the refrigerant-charge degradation was mostly less than 10%, which was significantly below the 30% threshold, so the embedded diagnostics did not report a charge fault for this unit. The condenser air flow degradation estimated by the embedded diagnostics ranged between 0% and 20%. The increase in pressure drop across the filter/dryer was between 10% and 15%. The results from the offline analysis were almost identical to the results from the embedded

algorithms, as shown in Figure 44.

Figure 45 shows the degradation of capacity or COP for a unit in AZ. Like the other unit reported previously (Figure 41), there is a relatively large deviation in the estimated capacity and COP primarily because of a large variation of indoor and/or outdoor conditions. However, these values are still below the fault threshold of 40%. The results from the offline analysis were almost identical to the results from the embedded algorithms, as shown in Figure 46.

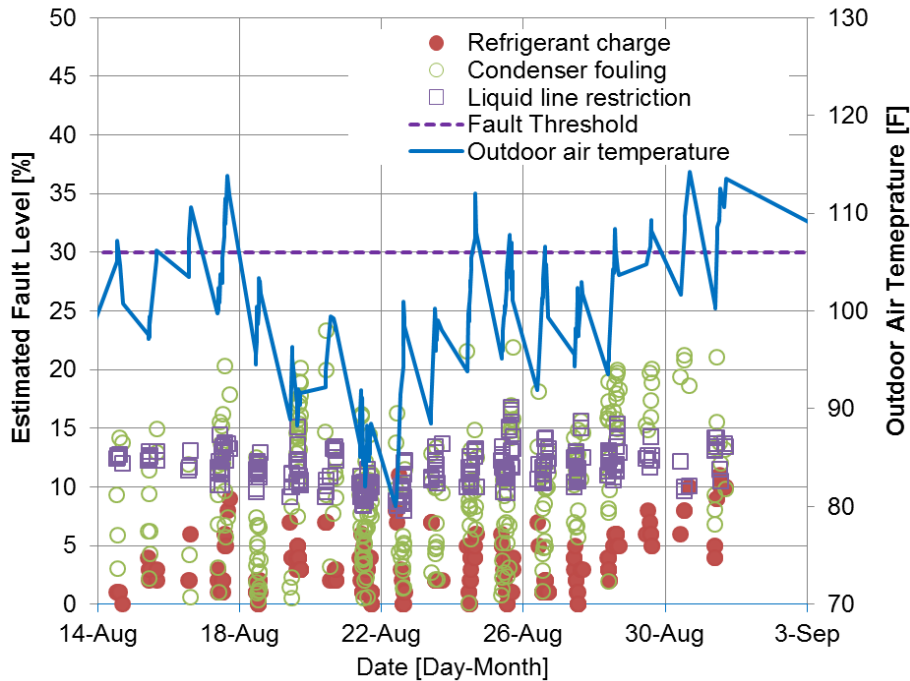


Figure 43 Outputs Showing the Estimated Fault Level from the Embedded Diagnostics for Refrigerant Charge, Liquid line Restriction, and Condenser Fouling for one Unit in AZ

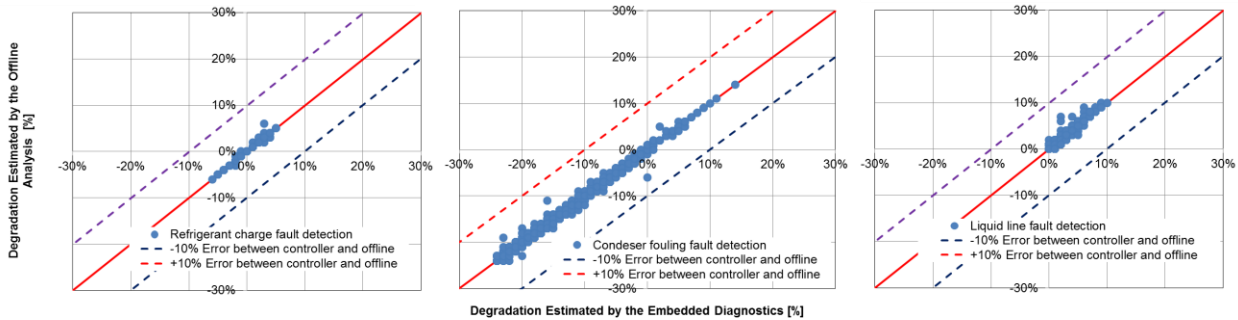


Figure 44: Comparison of Degradation Parameters Generated by the Embedded Diagnostics and Offline Analysis

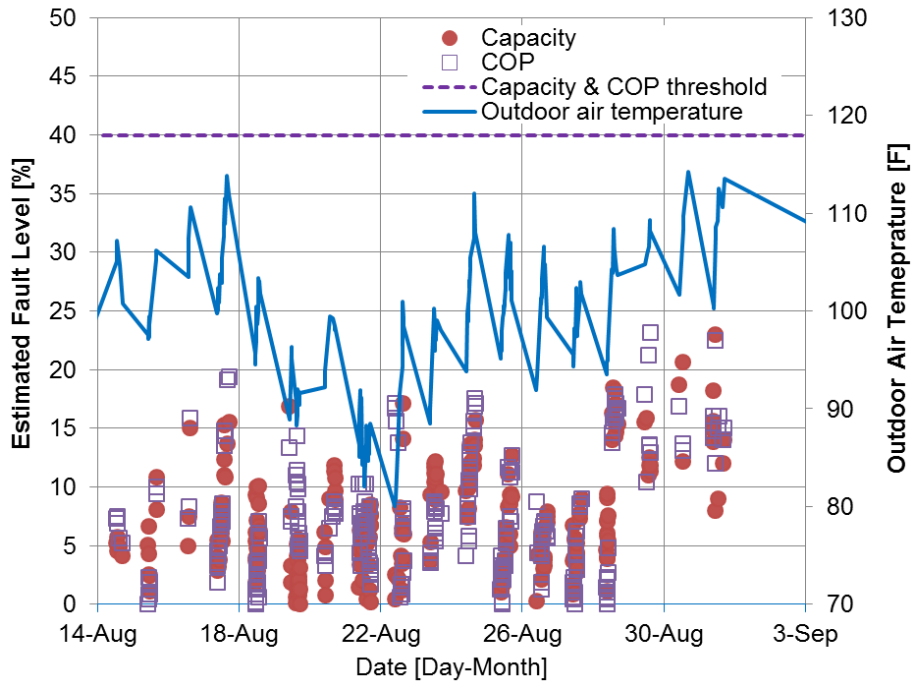


Figure 45 Outputs Showing the Performance Impact Estimated by the Embedded Diagnostics for Refrigerant Charge, Liquid line Restriction, and Condenser Fouling for one Unit in AZ

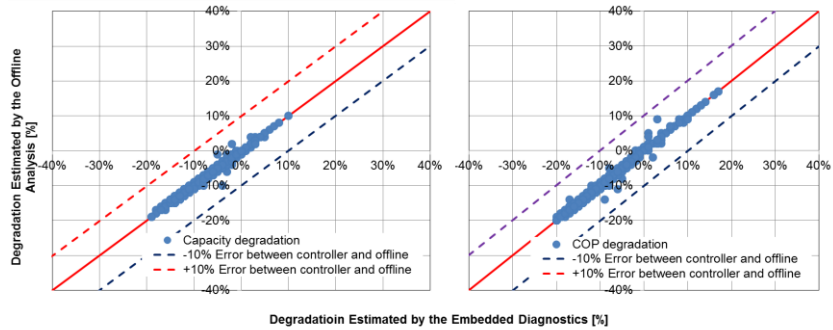


Figure 46: Comparison of Capacity and COP degradation Estimated by the Embedded Diagnostics and Offline Analysis

IX. Summary and Discussion

This report documented the development, testing and field validation of the integrated AFDD and advanced RTU controls using a single controller. The AFDD included both the air-side and the refrigerant-side faults that are commonly found in the RTUs.

Seven AFDD algorithms were developed, deployed and tested on the RTU controller for detecting and diagnosing faults with RTU economizer and ventilation operations using sensors that are commonly installed for advanced control purposes. The algorithms utilize rules derived from engineering principles of proper and improper RTU operations:

- Compare discharge-air temperatures (DAT) with mixed-air temperatures (MAT) for consistency (AFDD0)
- Check if the outdoor-air damper (OAD) is modulating (AFDD1)
- Detect RTU sensor faults (outdoor-air, mixed-air and return-air temperature sensors) (AFDD2)
- Detect if the RTU is not economizing when it should (AFDD3)
- Detect if the RTU is economizing when it should not (AFDD4)
- Detect if the RTU is using excess outdoor air (AFDD5)
- Detect if the RTU is bringing in insufficient ventilation air (AFDD6).

The intent of these algorithms is to provide actionable information to building owners and operations staff while minimizing false alarms. Therefore, the algorithms have been designed to minimize false alarms. These seven algorithms were embedded in the RTU controller. This implementation has been validated by comparing the outputs from the embedded diagnostics with output generated by offline analysis.

In addition to the air-side diagnostics, refrigerant-side diagnostics were also deployed on the RTU controller. The refrigerant-side diagnostics included: 1) low and high refrigerant charge, 2) condenser fouling and 3) liquid line restriction. Similar to the air-side diagnostics, the refrigerant-side diagnostics were also validated by comparing the outputs from the embedded diagnostics with the output generated by offline analysis.

A. Discussion and Lessons Learned

The project has shown that air-side and refrigerant-side AFDD can be easily integrated with advanced RTU controls. With the exception of the mixed-air temperature sensor, all other sensors required to conduct the air-side AFDD are readily available on the RTU controller because they are needed for the advanced control operations. Therefore, the incremental cost of adding air-side diagnostics is minimal. Although the project has shown that integration of the refrigerant-side diagnostics on to the RTU controller are possible, there are a number of additional sensors that are needed to deploy the refrigerant-side diagnostics.

In addition to the cost for the additional sensors, locating the sensors in the correct location to measure the parameters also turned out to be a challenge. Because temperature sensors were being used as proxies for pressure measurements, mounting these sensors in the right location is critical; otherwise, the uncertainty in the measurement will be high. Accommodating additional sensors also means either increasing the input/output capability of the RTU controller or adding another controller to handle the additional sensors, which increase the cost of deployment significantly.

Therefore, for deploying refrigerant-side diagnostics along with advanced RTU controls three hurdles have to be overcome: 1) cost of additional sensors, 2) cost of upgrading the RTU controller to handle additional sensors and 3) overcoming the installation of the sensors in the right location.

X. References

- AEC (Architectural Energy Corporation). 2003. Final Report: Energy efficient and affordable commercial and residential buildings. Report prepared for the California Energy Commission. Report number P500-03-096, Architectural Energy Corporation, Boulder, Colorado. Available on the Web at <http://www.archenergy.com/cec-eeb/P500-03-096-rev2-final.pdf>.
- DOE. 2013. High performance rooftop unit. U.S. Department of Energy, Washington, D.C. Retrieved January 2013 from http://www1.eere.energy.gov/buildings/commercial/bba_rtu_spec.html.
- DOE. 2014. http://apps1.eere.energy.gov/buildings/energyplus/energyplus_about.cfm last accessed on October 10, 2014.
- EIA. 2003. <http://www.eia.gov/consumption/commercial/data/2003/> last accessed on October 10, 2014.
- Criscione P. 2011. "A dramatic boost for existing RTUs." E Source Research Brief, TAS-RB-47.
- Katipamula S, W Wang, and M Vowles. 2014. "Improving the Operating Efficiency of Packaged Air Conditioners and Heat Pumps." ASHRAE Journal 56(3):36-42.
- Kim, W. and Braun, J., 2012a, Performance evaluation of a virtual refrigerant charge sensor, International Journal of Refrigeration, 36(3): 1130-1141.
- Kim,W. 2013. "Fault detection and diagnosis for air conditioners and heat pumps based on virtual sensors.", Thesis, Purdue University, West Lafayette, IN.
- Kim, W and J Braun. 2012a. "Performance evaluation of a virtual refrigerant charge sensor," International Journal of Refrigeration, 36(3): 1130-1141.
- Kim, W and J Braun. 2012b. "Evaluation of the Impact of Refrigerant Charge on Air Conditioner and Heat Pump Performance," International Journal of Refrigeration, 35(7): 1805-1814.
- Kim, W and J Braun. 2012c. "Evaluation of virtual refrigerant mass flow sensors," International Refrigerant and Air conditioning Conference, West Lafayette, IN, No. 2299.
- New Buildings Institute, 2003, Integrated Energy Systems: Productivity & Building Science, Vancouver, WA, Available online: http://www.energy.ca.gov/pier/project_reports/
- Quimby P W, Khire R, Leonardi F, and Sarkar S. 2014. "A Novel Human Machine Interface for Advanced Building Controls and Diagnostics." International High Performance Buildings Conference, West Lafayette, IN.
- Smith V. and Braun J. 2003. Final Report Compilation for Fault Detection and Diagnostics for Rooftop Air Conditioners, Available online: <http://www.energy.ca.gov/2003publications/CEC-500-2003-096/CEC-500-2003-096-A01.PDF>
- Wang W, S Katipamula, Y Huang, and MR Brambley. 2011. [Energy Savings and Economics of Advanced Control Strategies for Packaged Air-Conditioning Units with Gas Heat](#). PNNL-20955, Pacific Northwest National Laboratory, Richland, WA.

Wang W, Y Huang, and S Katipamula. 2012. [Energy Savings and Economics of Advanced Control Strategies for Packaged Heat Pumps](#). PNNL-21944, Pacific Northwest National Laboratory, Richland, WA.

Wang W, S Katipamula, H Ngo, RM Underhill, DJ Taasevigen, and RG Lutes. 2013. [Advanced Rooftop Control \(ARC\) Retrofit: Field-Test Results](#). PNNL-22656, Pacific Northwest National Laboratory, Richland, WA.

Appendix - Refrigerant Property Table

Table A- 1 Saturation lookup table of refrigerant R410A

Temperature	pressure	Liquid enthalpy	Vapor enthalpy
°F	pisa	Btu/lb	Btu/lb
-20.00	41.58	4.99	110.56
-10.00	51.53	7.64	111.7
0	63.27	10.41	112.78
10	77.03	13.29	113.81
12	80.05	13.88	114.01
14	83.15	14.47	114.21
16	86.35	15.08	114.4
18	89.64	15.68	114.59
20	93.03	16.29	114.78
22	96.52	16.91	114.96
24	100.11	17.53	115.14
26	103.81	18.16	115.32
28	107.6	18.79	115.5
30	111.51	19.43	115.67
32	115.52	20.08	115.85
34	119.65	20.73	116.01
36	123.89	21.38	116.18
38	128.24	22.05	116.34
40	132.71	22.71	116.5
42	137.3	23.39	116.65
44	142.01	24.07	116.8
46	146.85	24.76	116.95
48	151.81	25.45	117.09
50	156.89	26.15	117.23
52	162.11	26.85	117.37
54	167.46	27.57	117.5
56	172.94	28.28	117.63
58	178.56	29.01	117.76
60	184.32	29.74	117.88
62	190.21	30.48	118
64	196.25	31.23	118.11
66	202.44	31.99	118.22
68	208.77	32.75	118.32
70	215.25	33.52	118.42
72	221.88	34.3	118.52
74	228.67	35.09	118.61
76	235.61	35.88	118.69
78	242.71	36.68	118.77
80	249.97	37.5	118.85
82	257.39	38.32	118.92
84	264.98	39.15	118.98

Temperature	pressure	Liquid enthalpy	Vapor enthalpy
86	272.74	39.99	119.04
88	280.66	40.84	119.1
90	288.76	41.7	119.14
92	297.03	42.57	119.19
94	305.47	43.45	119.22
96	314.1	44.34	119.25
98	322.9	45.24	119.27
100	331.89	46.15	119.29
102	341.06	47.08	119.29
104	350.43	48.02	119.3
106	359.98	48.98	119.29
108	369.72	49.94	119.27
110	379.66	50.93	119.25
112	389.79	51.92	119.22
114	400.13	52.94	119.18
116	410.66	53.97	119.13
118	421.4	55.02	119.07
120	432.35	56.09	119
122	443.5	57.18	118.92
124	454.87	58.3	118.82
126	466.44	59.44	118.72
128	478.24	60.6	118.6
130	490.25	61.8	118.47
132	502.48	63.02	118.32
134	514.93	64.29	118.16
136	527.61	65.59	117.97
138	540.51	66.93	117.77
140	553.64	68.33	117.55
142	567.01	69.78	117.3
144	580.61	71.31	117.02
146	594.44	72.91	116.71
148	608.52	74.61	116.37
150	622.83	76.43	115.97
152	637.39	78.4	115.52
154	652.19	80.58	114.99
156	667.24	83.06	114.35
158	682.54	86.01	113.54
160	698.09	89.87	112.41

Table A- 2 Saturation lookup table of refrigerant R22

Temperature	Pressure	Liquid enthalpy	Vapor enthalpy
°F	pisa	Btu/lb	Btu/lb

Temperature	Pressure	Liquid enthalpy	Vapor enthalpy
-30	19.573	2.547	101.348
-28	20.549	3.061	101.564
-26	21.564	3.576	101.778
-24	22.617	4.093	101.992
-22	23.711	4.611	102.204
-20	24.845	5.131	102.415
-18	26.02	5.652	102.626
-16	27.239	6.175	102.835
-14	28.501	6.699	103.043
-12	29.809	7.224	103.25
-10	31.162	7.751	103.455
-8	32.563	8.28	103.66
-6	34.011	8.81	103.863
-4	35.509	9.341	104.065
-2	37.057	9.874	104.266
0	38.657	10.409	104.465
2	40.309	10.945	104.663
4	42.014	11.483	104.86
6	43.775	12.022	105.056
8	45.591	12.562	105.25
10	47.464	13.104	105.442
12	49.396	13.648	105.633
14	51.387	14.193	105.823
16	53.438	14.739	106.011
18	55.551	15.288	106.198
20	57.727	15.837	106.383
22	59.967	16.389	106.566
24	62.272	16.942	106.748
26	64.644	17.496	106.928
28	67.083	18.052	107.107
30	69.591	18.609	107.284
32	72.169	19.169	107.459
34	74.818	19.729	107.632
36	77.54	20.292	107.804
38	80.336	20.856	107.974
40	83.206	21.422	108.142
42	86.153	21.989	108.308
44	89.177	22.558	108.472
46	92.28	23.129	108.634
48	95.463	23.701	108.795

Temperature	Pressure	Liquid enthalpy	Vapor enthalpy
50	98.72	24.275	108.953
52	102.07	24.851	109.109
54	105.5	25.429	109.263
56	109.02	26.008	109.415
58	112.62	26.589	109.564
60	116.31	27.172	109.712
62	120.09	27.757	109.857
64	123.96	28.344	110
66	127.92	28.932	110.14
68	131.97	29.523	110.278
70	136.12	30.116	110.414
72	140.37	30.71	110.547
74	144.71	31.307	110.677
76	149.15	31.906	110.805
78	153.69	32.506	110.93
80	158.33	33.109	111.052
82	163.07	33.714	111.171
84	167.92	34.322	111.288
86	172.87	34.931	111.401
88	177.93	35.543	111.512
90	183.09	36.158	111.619
92	188.37	36.774	111.723
94	193.76	37.394	111.824
96	199.26	38.016	111.921
98	204.87	38.64	112.015
100	210.6	39.267	112.105
102	216.45	39.897	112.192
104	222.42	40.53	112.274
106	228.5	41.166	112.353
108	234.71	41.804	112.427
110	241.04	42.446	112.498
112	247.5	43.091	112.564
114	254.08	43.739	112.626
116	260.79	44.391	112.682
118	267.63	45.046	112.735
120	274.6	45.705	112.782
122	281.71	46.368	112.824
124	288.95	47.034	112.86
126	296.33	47.705	112.891
128	303.84	48.38	112.917

Temperature	Pressure	Liquid enthalpy	Vapor enthalpy
130	311.5	49.059	112.936
132	319.29	49.743	112.949
135	331.26	50.778	112.956
140	351.94	52.528	112.931
145	373.58	54.315	112.858
150	396.19	56.143	112.728
160	444.53	59.948	112.263
170	497.26	64.019	111.438
180	554.78	68.498	110.068
190	617.59	73.711	107.734
200	686.36	80.862	102.853

Table A- 3 Superheated lookup tables of refrigerant R410A

Absolute pressure	Temperature	Enthalpy
psia	F	Btu/lb
30	-30	115.8
30	0	121.8
30	30	127.8
30	60	133.9
30	90	140
30	120	146.2
30	150	152.6
30	180	159
30	210	165.7
30	240	172.5
50	0	119.9
50	30	126.3
50	60	132.6
50	90	139
50	120	145.4
50	150	151.9
50	180	158.4
50	210	165.2
50	240	172
50	270	179
70	30	124.7
70	60	131.4
70	90	137.9

Absolute pressure	Temperature	Enthalpy
70	120	144.5
70	150	151.1
70	180	157.8
70	210	164.6
70	240	171.5
70	270	178.5
70	300	185.7
100	30	122
100	60	129.3
100	90	136.3
100	120	143.2
100	150	150
100	180	156.9
100	210	163.8
100	240	170.8
100	270	177.9
100	300	185.1
130	60	127.2
130	90	134.7
130	120	141.9
130	150	148.9
130	180	155.9
130	210	163
130	240	170.1
130	270	177.3
130	300	184.5
130	330	191.9
150	60	125.6
150	90	133.5
150	120	140.9
150	150	148.1
150	180	155.3
150	210	162.4
150	240	169.6
150	270	176.8
150	300	184.2
150	330	191.6
170	60	123.9
170	90	132.2
170	120	139.9

Absolute pressure	Temperature	Enthalpy
170	150	147.4
170	180	154.6
170	210	161.9
170	240	169.1
170	270	176.4
170	300	183.8
170	330	191.2
200	90	130.2
200	120	138.4
200	150	146.1
200	180	153.6
200	210	161
200	240	168.4
200	270	175.7
200	300	183.2
200	330	190.7
200	360	198.3
220	90	128.8
220	120	137.4
220	150	145.3
220	180	152.9
220	210	160.4
220	240	167.8
220	270	175.3
220	300	182.8
220	330	190.3
220	360	198
240	90	127.3
240	120	136.3
240	150	144.4
240	180	152.2
240	210	159.8
240	240	167.3
240	270	174.8
240	300	182.4
240	330	190
240	360	197.7
260	90	125.7
260	120	135.1
260	150	143.6

Absolute pressure	Temperature	Enthalpy
260	180	151.5
260	210	159.2
260	240	166.8
260	270	174.4
260	300	182
260	330	189.6
260	360	197.3
280	120	133.9
280	150	142.6
280	180	150.8
280	210	158.6
280	240	166.3
280	270	173.9
280	300	181.6
280	330	189.3
280	360	197
300	120	132.7
300	150	141.7
300	180	150
300	210	158
300	240	165.8
300	270	173.5
300	300	181.2
300	330	188.9
300	360	196.7
320	120	131.4
320	150	140.7
320	180	149.3
320	210	157.4
320	240	165.2
320	270	173
320	300	180.8
320	330	185.9
320	360	196.3
320	390	204.2
340	120	130
340	150	139.7
340	180	148.5
340	210	156.7
340	240	164.7

Absolute pressure	Temperature	Enthalpy
340	270	172.5
340	300	180.3
340	330	188.2
340	360	196
340	390	203.9
360	120	128.5
360	150	138.7
360	180	147.7
360	210	156.1
360	240	164.2
360	270	172.1
360	300	179.9
360	330	187.8
360	360	195.7
360	390	203.6
400	150	136.5
400	180	146
400	210	154.8
400	240	163
400	270	171.1
400	300	179.1
400	330	187
400	360	195
400	390	203
400	420	208.4
450	150	133.5
450	180	143.9
450	210	153
450	240	161.6
450	270	169.9
450	300	178
450	330	186.1
450	360	194.2
450	390	202.2
450	420	210.4
500	150	130.1
500	180	141.5
500	210	151.2
500	240	160.1
500	270	168.7

Absolute pressure	Temperature	Enthalpy
500	300	177
500	330	185.2
500	360	193.3
500	390	201.5
500	420	209.7

Table A- 4 Superheated lookup tables of refrigerant R410A

Absolute pressure	Temperature	Enthalpy
psia	F	Btu/lb
30	-10	103.64
30	0	105.19
30	10	106.74
30	20	108.3
30	30	109.86
30	40	111.43
30	50	113.01
30	60	114.6
30	70	116.19
30	80	117.8
30	90	119.41
30	100	121.04
60	30	108
60	40	109.7
60	50	111.39
60	60	113.07
60	70	114.76
60	80	116.44
60	90	118.13
60	100	119.82
60	110	121.52
60	120	123.22
60	130	124.93
60	140	126.65
80	40	108.42
80	50	110.2
80	60	111.97
80	70	113.73

Absolute pressure	Temperature	Enthalpy
80	80	115.48
80	90	117.22
80	100	118.97
80	110	120.71
80	120	122.45
80	130	124.2
80	140	125.96
80	150	127.72
100	60	110.79
100	80	114.46
100	100	118.07
100	120	121.66
100	140	125.24
100	160	128.83
100	180	132.45
100	200	136.08
100	220	139.75
100	240	143.45
100	260	147.19
100	280	150.97
100	300	154.78
120	80	113.37
120	100	117.13
120	120	120.83
120	140	124.5
120	160	128.16
120	180	131.84
120	200	135.53
120	220	139.24
120	240	142.98
120	260	146.75
120	280	150.55
120	300	154.39
140	80	112.2
140	100	116.14
140	120	119.96
140	140	123.73
140	160	127.48
140	180	131.21
140	200	134.96

Absolute pressure	Temperature	Enthalpy
140	220	138.71
140	240	142.49
140	260	146.3
140	280	150.13
140	300	154
140	320	157.89
160	100	115.08
160	120	119.06
160	140	122.94
160	160	126.77
160	180	130.57
160	200	134.37
160	220	138.18
160	240	142
160	260	145.84
160	280	149.7
160	300	153.6
160	320	157.62
180	100	113.95
180	120	118.11
180	140	122.11
180	160	126.04
180	180	129.92
180	200	133.78
180	220	137.64
180	240	141.5
180	260	145.38
180	280	149.28
180	300	153.2
180	320	157.15
180	340	161.12
200	100	112.73
200	120	117.1
200	140	121.25
200	160	125.28
200	180	129.25
200	200	133.17
200	220	137.08
200	240	140.99
200	260	144.91

Absolute pressure	Temperature	Enthalpy
200	280	148.84
200	300	152.79
200	320	156.77
200	340	160.77
225	120	115.75
225	140	120.12
225	160	124.3
225	180	128.38
225	200	132.4
225	220	136.38
225	240	140.35
225	260	144.32
225	280	148.29
225	300	152.28
225	320	156.29
225	340	160.32
225	360	164.38
250	120	114.27
250	140	118.91
250	160	123.27
250	180	127.48
250	200	131.59
250	220	135.66
250	240	139.69
250	260	143.71
250	280	147.73
250	300	151.76
250	320	155.81
250	340	159.87
250	360	163.95
275	140	117.61
275	160	122.19
275	180	126.54
275	200	130.77
275	220	134.91
275	240	139.02
275	260	143.1
275	280	147.17
275	300	151.24
275	320	155.32

Absolute pressure	Temperature	Enthalpy
275	340	159.41
275	360	163.53
300	140	116.2
300	160	121.04
300	180	125.56
300	200	129.91
300	220	134.15
300	240	138.33
300	260	142.47
300	280	146.59
300	300	150.71
300	320	154.83
300	340	158.95
300	360	163.09
325	140	114.63
325	160	119.81
325	180	124.53
325	200	129.02
325	220	133.37
325	240	137.63
325	260	141.83
325	280	146.01
325	300	150.17
325	320	154.33
325	340	158.49
325	360	162.66
325	380	166.85
350	140	112.86
350	160	118.3
350	180	123.38
350	200	128.1
350	220	132.53
350	240	136.89
350	260	141.18
350	280	145.41
350	300	149.62
350	320	153.82
350	340	158.02
350	360	162.23
350	380	166.43

U.S. DEPARTMENT OF
ENERGY | Energy Efficiency &
Renewable Energy

Tech Demo Reports
techdemo@ee.doe.gov
May 2015

Printed with a renewable-source ink on paper containing at least 50% wastepaper, including 10% post-consumer waste.